


ISSN 0503-1540

La mer



Tome 40 Numéro 3 Août 2002

La Société franco-japonaise

d'océanographie

Tokyo, Japon

SOCIÉTÉ FRANÇO-JAPONAISE D'OcéANOGRAPHIE

Comité de Rédaction

(de l'exercice des années de 2002 et 2003)

Directeur et rédacteur: J. YOSHIDA

Comité de lecture: M. OCHIAI, Y. TANAKA, H. NAGASHIMA, M. MAEDA, S. MONTANI, T. YANAGI, S. WATANABE

Rédacteurs étrangers: H. J. CECCALDI (France), E. D. GOLDBERG (Etats-Unis), T. R. PARSONS (Canada)

Services de rédaction et d'édition: Y. TANAKA, Y. KITADE

Note pour la présentation des manuscrits

La mer, organe de la Société franco-japonaise d'océanographie, publie des articles et notes originaux, des articles de synthèse, des analyses d'ouvrages et des informations intéressant les membres de la société. Les sujets traités doivent avoir un rapport direct avec l'océanographie générale, ainsi qu'avec les sciences halieutiques.

Les manuscrits doivent être présentés avec un double, et dactylographiés, en *double interligne*, et au recto exclusivement, sur du papier blanc de format A4 (21×29.7 cm). Les tableaux et les légendes des figures seront regroupés respectivement sur des feuilles séparées à la fin du manuscrit.

Le manuscrit devra être présenté sous la forme suivante:

1° Il sera écrit en japonais, français ou anglais. Dans le cadre des articles originaux, il comprendra toujours le résumé en anglais ou français de *200 mots* environ. Pour les textes en langues européennes, il faudra joindre en plus le résumé en japonais de *500 lettres* environ. Si le manuscrit est envoyé par un non-japonophone, le comité sera responsable de la rédaction de ce résumé.

2° La présentation des articles devra être la même que dans les numéros récents; le nom de l'auteur précédé du prénom *en entier*, en minuscules; les symboles et abréviations standards autorisés par le comité; les citations bibliographiques seront faites selon le mode de publication: article dans une revue, partie d'un livre, livre entier, etc.

3° Les figures ou dessins originaux devront être parfaitement nettes en vue de la réduction nécessaire. La réduction sera faite dans le format 14.5×20.0 cm.

La première épreuve seule sera envoyée à l'auteur pour la correction.

Les membres de la Société peuvent publier 7 pages imprimées sans frais d'impression dans la mesure où leur manuscrit qui ne demande pas de frais d'impression excessifs (pour des photos couleurs, par exemple). Dans les autres cas, y compris la présentation d'un non-membre, tous les frais seront à la charge de l'auteur.

Cinquante tirés-à-part peuvent être fournis par article aux auteurs à titre gratuit. On peut en fournir aussi un plus grand nombre sur demande, par 50 exemplaires.

Les manuscrits devront être adressés directement au directeur de publication de la Société: Y. YAMAGUCHI, Université des Pêches de Tokyo, Konan 4-5-7, Minato-ku, Tokyo, 108 Japon; ou bien au rédacteur étranger le plus proche: H. J. CECCALDI, EPHE, Station marine d'Endoume, rue Batterie-des-Lions, 13007 Marseille, France; E. D. GOLDBERG, Scripps Institution of Oceanography, La Jolla, California 92093, Etats-Unis; ou T. R. PARSONS, Institute of Ocean Sciences, P.O.Box 6000, 9860W, Saanich Rd., Sidney, B. C., V8L 4B2, Canada.

サンゴ礁海域における二酸化炭素分圧と大気-海洋間のCO₂フラックス

藤村弘行*, 大森 保*, 北田幸男*, 真栄平司*

Carbon Dioxide and Air-Sea CO₂ Flux in Coral Reef

Hiroyuki FUJIMURA, Tamotsu OOMORI, Yukio KITADA, Tsukasa MAEHIRA

Abstract: In order to obtain long term CO₂ monitoring data in coral reef, studies on the methods of *p*CO₂ measurement in seawater (*p*CO_{2seawater}) and air-sea CO₂ flux estimate have been carried out; 1) Conventional *p*CO_{2seawater} estimation by pH-alkalinity method is well correlated ($R^2 = 0.962$) with the *p*CO_{2seawater} measurements by NDIR method, and is applicable to the long term monitoring of *p*CO_{2seawater} in coral reef.

- 2) Air-sea CO₂ flux measured by "chamber method" is largely dependent on the difference in *p*CO₂ between air and seawater, and wind velocity. Gas exchange coefficient values obtained in this study are in good agreement with those of previously reported values.
- 3) Preliminary long term monitoring of *p*CO_{2seawater} and air-sea CO₂ flux in coral reef has been carried out for 6 months by pH-alkalinity method; daily, monthly and seasonal variations of *p*CO_{2seawater} in coral reef are clearly seen. Rather low *p*CO_{2seawater} values are seen typically in daytime of low tide hours, and high *p*CO_{2seawater} values are seen at nighttime with low tide, respectively throughout the monitoring period. Air-sea CO₂ flux is largely dependent on the daily *p*CO_{2seawater} variation and on the wind velocity.
- 4) Monthly balance of CO₂ budget demonstrates that evasion of CO₂ from sea to air is seen during summer season, which is caused by relatively high *p*CO_{2seawater}, high water temperature and temporally strong winds, while invasion of CO₂ from air to sea is seen in spring.

Key words : coral reef, carbon dioxide, CO₂ flux, monitoring

1. はじめに

サンゴ礁は、貧栄養の海に多様な生物が生息し、生物による有機・無機炭素生産が活発におこなわれる熱帯・亜熱帯域の生物圏である。近年、化石燃料の大量消費が主要な原因となって大気中の二酸化炭素分圧が顕著に増加し、グローバルな温暖化の傾向が進行しつつある。これらの進行しつつあるグローバルな環境変動に対しサンゴ礁はどのように応答するのであろうか？ サンゴ礁における生物生産（光合成・石灰化）は、海水中の二酸化炭素分圧変動や大気-海洋間の二酸化炭素フラックスを通して、大気中の二酸化炭素分圧と密接な関係がある。

サンゴ礁における主要な炭素循環過程は、有機炭素生

産（光合成-呼吸）と無機炭素生産（石灰化-炭酸塩の溶解）である。光合成と炭酸塩の溶解は二酸化炭素の吸収過程であり、呼吸と石灰化は二酸化炭素の放出過程であることが知られている。サンゴ礁では、これらが相互に複合的に関連しながら同時に進行し、熱帯雨林に匹敵する高い生産性を有することに特徴がある。サンゴ礁における総有機炭素生産量は700~3000gCm⁻²y⁻¹であり、無機炭素生産量は12~480gCm⁻²y⁻¹である（KINSEY, 1985）。しかし、サンゴ礁群集は高い有機炭素生産を有するにもかかわらず、群集呼吸量が高いために過剰の有機生産量（純有機炭素生産量）はほとんどゼロであるか、わずかにゼロより大きい程度であると考えられている（KINSEY, 1985; CROSSLAND *et al.*, 1991）。

大気中の二酸化炭素に対してサンゴ礁が吸収源（シンク）になるか、それとも供給源（ソース）になるかについて議論がされ、通常のサンゴ礁海域では総有機炭素生産量（P_{gross}）/呼吸量（R）比>1および純有機炭素生

*琉球大学理学部海洋自然科学科

Department of Chemistry, Biology and Marine Science, University of the Ryukyus

〒903-0213 沖縄県中頭郡西原町字千原1番地
Senbaru 1, Nishihara, Okinawa, 903-0213 Japan

産量 (P_{net}) / 石灰化量 (G) 比) 0.6 が吸収源としてのポテンシャルを有することが示された (WARE *et al.*, 1992; 加納, 1990; FRANKIGNOULLE *et al.*, 1994; SUZUKI *et al.*, 1995)。

最近, サンゴ礁における生物生産や二酸化炭素分圧と関係した二酸化炭素フラックスの研究がおこなわれている。モーレア島とグレートバリアリーフの Yonge Reef では, 海水中の二酸化炭素分圧の変動に伴って大気-海洋間の CO_2 フラックスが最大で $-900 \sim +2500 \mu mol m^{-2} h^{-1}$ の範囲で変動し, 放出の傾向にあることが観測された (FRANKIGNOULLE *et al.*, 1996; GATTUSO *et al.*, 1996)。KAWAHATA *et al.* (1997) はパラオ堡礁で外洋の 316ppm に対して礁湖内で 414ppm の高い二酸化炭素分圧を測定し, サンゴ礁が二酸化炭素の放出源になることを示唆した。他方, 沖縄本島の南西に位置するルカン礁では短期間の観測が断続的に3年間おこなわれ, 昼間の二酸化炭素の吸収量と夜間の放出量が釣り合う結果が得られた (OHDE, 1995; OHDE and van WOESIK, 1999)。裾礁である石垣島の白保サンゴ礁では高い有機炭素生産量と約 200~500ppm の範囲の二酸化炭素分圧の日周変動を観測し, サンゴ礁が二酸化炭素を吸収することが示された (KAYANNE *et al.*, 1995)。サンゴ礁メソコズム (隔離水界) においては, サンゴ礁群集の生物活動が高く, 日周変動を繰り返しながら二酸化炭素が吸収される結果がえられた (大森, 1993; FUJIMURA *et al.*, 2001)。

サンゴ礁における活発な生物活動は, 昼間の光合成によって二酸化炭素を吸収し, 反対に, 石灰化と夜間における呼吸によって二酸化炭素を放出するが, 時間と場所, 季節によってその差が大きい。従来の研究は, 短期的あるいは, 任意の季節における観測に基づくものが多く, 必ずしもサンゴ礁の全体的な姿を示してはいない。地球規模の環境変動に対するサンゴ礁の応答を研究するためには, 有機炭素・無機炭素生産, 二酸化炭素分圧および二酸化炭素フラックスに関する系統的な観測をおこない, 精度の高い長期的な時系列データを得ることが要求される。

本研究では, サンゴ礁における二酸化炭素変動と大気-海洋間の二酸化炭素フラックスの長期にわたる連続的な時系列データを取得するための基礎的な研究として, (1) 海水中の二酸化炭素分圧の測定法のクロスチェック, (2) サンゴ礁における大気-海洋間の CO_2 フラックスの測定と気体交換係数の検討, および (3) サンゴ礁における海水中の二酸化炭素分圧の時系列連続測定と大気-海洋間の二酸化炭素フラックスの見積り可能性について検討した。

2. 方法

海水中の二酸化炭素分圧の測定は一般に気液平衡器を装備した非分散型赤外線ガス分析計 (NDIR) 法によって精度よく測定されている (INOUE *et al.*, 1987)。しか

し, サンゴ礁で長期間の連続測定を行なうには大がかりな装置を必要とし, 費用やメンテナンスにかかる負担が非常に大きい。他方, 海水の化学分析と化学平衡計算に基づく pH-アルカリ度法は平衡器-NDIR 法に比べると, 大がかりな装置を必要とせず簡便である。本研究では, まず海水中の二酸化炭素分圧の信頼性を確認するために pH-アルカリ度法による測定値を平衡器-NDIR 法によりクロスチェックをおこなった。

次に, 大気-海洋間の CO_2 フラックスの算出に必要な気体交換係数の検討を行なった。一般に大気-海洋間の CO_2 フラックスは大気と海水の二酸化炭素分圧の差および風速の関数として表される気体交換係数を基にして見積られている。これは外洋での観測に適した見積りであり, サンゴ礁のように水深の浅い, 地形の複雑な沿岸域では, 潮流等の影響によって気体交換係数が変化し, 乱流の効果が無視できない (FRANKIGNOULLE *et al.*, 1996)。サンゴ礁における連続的な長期間の CO_2 フラックスを算出するには, より正確な交換係数が必要である。そこで, 大気-海洋間の CO_2 フラックスをサンゴ礁の現場でチャンパー法によって測定し, これまでの風速依存の気体交換係数との関係を検討した。

さらに, 実際のサンゴ礁において pH と溶存酸素濃度の連続測定を行ない, pH-アルカリ度法を基礎とした二酸化炭素分圧と大気-海洋間の CO_2 フラックスを算出することにより, その変動性を確かめた。

2.1 海水の二酸化炭素分圧測定法のクロスチェック

1996年11月に, 琉球大学熱帯生物圏研究センター瀬底実験所において, サンゴを飼育している屋外大型水槽中の二酸化炭素分圧を, 平衡器-NDIR 法および pH-アルカリ度法によって1時間ごとに27時間測定した。

平衡器-NDIR 法では, 気液平衡器にシャワー型平衡器 (気象研究所仕様) を使用した。また, NDIR は LI 6252 (LI-COR 社) を用い, N_2 ガス (0ppm) と 151 ppm, 259ppm, 355ppm の CO_2 標準ガス (空気ベース, 日本酸素 KK) で検量線を作成し, 装置の校正を行った。次に水槽内の海水を気液平衡器へ流し, 海水シャワーと気体を平衡にし, NDIR で二酸化炭素分圧の測定を行なった。一連の測定が終了した後は, 校正に使用した同じ N_2 ガスと CO_2 標準ガスを測定し, ドリフトのチェックを行った。この NDIR は 0.1ppm の分解能の読みとりが可能で, 海水中の二酸化炭素分圧測定の繰り返し精度は ± 1 ppm である。クロスチェックのために二酸化炭素分圧の測定値は, 25°C に規格化した。

pH-アルカリ度法では, 大型水槽内の海水を1時間ごとに採水し pH と全アルカリ度の測定を行なった。pH は採水後数時間以内に NBS スケールの標準溶液 (pH 6.863, pH 4.006 Golden Buffer, TOA) で校正した pH メータ (PHM95 pH/ion meter, Radiometer 社) を用いて 25.0°C で測定した (± 0.002 pH)。全アルカリ度は自動滴定

装置 (ABU93 TIM90, Radiometer社) を用いて滴定を行ない, グランプロット法 (STUMM and MORGAN, 1981) によって終点を決定した ($\pm 0.1\%$)。海水中の二酸化炭素分圧 ($p\text{CO}_{2\text{sea}}$) は (1) 式より算出した。

$$p\text{CO}_{2\text{sea}} = \frac{A_c \cdot a_{\text{H}^+}}{K'_0 K'_1 (2K'_2 + a_{\text{H}^+})} \quad (1)$$

ここで, A_c は炭酸アルカリ度, a_{H^+} は水素イオンの活量, K'_0 は CO_2 の溶解度 (Plummer and Busenberg, 1982), K'_1 , K'_2 は NBS スケールのみかけの炭酸の第 1, 第 2 平衡定数 (MEHRBACH *et al.*, 1973) であり, 水温と塩分の測定値からそれぞれ算出した。

炭酸アルカリ度 (A_c) は (2) 式によって全アルカリ度 (A_T) の測定値からホウ酸アルカリ度 (A_B) の寄与分を差し引くことによって求めた。

$$A_c = A_T - A_B \quad (2)$$

ここで, A_B は次式により求められる (MILLERO, 1979)。

$$A_B = \frac{K'_B \cdot 1.212 \times 10^{-5} \cdot S}{a_{\text{H}^+} + K'_B} \quad (3)$$

但し, K'_B はホウ酸のみかけの平衡定数 (LYMAN, 1957), S は塩分を表す。

本研究においては pH と全アルカリ度の繰り返しの測定誤差は, それぞれ $\pm 0.002\text{pH unit}$ と $\pm 2 \mu\text{mol kg}^{-1}$ であり, この誤差からくる二酸化炭素分圧の誤差は $\pm 2\text{ppm}$ である。

2.2 サンゴ礁における大気-海洋間二酸化炭素フラックスの測定

海洋における二酸化炭素フラックス (FCO_2) は, 大気-海洋間の CO_2 分圧差 ($\Delta p\text{CO}_2$), CO_2 の気体交換係数 (k_t) および CO_2 の溶解度 (K'_0) に依存し, 次のような関係にある (LISS and MERLIVAT, 1986)。

$$\text{FCO}_2 = k_t \cdot K'_0 \cdot \Delta p\text{CO}_2 \quad (4)$$

本研究ではサンゴ礁における CO_2 フラックスをチャンバー法によって現場測定するとともに, 大気および海水中の二酸化炭素分圧を測定し, 現場における気体交換係数を見積り, 文献値と比較した。

チャンバー法による CO_2 フラックスの現場測定は, 1999年12月31日, 2000年1月4日と1月7日に, 瀬底実験所前のサンゴ礁においておこなわれた。サンゴ礁海水の表面状態は風の他に潮流などの影響を受けると考えられる。海面での潮流の影響をみるために満潮停留時 (12月31日), 干潮から満潮へ向かう上げ潮時 (1月4日), 満潮から干潮へ向かう下げ潮時 (1月7日) にそれぞれ15分~30分ごとに約10分間の測定を行なった。

用いた測定システムの概念図を Fig. 1 に示す。このシステムは非分散型赤外線ガス分析計 (NDIR) と箱型のチャンバー, ポンプ, 除湿剤 (過塩素酸マグネシウムと塩化カルシウム), フィルターなどで構成されている。

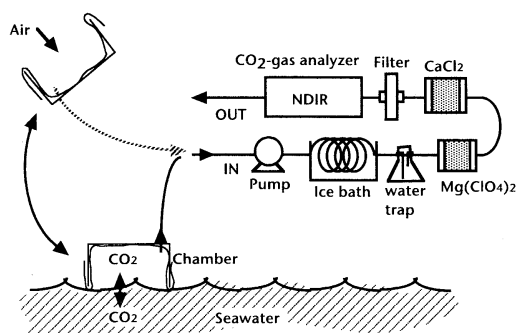


Fig. 1. Measurement system for air-sea CO_2 flux.

本研究では従来のチャンバー法 (FRANKIGNOULLE, 1988; FUJIMURA *et al.*, 1999) を改良し, チャンバーの内圧を常に大気圧に維持するためにフレキシブルな体積バッファを有した構造にし, ポンプで吸引した気体を測定後に排気して, チャンバー内へ戻さない半閉鎖型とした。チャンバーの容積は $33.6 \pm 0.3\text{L}$ であり, 海面に接している断面積は 0.14m^2 ($0.45 \times 0.31\text{m}$) である。

チャンバー法による CO_2 フラックス ($\text{FCO}_{2\text{chamber}}$) は以下のようにして得られる。まず, 時間 t におけるチャンバー内の CO_2 フラックス ($\text{FCO}_{2\text{chamber},t}$) は, 次の式で与えられる。

$$\text{FCO}_{2\text{chamber},t} = - \frac{V}{RTS_A} \cdot \frac{d\Delta p\text{CO}_2}{dt} \quad (5)$$

ここで, $d\Delta p\text{CO}_2/dt$ はチャンバー内空気と海水間の二酸化炭素分圧差の変化速度, V はチャンバーの容積, R は気体定数, T は絶対温度, S_A はチャンバーが海面と接する開口部の断面積を表す。

(4), (5) 式より $k_t K'_0 RTS_A / V = \lambda$ とおくと, 次の式が導かれる。

$$\frac{d\Delta p\text{CO}_2}{dt} = -\lambda \Delta p\text{CO}_2 \quad (6)$$

ここで, λ はチャンバー内の分圧差が変化するときの速度定数である。この式はチャンバー内の二酸化炭素分圧が, 大気-海洋間の分圧差に応じて一次反応的に変化 (吸収または放出) するという SUGIURA *et al.* (1963) の結果と合致している。

次に速度定数 λ を求めるために (6) 式の微分方程式を解くと (7) 式を得る。

$$\ln(\Delta p\text{CO}_{2,t} / \Delta p\text{CO}_{2,0}) = -\lambda t \quad (7)$$

ここで, $\Delta p\text{CO}_{2,0} (= p\text{CO}_{2\text{sea}} - p\text{CO}_{2\text{air},0})$ はチャンバーを海水面に浮かべた瞬間における大気-海洋間の二酸化炭素分圧差, $\Delta p\text{CO}_{2,t} (= p\text{CO}_{2\text{sea}} - p\text{CO}_{2\text{air},t})$ は t 時間後の分圧差である。海水の二酸化炭素分圧とチャンバー内の二酸化炭素分圧の経時変化を測定し, 時間 t に対して $\ln(\Delta p\text{CO}_{2,t} / \Delta p\text{CO}_{2,0})$ をプロットすると, その傾きから速度定数を求めることができる (チャンバー内の CO_2 が

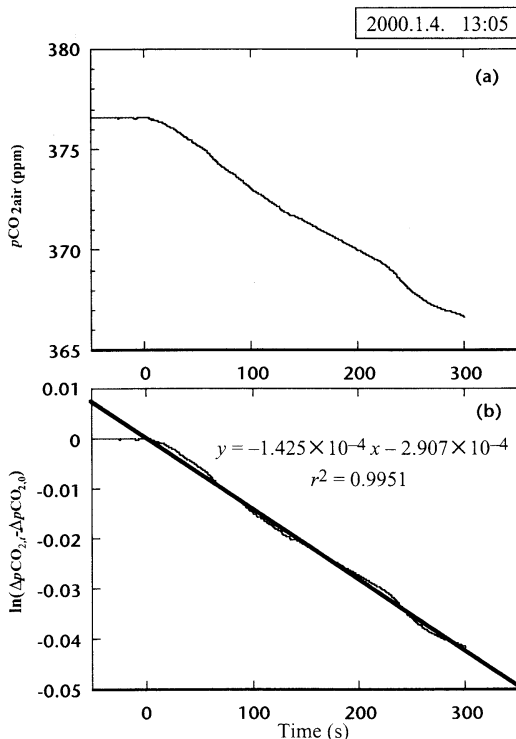


Fig. 2. An example of measurement of CO_2 flux by chamber method.

増加すれば $-\lambda$ は正の値(放出)となり、減少すれば負の値(吸収)となる。

(7)式で得られた λ 値と $t=0$ における分圧差($\Delta p\text{CO}_{2,0}$)を(6)式に代入するとチャンバーをかぶせた瞬間における二酸化炭素分圧差の変化速度($d\Delta p\text{CO}_2/dt$)が得られる。これを(5)式に代入するとチャンバー法による大気-海洋間の CO_2 フラックス値($\text{FCO}_{2\text{chamber}}$)が求められる。

チャンバー内の二酸化炭素分圧の値を1秒ごとに測定した測定例(2000年1月4日13時05分のデータ)をFig. 2(a)に示す。チャンバーを海面に浮かべたときの二酸化炭素分圧(376.6ppm)が5分間に約10ppm減少した。Fig. 2(b)の直線の傾きより、このときの速度定数 λ は $-1.43 \times 10^{-4} \text{ s}^{-1}$ となり、大気-海洋間の CO_2 フラックスは $-1241 \mu\text{mol m}^{-2} \text{ h}^{-1}$ となった。

なお、本研究ではチャンバー内の空気を吸引することによって気体の体積が減少するので、見かけ上(7)式における $p\text{CO}_{2,t}$ の変化が大きくなる。排出した空気をチャンバーへ戻したと仮定して $p\text{CO}_{2\text{air},t}$ について(8)式のように近似的な体積補正を試みた。

$$p\text{CO}_{2\text{air},t} = \frac{\sum_{n=1}^t (p\text{CO}_{2\text{air},n-1} \cdot \Delta V) + p\text{CO}_{2\text{air},t} \cdot V_t}{V} \quad (8)$$

ここで、 $p\text{CO}_{2\text{air},t}$ 、 $p\text{CO}_{2\text{air},n-1}$ はそれぞれ t 、 $n-1$ 秒後のチャンバー内の二酸化炭素分圧の実測値、 V_t は t 秒後のチャンバーの容量、 ΔV は1秒間の吸引容量をそれぞれ示す。

本研究では、すべての測定において ΔV は 5 ml s^{-1} としたので、(8)式の補正にともなう二酸化炭素分圧の補正値は5分後の測定で約0.18ppm(0.05%)であった。したがって、本研究では測定後の気体を排気することによって生じる体積変化の効果は、ほとんど無視できるものであった。

2.3 水質モニターゾンデによるサンゴ礁の連続観測

琉球大学熱帯生物圏研究センター瀬底実験所前のサンゴ礁にて、2000年5月~10月までの6ヶ月間、棧橋の先端に水質モニターゾンデ(YSI-6600)を設置し、海水中のpH、溶存酸素、塩分、水温を15分ごとに取得した。約3週間ごとにゾンデを引き上げ、データの回収とセンサーの校正を行った。また、ゾンデを引き上げる前と後にセンサー周辺の海水を採水し、実験室においてpH、溶存酸素(ウィンクラー法)、全アルカリ度(グランプロット法によるHCl滴定)の精密測定を行った。この高精度のpHと溶存酸素の分析値を用いて、ゾンデによるpHと溶存酸素の現場における観測値を校正した。

海水中の二酸化炭素分圧は(1)式より算出できる。但し、二酸化炭素分圧の算出に必要な炭酸アルカリ度の値は現場におけるアルカリ度の連続測定が難しいので、次に示す方法で求めた。

まず、サンゴ礁における有機炭素生産量(OP)と無機炭素生産量(IP)は、全炭酸の変化量(ΔC_T)と次の関係にある

$$-\Delta C_T = OP + IP + \text{FCO}_2 \quad (9)$$

ここで、実際のサンゴ礁では生物生産量が大きいため FCO_2 は、OPとIPに比べて小さく、全炭酸の変化量にほとんど影響しないため無視できる(SMITH 1973)。

有機炭素生産量(OP)は、溶存酸素の変化量(ΔDO)から(10)式で与えられる。

$$OP = Q(\Delta \text{DO} + \text{FO}_2) \quad (10)$$

ここで、 FO_2 は大気-海洋間の酸素フラックスを示し、KANWISHER(1963)の風速依存式を用いて風速と酸素飽和度から算出される。OPに対する FO_2 の割合は、溶存酸素の変化量が小さい明け方と夕方の時間帯に約20%に達する。しかし、それ以外の大部分の時間帯は0.5%以下である。Qは光合成商または呼吸商を表す。多くのサンゴ礁群集で光合成商と呼吸商はほぼ1.0であることが報告されており(GATTUSO *et al.*, 1999)、(10)式においてもQは1.0とした。

無機炭素生産量(IP)は炭酸アルカリ度(A_c)の変化量から算出される。サンゴ礁における無機炭素生産量

は全アルカリ度 (A_T) を基礎にしても求められる (SMITH and KEY, 1975) が、通常の海水条件ではどちらも同じ値が得られ、本質的な違いはない。

$$IP = -\Delta A_c / 2 \quad (11)$$

また、全炭酸は、化学平衡にあるとき炭酸アルカリ度と次の関係にある。

$$C_T = \alpha \cdot A_c \quad (12)$$

ここで、 α は平衡定数と水素イオンの活量を含む係数であり次の式で表す。

$$\alpha = (1 + K'_2/a_{H^+} + a_{H^+}/K'_1)(1 + 2K'_2/a_{H^+})^{-1} \quad (13)$$

(9) 式に (10), (11), (12), (13) 式を代入して (14) 式を得る。結局、ある時間における炭酸アルカリ度 ($A_{c,t}$) は、ゾンデ投入直後の海水の全アルカリ度 ($A_{T,i}$) と、15分ごとの pH と溶存酸素の測定値を与えることによって算出される。

$$A_{c,t} = \frac{(\alpha_t - 0.5)(A_{T,i} - A_{B,i}) - \Delta DO - FO_2}{\alpha_t - 0.5} \quad (14)$$

ここで、添字の i と t はそれぞれ初期の値と t 時間後の値を表す。

(14) 式によって得られた炭酸アルカリ度の値を (1) 式に代入して15分ごとの連続的な海水中の二酸化炭素分圧を算出した。ゾンデによる測定時の繰り返し誤差は pH: ± 0.01 , DO: $\pm 0.07 \text{ mg O}_2 \text{ l}^{-1}$, 水温: $\pm 0.02^\circ \text{C}$, 塩分: $\pm 0.15\text{‰}$ であった。

15分ごとの連続的な大気-海洋間 CO_2 フラックスの計算値は15分ごとの海水中の二酸化炭素分圧の値と大気中の二酸化炭素分圧の値 (366 ppm), LISS and MERLIVAT (1986) の風速依存の気体交換係数 (k_t), そして WEISS (1974) の CO_2 の溶解度 (K') を用いて (4) 式より算出した。

2.4 風速の観測

大気-海洋間の CO_2 フラックスの計算に必要な風速のデータは風速計 (Met-One model 038) を棧橋に設置しデータロガー (LI-COR LI-1000) で収集した。

3 結果と考察

3.1 海水中の二酸化炭素分圧測定法のクロスチェック

NDIR-平衡器法による測定と pH-全アルカリ度の平衡計算を用いた測定の結果を Fig. 3 に示す。両者はほぼ直線的な関係にある。350 ppm 付近ではおよそ 3 ppm の違いであり、250 ppm 付近では pH-全アルカリ度法で求めた分圧が 16 ppm 程低い値を示した。これは、海水温度や pH の測定誤差、使用した平衡定数の違い、シャワー型平衡器の測定条件などにより、両者の間に系統的に生じた差であると考えられる。

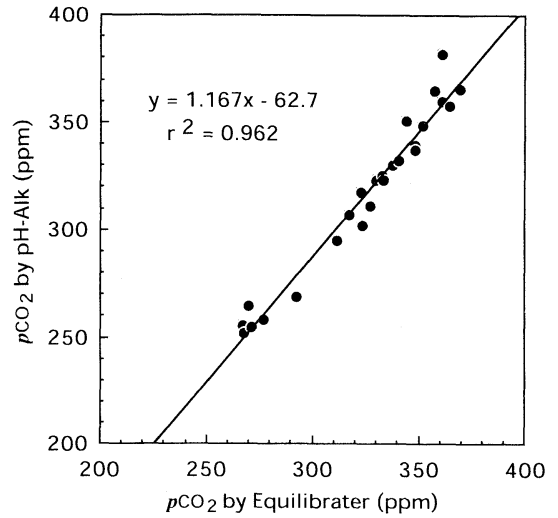


Fig. 3. $p\text{CO}_{2\text{sea}}$ values measured by pH-alkalinity method versus NDIR method.

MILLERO *et al.* (1993) は二酸化炭素分圧が 336~364 ppm の太平洋表層水のクロスチェックを行ない、pH-全アルカリ度と MEHRBACH *et al.* (1973) の平衡定数を組み合わせた時の二酸化炭素分圧は NDIR-平衡器法の実測値と $\pm 5 \text{ ppm}$ の範囲で一致することを示した。したがって、本研究における 350 ppm 付近での pH-全アルカリ度法と NDIR-平衡器法の結果はよく一致しているものと考えられる。ただし Fig. 3 が示すように、pH-全アルカリ度法は二酸化炭素分圧が 350 ppm よりも低い時に過小評価となり、大きい時に過大評価となるため、今後は 2 つの方法の系統誤差を取り除く必要がある。

3.2 大気-海洋間二酸化炭素フラックスの測定と気体交換係数の検討

1999年12月31日, 2000年1月4日, 1月7日の瀬底島サンゴ礁における大気-海洋間の CO_2 フラックスと大気中の二酸化炭素分圧, pH-全アルカリ度による海水の二酸化炭素分圧の結果を Table 1 に示す。

チャンバー法により得られた大気-海洋間の CO_2 フラックスは $-2 \mu \text{ mol m}^{-2} \text{ h}^{-1}$ から、最大で $-1241 \mu \text{ mol m}^{-2} \text{ h}^{-1}$ までの負の値であり、大気から海水へ CO_2 が吸収されていることを示した。このことは大気中の二酸化炭素分圧が 373.8~384.8 ppm であるのに対して、海水の二酸化炭素分圧は 119.1~249.9 ppm と低いことと合致している。

測定した大気-海洋間の CO_2 フラックスと大気中の二酸化炭素分圧差から (4) 式により各測定における CO_2 の気体交換係数を求めた (Table 1)。この気体交換係数を風速に対してプロットし、これまで一般に使われている風速依存性の文献値と比較した (Fig. 4)。風速依存性は海水表面での乱流や気泡の巻き込み、薄層

Table 1 Data for air-sea CO₂ flux and gas exchange coefficient

Date	Time	$-\lambda$ (S ⁻¹)	$FCO_{2\text{chamber}}$ ($\mu\text{molm}^{-2}\text{h}^{-1}$)	$pCO_{2\text{sea}}$ (ppmv)	$pCO_{2\text{air}}$ (ppmv)	K'_0 ($\text{mol kg}^{-1}\text{atm}^{-1}$)	Wind speed (ms^{-1})	Gas exchange coefficient(k_t) (ms^{-1})
1999.12.31	14 : 05	-5.13×10^{-5}	-413	147.7	375.4	0.02999	6.8	1.68×10^{-5}
	14 : 20	-8.75×10^{-5}	-693	152.0	376.0	0.02998	6.8	2.87×10^{-5}
	14 : 35	-7.26×10^{-5}	-574	152.2	374.8	0.02997	6.8	2.39×10^{-5}
	14 : 50	-1.10×10^{-4}	-869	152.3	374.6	0.02995	6.8	3.62×10^{-5}
	15 : 05	-1.14×10^{-4}	-917	148.1	375.5	0.02991	7.0	3.75×10^{-5}
	15 : 20	-1.18×10^{-4}	-912	156.5	374.1	0.02993	7.0	3.89×10^{-5}
	15 : 35	-1.57×10^{-4}	-1217	157.1	374.3	0.02994	7.0	5.20×10^{-5}
	15 : 50	-1.04×10^{-4}	-804	157.2	373.8	0.02994	7.0	3.44×10^{-5}
	2000.1.4	11 : 35	-9.34×10^{-5}	-740	156.3	377.3	0.03086	4.3
11 : 50		-7.80×10^{-5}	-606	160.3	377.0	0.03075	4.3	2.52×10^{-5}
12 : 05		-9.74×10^{-5}	-752	160.9	376.6	0.03066	4.5	3.16×10^{-5}
12 : 20		-9.04×10^{-5}	-727	152.2	376.8	0.03059	3.9	2.94×10^{-5}
12 : 35		-9.55×10^{-5}	-781	147.7	376.6	0.03054	4.0	3.11×10^{-5}
12 : 50		-1.36×10^{-4}	-1147	140.2	376.6	0.03048	3.8	4.42×10^{-5}
13 : 05		-1.43×10^{-4}	-1241	132.6	376.5	0.03041	3.5	4.65×10^{-5}
13 : 20		-1.10×10^{-4}	-994	123.0	376.2	0.03035	3.7	3.59×10^{-5}
13 : 35		-1.09×10^{-4}	-1001	119.1	376.0	0.03025	4.3	3.58×10^{-5}
2000.1.7		7 : 30	-4.30×10^{-6}	-25	224.7	384.8	0.03099	2.6
	8 : 00	-5.91×10^{-6}	-30	244.1	385.0	0.03102	3.4	1.92×10^{-6}
	8 : 20	-4.67×10^{-6}	-23	249.9	384.2	0.03110	3.0	1.51×10^{-6}
	8 : 36	-2.55×10^{-6}	-12	255.3	383.8	0.03118	2.6	8.20×10^{-7}
	8 : 50	-3.97×10^{-6}	-18	254.4	383.4	0.03126	3.1	1.27×10^{-6}
	9 : 05	-2.80×10^{-6}	-14	248.0	383.8	0.03121	3.2	9.02×10^{-7}
	9 : 20	-0.33×10^{-6}	-2	247.4	383.7	0.03123	3.0	1.07×10^{-7}
	9 : 35	-6.39×10^{-6}	-32	246.5	383.3	0.03126	3.0	2.05×10^{-6}
	9 : 52	-6.29×10^{-6}	-31	244.7	382.8	0.03132	3.0	2.02×10^{-6}
	10 : 05	-1.11×10^{-5}	-58	238.5	383.0	0.03134	3.5	3.56×10^{-6}
	10 : 21	-2.10×10^{-5}	-110	236.8	382.0	0.03134	3.8	6.73×10^{-6}
	10 : 35	-3.55×10^{-5}	-201	224.9	382.0	0.03131	4.1	1.14×10^{-5}
	11 : 00	-4.30×10^{-5}	-253	218.2	381.4	0.03125	4.6	1.38×10^{-5}

(Stagnant Film) の厚み変化などによる気体交換係数への影響を、一義的に風速の関数として表わしている。風速依存式は文献によって異なっており、湖と風洞実験での結果を基にして作られた Liss and MERLIVAT (1986) の式が海洋における CO₂ フラックスの見積りにもっともよく用いられている。UPSTILL-GODDARD *et al.* (1990) の SF₆ を用いた湖での測定結果から作られた式は風速の大きな時に比較的低い値を示し、KOMORI and SHIMADA (1995) の乱流渦の影響を反映した風洞実験によって得られた式は風速の小さいときに比較的高い値を示している。また、最近では WANNINKHOF (1992) の SF₆ の実験結果から得られた風速依存式もよく用いられている。

今回の測定値は、下げ潮時 (1月7日) の気体交換係数は Liss and MERLIVAT (1986) のこれまでの風速依存則と比較的よい一致を示した (Fig.4)。下げ潮時の結果は打ち寄せる波の影響が少なく、風による海面の攪乱のみ

が気体交換に影響していることが考えられる。満潮時 (12月31日) の気体交換係数は $1.7 \sim 5.2 \times 10^{-5} \text{ms}^{-1}$ の幅広い値であった。これらの値は、Liss and MERLIVAT (1986) の風速依存式に比較的近い値を示した。上げ潮 (1月4日) の時間帯では風速が $3 \sim 5 \text{ms}^{-1}$ と下げ潮時の風速と同程度であるのに対して $2.5 \sim 4.6 \times 10^{-5} \text{ms}^{-1}$ の高い気体交換係数を示した。上げ潮の時間帯は、外洋からサンゴ礁に波が打ち寄せているために、乱流の影響を受けて通常の風速依存の気体交換係数よりも高い値を示したと考えられる。FRANKIGNOULLE *et al.* (1996) のムルロワ環礁での CO₂ フラックスの測定でも、風速が 3ms^{-1} 以下のときに $1 \sim 7 \times 10^{-5} \text{ms}^{-1}$ の高い気体交換係数が観測されている。

したがって、サンゴ礁の気体交換係数は基本的には下げ潮時 (1月7日) のデータが示すように一般に用いられている Liss and MERLIVAT (1986) の風速依存式に従っている。ただし、潮の干満による影響で一時的にやや大

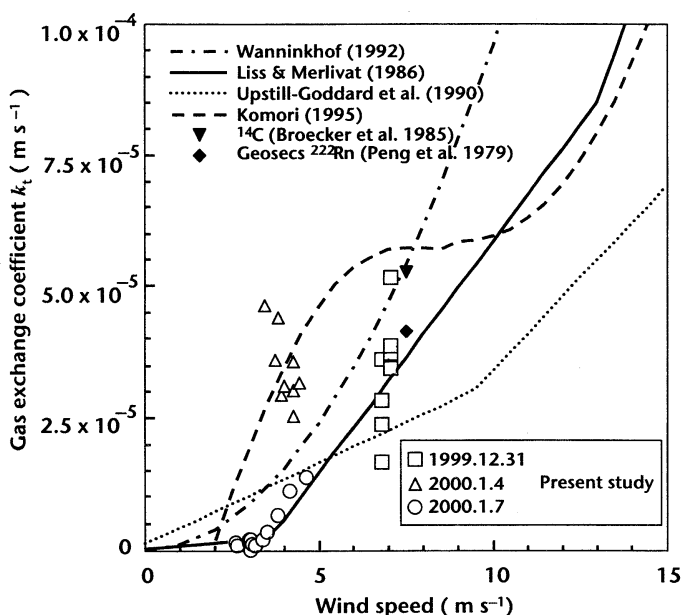


Fig. 4. Gas exchange coefficient versus wind speed.

きなフラックスが得られたことから、サンゴ礁のような沿岸域で風速依存の式を用いることは、二酸化炭素フラックスの見積りを過小評価してしまう可能性がある。サンゴ礁のような沿岸域では風速に依存しない乱流の影響をいかに捉えるかが今後の課題となる。

3.3 瀬底島サンゴ礁における二酸化炭素分圧の連続観測

瀬底島サンゴ礁における二酸化炭素分圧の15分ごとの連続測定の結果を時系列図としてFig. 5 (a) に示す。縦軸は一日の時刻を示し、横軸は暦日を示す。青系色は大気中の二酸化炭素分圧より低い366ppm以下の部分を示し、200ppm以下の値は濃い紫色で示す。緑 (366ppm) から黄 (460ppm) まで、オレンジ (560ppm) まで、赤 (660~800ppm) 系色の部分は大気中の値より高い部分を示す。

二酸化炭素の時系列図からサンゴ礁における二酸化炭素分圧変動の詳細な情報をみることができる。まず、海水中の二酸化炭素分圧は昼間に減少し、夜間に増加する周期的な日変動を繰り返す。5月から6月初旬までは、正午から午後6時までの間に200~300ppmと大気中の二酸化炭素分圧より低い値を示し、0時から午前6時までの時間帯に大気より高い400~500ppmに達した。5月下旬から6月上旬にかけて海水中の二酸化炭素分圧は全体的に大気中の値より低いことが多い。時系列図において、二酸化炭素分圧が夜間には極大値を示し、昼間には極小値を示す。しかし、極大値、極小値を示す時間帯が一日ごとに遅れることが時系列図からわかる。これは潮位に関係

し、干潮時に水深が浅くなると共に生物活動の効果が顕著に水質に反映される結果である。

海水中の二酸化炭素分圧が5月~6月初旬に低く、6月中旬~9月に高い傾向にあるのは海水温の上昇が主な要因であると考えられる。6月初旬から下旬にかけて、平均水温は24℃から29℃へと約5℃上昇した。海水中の二酸化炭素分圧は海水温度に依存し水温が1℃上昇すると14.8ppm上昇する (GORDON and JONES, 1973) ので、一ヶ月の間に二酸化炭素分圧が水温の影響で70ppmほど上昇したことになる。6月中旬から9月は全体的に二酸化炭素分圧が高い傾向にあり、夜間に600ppm~700ppmに達する期間がある。

特異的なこととして8月5~9日あるいは9月9~17日の台風通過時には昼間も夜間も海水中の二酸化炭素分圧は一時的に減少し、一日中はほぼ定常的な値を示した。これは台風によって海水が攪乱され、大気との濃度差が小さくなっていったと考えられる。

また、7月2日から4日には昼間であるにもかかわらず午後12時から4時頃にかけて二酸化炭素分圧の高い時間帯がある。これは大潮の最干潮時に相当し、水深が浅い (0.5m) ために海水の化学成分が生物活動の影響を受けやすい状態であった。さらにこの期間は天候が悪く、7月3日のこの時間帯 (12:00から13:00) の光量は100~200 $\mu\text{mol m}^{-2} \text{s}^{-1}$ の非常に低い状態であった。この時の溶解酸素の値は大きく減少しており、光合成量よりも呼吸量が卓越していた。このような状況が重なり、昼間の時間帯としては異常な二酸化炭素分圧の高い値を示した (7/3 14:00 796ppm)。このように二酸化炭素分圧の変

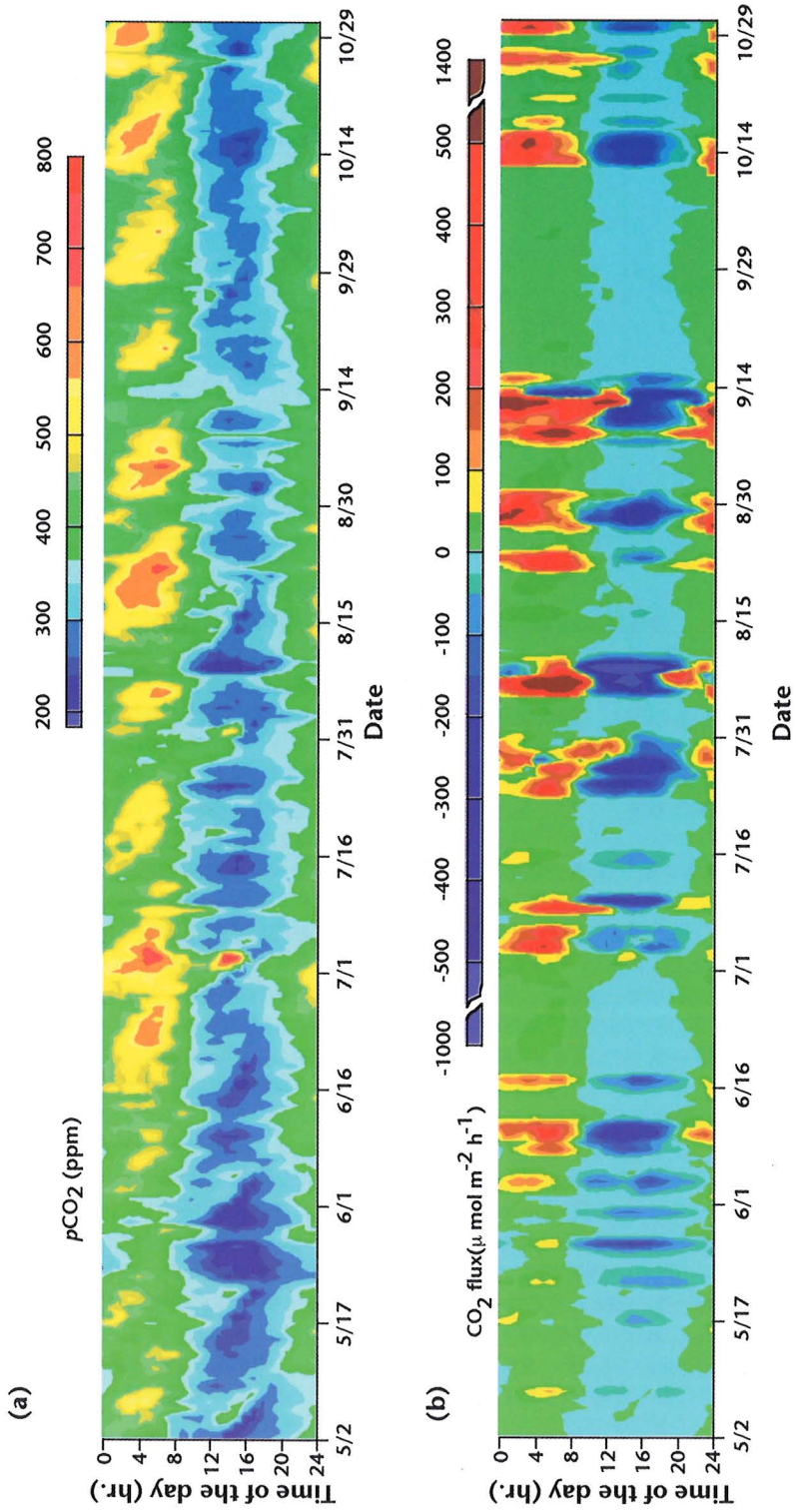


Fig. 5. Time series data of $p\text{CO}_{2,\text{sea}}$ (a) and air-sea CO_2 flux (b) from May to October, 2000.

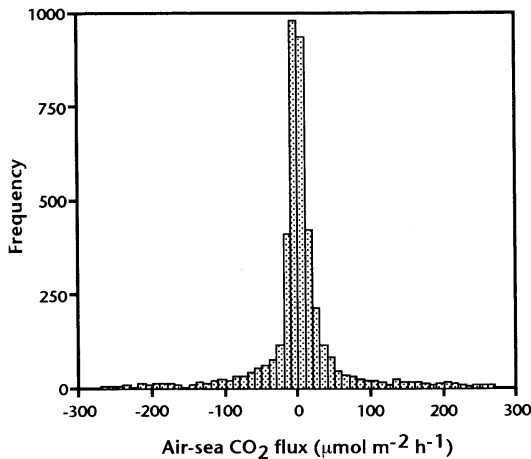


Fig. 6. Frequency histogram of air-sea CO₂ flux values.

動は周期的な潮の干満による影響や天候による生物活動の影響を常に受けている。

3.4 大気-海洋間の二酸化炭素フラックス

サンゴ礁の気体交換係数が基本的には Liss and MERLIVAT (1986) の風速依存式に従っている結果が得られたことから、瀬底島サンゴ礁における二酸化炭素分圧の連続測定値と風速の値を用いて (4) 式により長期間の大気-海洋間の二酸化炭素フラックスを算出した。大気-海洋間の二酸化炭素フラックスの結果を時系列図に示す (Fig. 5(b))。大気から海水へ二酸化炭素が吸収されている吸収帯を青 ($-300 \sim 0 \mu\text{mol m}^{-2} \text{h}^{-1}$) 系色と濃い紫 ($-300 \mu\text{mol m}^{-2} \text{h}^{-1}$ 以下) で示す。海水から大気へ二酸化炭素が放出されている放出帯を緑 ($0 \sim +50 \mu\text{mol m}^{-2} \text{h}^{-1}$)、黄 ($+50 \sim +100 \mu\text{mol m}^{-2} \text{h}^{-1}$)、オレンジ ($+100 \sim +200 \mu\text{mol m}^{-2} \text{h}^{-1}$)、赤 ($+200 \sim +300 \mu\text{mol m}^{-2} \text{h}^{-1}$)、濃い赤 ($+300 \mu\text{mol m}^{-2} \text{h}^{-1}$ 以上) で示す。

サンゴ礁で観測された風速は 4 ms^{-1} 以下であることが多く、この風速以下では、大気-海洋間の CO₂ フラックスは薄い水色と緑色で示される $-25 \sim +25 \mu\text{mol m}^{-2} \text{h}^{-1}$ の範囲にある。通常の穏やかな日の CO₂ フラックスはこの範囲内での変動に対応して日変化を繰り返している。風速が 5 ms^{-1} 以上になると CO₂ フラックスは急激に大きくなり、濃い紫色と濃い赤色の部分で表される強い吸収と放出の領域が出現する。特に8月上旬と9月中旬の大きなフラックスは台風通過時に相当し、8月5~9日の台風ではフラックスが $-905 \sim +1370 \mu\text{mol m}^{-2} \text{h}^{-1}$ であり、9月9~17日の台風では $-483 \sim +1040 \mu\text{mol m}^{-2} \text{h}^{-1}$ であった。9月17日の台風通過後の穏やかな日 (9/18~10/10まで) のフラックスは $-16 \sim +39 \mu\text{mol m}^{-2} \text{h}^{-1}$ であることから、台風によるフラックスは通常時のおよそ30

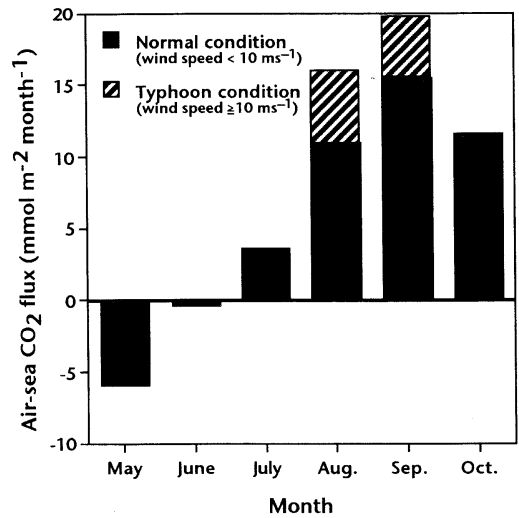


Fig. 7. Monthly budget of air-sea CO₂ flux.

倍である。このような台風による非常に大きな CO₂ フラックスは BATES *et al.* (1998) によっても報告されており、サルガッソ海では夏季の CO₂ の放出量の 55% が台風によるものであるとしている。

5月から10月までの15分ごとの大気-海洋間の CO₂ フラックスを積算して1時間ごとの値とし、約4400個のフラックスの頻度分布をとった (Fig. 6)。通常の瀬底島サンゴ礁における CO₂ フラックスの大部分は $-100 \sim +100 \mu\text{mol m}^{-2} \text{h}^{-1}$ の範囲にあり、特に $-30 \sim +30 \mu\text{mol m}^{-2} \text{h}^{-1}$ の範囲に多い。

季節変動では、大気-海洋間の CO₂ フラックスは海水の二酸化炭素分圧の変動と対応して青色の吸収帯が夏季に向かって狭くなり、放出の時間帯が増加している。そして、9月以降は再び吸収の時間帯が増加している。

大気-海洋間の二酸化炭素フラックスを月ごとに積算し、フラックスの収支を算出した (Fig. 7)。5月から6月の積算の CO₂ フラックスは海水への吸収ないしは、ほぼ釣り合っている。7月~10月までの夏期には海水から大気へ二酸化炭素が放出されていることが分かる。8、9月の放出量が高いのは主に台風時 (風速 10 ms^{-1} 以上) のフラックスの寄与が大きいことを示している。月毎の CO₂ フラックスのピークは9月であり、10月から減少している。1999年12月~2000年1月の冬の短期 (2週間) の測定では、吸収の結果が得られているので、瀬底島サンゴ礁では二酸化炭素を冬季は吸収し、夏季は放出するという季節変動が予想される。

今後、サンゴ礁における代謝活動と二酸化炭素分圧変動の時系列観測を続けることによって、増加しつつある大気中の二酸化炭素分圧変動や地球温暖化に対するサンゴ礁の応答について詳細な情報を得られるものと思われる。

4. おわりに

本研究により、サンゴ礁における二酸化炭素分圧と大気-海洋間の二酸化炭素フラックスに関して以下のことが明らかになった。

- 1) サンゴ礁の生物生産と二酸化炭素分圧を測定できる pH-アルカリ度法は、高精度の標準的な赤外線ガス分析法 (NDIR) の二酸化炭素測定値と比較的よい一致を示した (350ppm付近において ± 3 ppm以内)。
- 2) 大気-海洋間の二酸化炭素フラックスの実測をおこない、サンゴ礁における二酸化炭素の気体交換係数を求めた。今回得られた気体交換係数と風速との関係は、一般的な外洋や湖を基礎にした風速依存式の範囲にあることがわかった。但し、サンゴ礁において潮流の影響を受けやすい上げ潮時にはやや大きめの気体交換係数がえられた。
- 3) pH-アルカリ度法に基づいて、サンゴ礁の二酸化炭素分圧と大気-海洋間の二酸化炭素フラックスを15分ごとに6ヶ月間継続して観測した。その結果、二酸化炭素分圧は、日射量、潮位および水温などの影響を受けて、顕著な日変動、月変動および季節変動を示した。
- 4) 大気-海洋間の二酸化炭素フラックスは、二酸化炭素分圧および風速や水温などの気象・海象の影響を強く反映した。月毎の二酸化炭素フラックス収支は、初夏の5、6月は、大気から海への吸収を示し、反対に、夏-初秋の7、8、9、10月には、大気への放出となった。夏季の大気-海洋間のフラックスは、とくに台風の影響が顕著であった。
- 5) 今後、サンゴ礁における代謝活動と二酸化炭素分圧変動の時系列観測を続けることによって、増加しつつある大気中の二酸化炭素分圧変動や地球温暖化に対するサンゴ礁の応答について詳細な情報を得られるものと思われる。

謝辞

瀬底島サンゴ礁における測定では、琉球大学熱帯生物圏研究センター瀬底実験所の中野義勝技官はじめ実験所の方々に大変お世話になりました。ここに感謝の意をこめ、厚くお礼を申し上げます。また、本研究の一部は文部省科学研究費補助金特定領域研究 (課題番号11131213および10144103) によっておこなわれました。

文 献

- BATES, N. R., A. H. KNAP and A. F. MICHAELS (1998) : Contribution of hurricanes to local and global estimates of air-sea exchange of CO_2 . *Nature*, **395**, 58-61.
- CROSSLAND, C. J., B. G. HATCHER and S.V. SMITH (1991): Role of coral reefs in global ocean production. *Coral Reefs*, **10**, 55-64.
- FRANKIGNOULLE, M. (1988) : Field measurements of air-sea CO_2 exchange. *Limnol. Oceanogr.*, **33** (3), 313-322.
- FRANKIGNOULLE, M., C. CANON and J.-P. GATTUSO (1994) : Marine calcification as a source of carbon dioxide: Positive feedback of increasing atmospheric CO_2 . *Limnol. Oceanogr.*, **39** (2), 458-462.
- FRANKIGNOULLE, M., J.-P. GATTUSO, R. BIONDO, I. BOURGE, G. COPIN-MONTÉGUT and M. PICHON (1996) : Carbon fluxes in coral reefs. II. Eulerian study of inorganic carbon dynamics and measurement of air-sea CO_2 exchanges. *Mar. Ecol. Prog. Ser.*, **145**, 123-132.
- FUJIMURA, H., T. OOMORI, T. MAEHIRA and K. MIYAHIRA (1999) : Air-sea CO_2 flux and the organic and inorganic carbon production in coral reef. *In Proc. 2nd Inter. Symp. CO_2 in the Oceans*. Y. Nojiri (ed.), CGER/NIES, Tsukuba, Japan, p. 413-419.
- FUJIMURA, H., T. OOMORI, T. MAEHIRA and K. MIYAHIRA (2001) : Change of coral carbon metabolism influenced by coral bleaching. *Galaxea, JCRS*, **3**, 41-50.
- GATTUSO, J.-P., M. PICHON, B. DELESALLE, C. CANON and M. FRANKIGNOULLE (1996) : Carbon fluxes in coral reefs. I. Lagrangian measurement of community metabolism and resulting air-sea CO_2 disequilibrium. *Mar. Ecol. Progr. Ser.*, **145**, 109-121.
- GATTUSO, J.-P., M. FRANKIGNOULLE and S. V. SMITH (1999) : Measurement of community metabolism and significance in coral reef CO_2 source-sink debate. *Proc. Natl. Acad. Sci. USA*, **96**, 13017-13022.
- GORDON, L. I. and L. B. JONES (1973) : The effect of temperature on carbon dioxide partial pressures in seawater. *Mar. Chem.*, **1**, 317-322.
- INOUE, H., Y. SUGIMURA and K. FUSHIMI (1987) : $p\text{CO}_2$ and ^{13}C in the air and surface sea water in the western North Pacific. *Tellus*, **39B**, 228-242.
- 加納 裕二 (1990) : サンゴの増殖と大気中の二酸化炭素分圧の関係. *海と空*, **65** 特別号, 259-265.
- KANWISHER, J. (1963) : On the exchange of gases between the atmosphere and the sea. *Deep Sea Res.*, **10**, 195-207.
- KAWAHATA, K., A. SUZUKI and K. GOTO (1997) : Coral reef ecosystems as a source of atmospheric CO_2 : evidence from measurements of surface waters. *Coral reefs*, **16**, 261-266.
- KAYANNE, H., A. SUZUKI and H. Saito (1995) : Diurnal changes in the partial pressure of carbon dioxide in coral reef water. *Science*, **269**, 214-216.
- KINSEY, D. W. (1985) : Metabolism, calcification and production: I systems level studies. *Proc. Fifth*

- Inter. Coral Reef Congr., Tahiti, **4**, 503-542.
- KOMORI, S. and T. SHIMADA (1995) : Gas transfer across a wind-driven air-water interface and effects of sea water on CO₂ transfer. *In* Air - Water Sea Transfer. JAHNE, B. and E. C. MONAHAN (eds.), Hanau, Germany, p. 553-569
- LISS, P. S. and L. MERLIVAT (1986) : Air-sea gas exchange rates: introduction and synthesis. *In* The role of air-sea exchange in geochemical cycling. BUAT-MENARD, P. (ed.), Dordrecht, Holland, p.113-127
- LYMAN, J. (1957) : Buffer mechanism of sea water. Ph. D. Thesis, University of California, Los Angeles, 196 pp.
- MILLERO, F. J. (1979) : The thermodynamics of the carbonate system in seawater. *Geochim. Cosmochim. Acta*, **43**, 1651-1661.
- MILLERO, F. J., R. H. BYRNE, R. WANNINKHOF, R. FEELY, T. CLAYTON, P. MURPHY and M. F. LAMB (1993) : The internal consistency of CO₂ measurements in the equatorial Pacific. *Marine Chemistry*, **44**, 269-280.
- MEHRBACH, C., C. H. CULBERSON, J. E. HAWLEY and R. M. PYTKOWICZ (1973) : Measurement of the apparent dissociation constants of carbonic acid in seawater at atmospheric pressure. *Limnol. Oceanogr.*, **18**, 897-907.
- OHDE, S. (1995) : Calcium carbonate production and carbon dioxide flux on coral reef, Okinawa. *In* Biochemical Processes and Ocean Flux in Western Pacific. SAKAI, H., NOZAKI, Y. (eds.), TERAPUB, Tokyo, p. 93-98
- OHDE, S. and R. van WOESIK (1999) : Carbon dioxide flux and metabolic processes of a coral reef, OKINAWA. *Bull. Mar. Sci.*, **65**, 559-576.
- 大森 保 (1993) : サンゴによる石灰化と二酸化炭素の固定 -サンゴ飼育水槽実験-. *地質ニュース*, **465**, 26-31.
- PLUMMER, L. M. and E. BUSENBERG (1982) : The solubilities of calcite, aragonite and vaterite in CO₂-H₂O solutions between 0 and 90°C and an evaluation of the aqueous model for the system CaCO₃-CO₂-H₂O. *Geochim. Cosmochim. Acta*, **46**, 1011-1040.
- SMITH, S. V. (1973) : Carbon dioxide dynamics: a record of organic carbon production, respiration, and calcification in the Eniwetok reef flat community. *Limnol. Oceanogr.*, **18** (1), 106-120.
- SMITH, S. V. and G. S. KEY (1975) : Carbon dioxide and metabolism in marine environments. *Limnol. Oceanogr.*, **20**, 493-495.
- STUMM, W. and J. J. MORGAN (1981) : *Aquatic Chemistry* 2nd Ed. Wiley-Interscience, New York, 226-229 pp.
- SUGIURA, Y., E. R. IBERT and D. W. HOOD (1963) : Mass transfer of carbon dioxide across sea surfaces. *J. Mar. Res.*, **21**, 11-24.
- SUZUKI, A., T. NAKAMORI and H. KAYANNE (1995) : The mechanism of production enhancement in coral reef carbonate system: model and empirical results. *Sed. Geol.*, **99**, 259-280.
- UPSTILL-GODDARD, R. C., A. J. WATSON, P. S. LISS and M. I. LIDDICOAT (1990) : Gas transfer velocities in lakes measured with SF₆. *Tellus*, **42B**, 364-377.
- WANNINKHOF, R. (1992) : Relationship between wind speed and gas exchange over the ocean. *J. Geophys. Res.*, **97**, 7373-7382.
- WARE, J. R., S. V. SMITH and M. L. REAKA-KUDLA (1992) : Coral Reefs: Sources or sinks of atmospheric CO₂? *Coral Reefs*, **11** (3), 127-130.
- WEISS, R. (1974) : Carbon dioxide in water and seawater: the solubility of a non-ideal gas. *Mar. Chem.*, **2**, 203-215.

Received June 22, 2001

Accepted August 29, 2002

Jellyfish Population Explosions : Revisiting a Hypothesis of Possible Causes

T.R. PARSONS* and C.M. LALLI*

Abstract : A hypothesis is discussed that relates the production of large blooms of jellyfish (medusae and/or ctenophores) to specific food chains in the sea that are based on the production of nanophytoplankton. Evidence is given from the fossil record and from the contemporary ocean to show how this type of low-energy food chain contrasts with a high-energy food chain, which is based on diatom ecology and supports the large raptorial feeders, fish and whales. Recent anthropogenic effects on the ocean, including pollution and overfishing, are discussed in terms of the proposed hypothesis. Natural events that can lead to an abundance of jellyfish are also considered.

Key words : *jellyfish blooms, food chain energetics, eutrophication, overfishing, pollution, climate change, evolution of marine ecosystems*

1. Introduction

In recent years, there has been a spate of publications noting unprecedented population explosions of “jellyfish” (medusae and/or ctenophores) which have been increasing in frequency and expanding in geographic coverage (e.g. PURCELL *et al.*, 2001a). These high densities result from increases in numbers through reproduction, and are not aggregations caused by physical advection or behavioural activities as described by GRAHAM *et al.* (2001). Table 1 gives some examples of such blooms, but the subject has recently been reviewed in more detail by MILLS (2001). Some of these blooms have occurred in endemic species, others result after invasions by species brought into new areas in ballast water. A number of causes have been advanced, including eutrophication, overfishing, pollution, global warming, and increases in artificial substrates which expand the potential attachment sites for polyp stages in the life cycles of some species. We believe that a commonality underlying these enhancements of jellyfish populations may be indica-

tive of major fundamental changes in marine ecosystems that are pushing the world's oceans into a less desirable state with respect to marine resources.

We recognize that the many species of jellyfish have different diets and feeding methods, and that populations of those larger species that feed on large-sized food (macrozooplankton) in the sea can be enhanced simply by the removal of top-level fish that are direct competitors for food. However, many ctenophores (e.g. GREVE, 1970; HARBISON *et al.*, 1978) and medusae including the young of large species (e.g. FRASER, 1969; MILLS, 1995; PURCELL and ARAI, 2001; PURCELL and STURDEVANT, 2001) are known to feed on smaller-sized particles (mesozooplankton) such as small copepods and other small crustaceans, meroplanktonic larvae, fish eggs and fish larvae and even microzooplankton such as ciliates (STOECKER *et al.*, 1987), and their numbers are not directly controlled by fish removal except perhaps by removal of fish such as anchovies that are also low in food chains. Although turtles and some fish may eat jellyfish (e.g. PURCELL and ARAI, 2001), top-down control of population numbers does not seem to be prevalent for most species except for those that are eaten by other jellies

*Institute of Ocean Sciences
Sidney, B.C., V8L 4B2 Canada
email: parsonstimothy@shaw.ca
lallm@shaw.ca

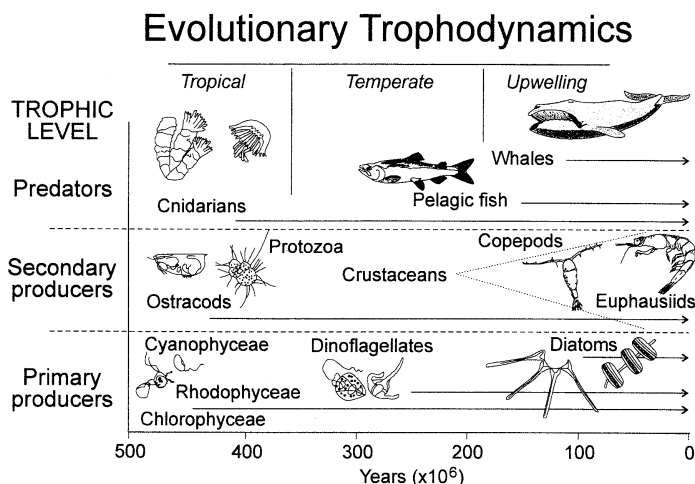


Fig. 1. The evolution of pelagic food chains in the ocean from the Cambrian to the present based on the fossil record and showing the approximate relationship in time between the evolution of low energy cnidarians (corals and "jellies") and higher energy requiring organisms (i.e. fish X 7, whales X 200) in association with the evolution of organisms at lower trophic levels from small to large primary producers. (Reprinted from PARSONS, 1979)

(PURCELL, 1991), as for example control of *Mnemiopsis* by *Beroe* (PURCELL *et al.*, 2001b; SHIGANOVA *et al.*, 2001; VINOGRADOV *et al.*, 2001). In order to find a general principle governing the outbreaks of jellyfish in different areas and at different times, we have re-examined the hypothesis put forward in 1977 by GREVE and PARSONS. These authors suggested that there are two basic food chains in the sea depending on the dominant type of primary producers. These are :

- (1) small flagellates* → small zooplankton → jellyfish*
- (2) large diatoms → large zooplankton → fish

These food chains represent pathways of energy flow in the pelagic ecosystem in the same sense as their use by others (e.g. RYTHER, 1969;

* "Flagellates" include autotrophic flagellates as well as heterotrophic zooflagellates produced in the microbial loop through the consumption of picoplankton; all of these are $<10 \mu\text{m}$ (i.e. nanoplankton). "Jellyfish" or "jellies" are not taxonomic categories, but are defined here and throughout this paper in an ecological sense to include all pelagic cnidarians and ctenophores.

SHELDON *et al.*, 1977) ; they are not a representation of a food web. One type of food chain in which flagellates are the dominant primary producers leads to production of jellies; we refer to this as a "low-energy" system. The other food chain, in which large phytoplankton prevail, leads to fish production and is a "high-energy" food chain. The concept of low- and high-energy food chains as described here (e.g. Fig. 1) does not depend on food chain length, but on the conditions for primary production and on the energy requirements of the terminal producer (s). RYTHER (1969) initially proposed that longer food chains (or increased number of trophic levels) were an impediment to the transfer of organic matter and resulted in lower terminal production. This is still a valid concept for very long food chains which involve active hunting and capture of prey at higher trophic levels. However, at the lowest trophic levels, as we have discussed in an earlier paper (PARSONS and LALLI, 1988), much higher ecological efficiencies between small-sized particles can result in almost equal energy flows in short and long food chains. As HEINBOKEL and BEERS (1979) have said, "relatively little of the energy and material fixed by

the nanoplankton may be lost to the larger consumers by the insertion of a ciliate extra link into the food chain". In our terminology, "high-energy" food chain refers to the terminal producers (i.e. fish or whales) as being high energy consuming organisms that must be supplied with an abundance of relatively large particles in order to meet their energy needs. Conversely, a "low-energy" food chain refers to terminal producers (e.g. jellies) that can feed efficiently off small particles in order to meet their lower metabolic demands. Hence the presence or absence of an additional link (e.g. picoplankton, including bacteria, being fed upon by zooflagellates) in the latter type of food chain is not nearly as important as the ecological conditions which favour the kind of primary producer. Thus the food chains depicted in Fig. 1 can be of equal length.

GREVE & PARSONS (1977) did not claim that these two different food chains were mutually exclusive, but suggested that one or the other could dominate at different times and/or in different ocean areas depending on environmental conditions. Environmental change causing shifts in dominance could either be induced by climate or pollution. Climate was cited in three references as causing at least two different conditions favoring flagellate production. The establishment of very stable, nutrient-poor water masses favors flagellate dominance, as these phytoplankton grow well under conditions of nutrient limitation. Flagellates also dominate in situations of light limitation, such as result from deep mixing of the water column. Diatom growth is at a disadvantage under both of these conditions, as physiological data have shown that high light intensity and abundant nutrients are necessary for diatoms to grow faster than flagellates. GREVE and PARSONS (1977) also cited literature references on grazing to further support their hypothesis that a flagellate-based, energy-poor food chain favors populations of jellyfish, and that an energy-rich food chain dominated by diatoms leads to fish production.

At the time of proposing this hypothesis, there was little evidence that large jellyfish population explosions were occurring in the sea, or that there were linkages with flagellate-

based food chains. However, GREVE and PARSONS gave some evidence concerning the preferential feeding of ctenophores on small prey items in the North Sea. They also pointed out that, on a seasonal scale in temperate waters, fish feeding and production maximize in early spring in association with diatom blooms, whereas jellyfish generally occur in large numbers later in the summer, when flagellates dominate in the nutrient-impoverished water column. This seasonal shift in the two different types of food chains has been noted in numerous publications (e.g., PARSONS *et al.*, 1970).

PARSONS later (1979, 1996) presented further evidence for the possible importance of these two food chains in pelagic marine ecology. These references drew attention to the size differential between small flagellates and large diatoms, which spans over six orders of magnitude in volumetric size. The first of these papers pointed out, that in evolutionary terms, the ancient ocean (500×10^6 ybp) was dominated by small phytoplankton (cyanobacteria, flagellates), small zooplankton and cnidarian ecology, including both coral reefs and pelagic jellyfish. It was argued that the later evolution of teleost fish (which appeared ca. 300×10^6 ybp) and whales (ca. 100×10^6 ybp) would have required a richer food chain in order to support the energy requirements of these animals (fish requiring approximately seven times and whales 200 times more energy than jellyfish on a weight specific basis according to FENCHEL, 1974). PARSONS (1979) suggested that this enrichment of the food chain of the pelagic environment came about from the evolution of larger phytoplanktonic forms, with diatoms appearing about 190 mya and becoming abundant by the time of the appearance of marine mammals (Fig. 1).

In contemporary terms, high and low energy food chains can be found in the present oceans. The greatest production of fish and whales in the world occurs in upwelling areas (e.g., the Peru Current or Benguela Current) on the western seabords of continents, whereas cnidarian ecology in terms of coral production is characteristic of convergent water masses on eastern seabords (e.g., the Caribbean and the Great Barrier Reef). These two different types

of ecologies are dominated by diatom and flagellate production, respectively. PARSONS (1996) further suggested that the fish/diatom food chain could be destabilized by overfishing. Two examples were given (AVIAN and SANDRIN, 1988; ZAITZEV, 1992) where jellyfish explosions had occurred in the ocean, although in neither case was it clear whether these may have been caused by overfishing, or by pollution to which diatoms are generally more susceptible than flagellates (e.g. THOMAS and SEIBERT, 1977).

Criticisms of GREVE and PARSONS' hypothesis on different ocean ecologies based on phytoplankton type have come mainly from two sources (LONGHURST, 1985; MILLS, 1995). Although LONGHURST (1985) agreed that different food chains developed seasonally in temperate waters, he did not believe there was definitive support for the existence of "two specific and separable pelagic food chains" elsewhere in the oceans. This may be partly a misinterpretation as GREVE and PARSONS did not claim that these food chains existed independently of each other, only that one or the other could dominate under different environmental conditions. LONGHURST also argued that he did not find a relationship between jellyfish and small zooplankton, and suggested that, on the contrary, jellies tend to eat larger organisms. More recent work has shown that there is considerable diversity in the diets of carnivorous cnidaria and ctenophores, and that many do indeed take small forms of zooplankton, predominantly small-sized copepods (e.g. GREVE, 1970; STOECKER *et al.*, 1987; MILLS, 1995; PURCELL and ARAI, 2001; PURCELL and STURDEVANT, 2001). The hypothesis being considered here was not intended to be mutually exclusive of jellyfish predation on larger zooplankton. It was intended to show that, in general, cnidarian ecology consumes small prey items compared with raptorial feeders, but there are certainly some biological exceptions.

In the second criticism, MILLS (1995) claimed that jellyfish are often abundant in upwelling (high-energy) environments. However, PAGÈS and GILI (1991) observed that the concentration of jellyfish in upwelled waters is the result of advection, not of increased reproduction. To quote these authors, "...a strong intrusion of

Angolan waters into the northern part of the Benguela system coincided with the abatement in the upwelling activity that characterizes the region. This important advective process facilitated penetration by large number of species and individuals of the gelatinous zooplankton...". MILLS (1995) also presented data indicating that the number of species of "jellies" found in high and low productive waters is about the same as observed from a submersible. However, the studies of the "high" productivity environment were in the N.W. Atlantic in July and August, when seasonal nutrient limitation would cause low productivity. In any event, the hypothesis being advanced here does not depend on the number of species but on the biomass of "jellies", which the author does not record. A further objection by this author is that "jellies" (quote) "... form a major part of the macroplankton of temperate fjords, which are generally considered to be high productivity systems." We agree that large concentrations of jellyfish are found at the head of many fjords but, as has been observed by a number of authors (e.g. PARSONS *et al.*, 1983; Hobson and MCQUOID, 2001), these areas generally have a low productivity, dominated by flagellate ecology. Where the impression of "high" productivity is gained, is from the frontal zone that sometimes occurs at the mouth of fjords. These areas are dominated by diatom ecology and by schools of fish, such as herring. Further, GRAHAM *et al.* (2001) have noted that aggregations of large medusae at fronts or other physical discontinuities must result from physical accumulation, because population increases of these animals is almost always decoupled from water column processes. MILLS (1995) also concluded that "jellies" are so ubiquitous that they are opportunistically positioned to utilize secondary production in the absence of fish. This may be correct, certainly in respect to their high reproductive rate. However, in coastal areas, changes caused by eutrophication, as discussed below, appear to enhance jellyfish production and not fish production. This indicates that a food chain favouring "jellies" occurs in these areas, rather than there simply being a vacancy for an opportunistic feeder at a higher trophic level.

Table 1. Some examples of jellyfish population explosions

Location	Date	Species	Suggested Causes	Reference
Bering Sea (eastern shelf)	1989 onward	Combined species, <i>Chrysaora melanaster</i> dominant	Climate change; overfishing	BRODEUR <i>et al.</i> , 1999
Black Sea	1970s- 1980s	<i>Rhizostoma pulmo</i> <i>Aurelia aurita</i>	Overfishing; eutrophication	KOVALEV & PIONTKOVSKI, 1998; SHIGANOVA, 1998; DASKALOV, 2002
	1982-	<i>Mnemiopsis leidyi</i>	Invasion & proliferation; overfishing	SHIGANOVA, 1998; DASKALOV, 2002
	1997-	<i>Beroe ovata</i>	Invasion & proliferation due to superabundant <i>Mnemiopsis</i> prey	SHIGANOVA <i>et al.</i> , 2001; VINOGRADOV <i>et al.</i> , 2001
Gulf of Mexico	1980s- 2000	<i>Chrysaora</i> <i>quinquecirrha</i> <i>Aurelia aurita</i>	Eutrophication; overfishing	GRAHAM, 2001 and pers. commun.
Mediterranean (western)	Periodic	<i>Pelagia noctiluca</i>	Climate change	GOY <i>et al.</i> , 1989
Tokyo Bay	1960s Onward	<i>Aurelia aurita</i>	Eutrophication	ISHII and TANAKA, 2001

2. Several Explanations for Population Explosions of Jellyfish based on the Energy Flow Hypothesis

Various causes of jellyfish population explosions have been advanced (see Table 1), but it is our contention that there is a general framework on which all of these events can be brought together, as outlined in the following sections.

Pollution and Eutrophication Effects

There are two aspects to consider in respect to increases in jellyfish populations in coastal areas. Firstly, heavy metals and petroleum hydrocarbons are highest in coastal areas associated with urban runoff; secondly, agricultural and sewage eutrophication are also highest in coastal zones.

GREVE and PARSONS (1977) drew attention to Controlled Ecosystem Pollution Experiments (CEPEX) which showed that hydrocarbons tended to enhance flagellate production, and pointed out that this effect was also observed after some oil spills. However, concentrations of jellyfish in oil-polluted waters have not been recorded following these events. CEPEX experiments with heavy metal additions also decreased diatom populations, while flagellates

survived and accounted for most of the primary production. In addition, heterotrophic zooflagellates may also be produced under conditions of high organic pollution and a large bacterial biomass (FENCHEL, 1982). This microbial loop (AZAM *et al.*, 1983) may become especially dominant in some forms of coastal eutrophication. Organic enrichment leading to enhanced bacterial production was studied during the CEPEX experiments (PARSONS *et al.*, 1981). The addition of small amounts (1 to 5 ppm) of glucose caused a depression in photosynthesis, increased bacterial production, and a bloom of larvaceans, copepods and meroplanktonic larvae, followed by a large bloom of jellies (mostly *Pleurobrachia* and *Aequorea aequorea*). Thus, under experimental conditions, it may be concluded that the heterotrophic cycle is another possible contribution to jelly production.

Eutrophication of coastal waters now appears to be the most severe form of coastal pollution and could be a cause of enhanced jellyfish production. The subject was reviewed by PURCELL *et al.* (1999), and later by ARAI (2001) who concluded that cnidarian populations appear to increase in eutrophied areas, but such increases can not be unequivocally attributed

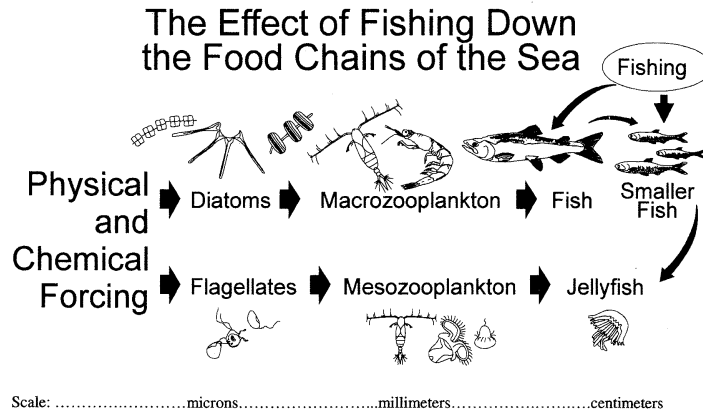


Fig. 2. The effect of overfishing on the high and low energy food chains of the sea. The elimination of large quantities of fish would initially cause an increase in the macroplankton and later a decrease in the diatom population through grazing. More nutrients then flow into the flagellate food chain resulting in an increased jellyfish population.

to nutrient enrichment since there are usually other coastal influences such as higher levels of heavy metals and hydrocarbons. In coastal eutrophication, the author correctly identifies the lack of silicate as the cause of flagellate blooms as diatoms require this nutrient for growth. Over the past four decades in eutrophied Tokyo Bay, a food chain based on microflagellates has developed which supports mainly small-sized copepods and jellyfish (*Aurelia aurita*), with very little fish production (NOMURA and MURANO, 1992; UYE, 1994; ISHII and TANAKA, 2001). This long-term change is what one would predict when eutrophication or pollution favors flagellate ecology and a low-energy food chain.

There are now a number of reports on the massive increases in jellyfish populations in the Black Sea (e.g. ZAITZEV, 1992; KOVALEV and PIONTKOVSKI, 1998; SHIGANOVA, 1998; SHIGANOVA *et al.*, 2001; VINOGRADOV *et al.*, 2001). In a modeling analysis of various causes for this effect, DASKALOV (2002) concluded that the two most probable causes were eutrophication and overfishing, with the latter being the stronger causative agent.

Effects of Overfishing

The effects of overfishing on the high-energy food chain are shown in Fig. 2. The initial effect of overfishing in reducing fish size, either

within the fished population or by supplanting it with another smaller species in the fish catch, has been known for some time (e.g. HEMPEL, 1978; SHERMAN *et al.*, 1981). It is also common knowledge that the effects of overfishing may result in a variety of ecological changes, such as increased penguin populations in the Antarctic or decreased bird populations off Peru (for summary, see PARSONS, 1992). In Fig. 2, however, the specific case of what could happen to the diatom/fish food chain is illustrated. In the absence of fish to graze the large-sized zooplankters, the numbers of these animals would increase and exert pressure on the diatom population. Diatoms in turn would diminish, leaving more of the available nutrients to flow into the flagellate/jellyfish part of the food chain - a result that would increase the jellyfish population. This kind of oscillation between phytoplankton and zooplankton has been observed experimentally on lakes (e.g. MCQUEEN *et al.*, 1989) and has been the subject of computer simulations (e.g. HASTINGS and POWELL, 1991). Is there any evidence that this has happened in the natural marine environment?

BRODEUR *et al.* (1999) described a large increase in the population of jellyfish in the Bering Sea where there has been a substantial pollock fishery in recent years (SPRINGER, 1992). To account for this increase in jellyfish

numbers, BRODEUR *et al.* favor an explanation based on climate change. Certainly this is possible and is allowed for in Fig. 2, if the physical /chemical environment changes in such a way as to preferentially favor one or the other of the food chains. However, the alternative explanation that the increase in jellyfish has been the result of overfishing can not be dismissed. There are several pieces of circumstantial evidence which favor the latter explanation.

Firstly, SPRINGER (1992) noted that whereas fishing may have reduced the numbers of fish-eating birds and mammals in the area due to a lack of prey, plankton-eating auklets actually increased in abundance, which might indicate that the macroplankton community had increased as a result of the decreased predation by fish. Another unusual occurrence in the Bering Sea was the development of a massive bloom of coccolithophorid flagellates that was accompanied by a large increase in small crustaceans (e.g. STOCKWELL *et al.*, 2001). An explanation for this phenomenon does not necessarily require changes in the growth conditions for phytoplankton; it could also be generated by a lack of predator (i.e. fish) control of the food chain, which would force more nutrients into flagellate production if large crustaceans were to control diatom production (Fig. 2 and HASTINGS and POWELL, 1991). Once a food chain has been destabilized in such a manner, the role of climate as an additional influence in these effects can not be ruled out. However, the role of pollutants or eutrophication, such as may have caused changes in the Black Sea and in coastal waters, is probably not significant in the Bering Sea.

DASKALOV'S (2002) conclusion that overfishing was the primary cause of the increase in "jellies" in the Black Sea is important to the concept of food chains as originally suggested by GREVE and PARSONS (1977). DASKALOV concluded that size-selective effects were crucial to biomass dynamics. Large zooplankton consumed by fish had a pronounced effect on size structure of the food chain. He found that total zooplankton and phytoplankton biomass were determined mainly by the dynamics of the large size fractions at each trophic level, and that it was these that were most sensitive to

top-down control by fish. However, these conclusions were based on a mathematical model and one result of this model, the dominance of large phytoplankton cells in the presence of jellyfish, is not consistent with direct observations of others (e.g. ISHII and TANAKA, 2001). Other possible effects of overfishing are discussed by PURCELL and ARAI (2001) ; they reviewed the disappearance of mackerel in the Black Sea due to overfishing and the subsequent abundance of "jellies" on which the mackerel preyed. This type of direct predator /prey interaction with jellyfish does not appear to be common in the sea, but where it occurs, it must be included as a possible cause of jellyfish population explosions.

Effects of Climate Change

Climate changes, whether induced by global warming or not, can have profound effects on marine ecosystems. BRODEUR *et al.* (1999) consider that the production of jellyfish in the Bering Sea, which started in about 1990 and has continued strongly ever since, was due to a regime shift brought about by a change in climate. They pointed out that the extent of ice cover in the Bering Sea is highly variable but, if the survival of early life stages of jellyfish depended on ice-associated phytoplankton blooms and attendant secondary production, then in terms of both its persistence and spatial extent, more favorable conditions existed after 1990, which was when the jellyfish population started to increase. If these events were associated with the physical/chemical regime in Fig. 2, then ensuing flagellate production could come about through quite different mechanisms, either by development of a very stable, nutrient-poor water column, or by formation of an unstable deeply-mixed water column (see PARSONS and TAKAHASHI, 1973 for discussion). Either condition favors flagellate growth over diatom production.

Jellyfish abundance in the Mediterranean Sea has been directly linked to climate by GOY *et al.* (1989), although an earlier report (AVIAN and SANDRIN, 1988) attributed an increase in jellyfish in the Adriatic Sea to overfishing. GOY *et al.* analysed long-term data sets and concluded that warmer waters gave

rise to more jellyfish, and suggested that this may have been due to increased production of microzooplankton.

3. Conclusions

It has not been our purpose to give specific reasons for any particular jellyfish population explosion listed in Table 1, but rather to establish a framework that could be used to explain any one of the observations. This framework is based on two very different pelagic food chains, which we believe evolved over time and which coexist in the contemporary ocean. These food chains are based on the amount of energy supplied by the different types of primary producers. The low-energy food chain is based on very small phytoplankton, generally referred to as flagellates (also as nanoplankton). These cells are at least six orders of magnitude smaller than the large phytoplankton, which are most often represented by the diatoms (or microplankton). Food chains based on very small phytoplankton support micro- and mesozooplankton that are mostly too little for large raptorial fish, because it is energetically too costly to feed on such small prey. Instead, these small zooplankton are easily fed on by the "jellies" of the sea. The conditions under which one or the other of these two food chains can dominate are determined by at least three events, including natural changes in the physical-chemical environment, various forms of pollution including eutrophication, and overfishing. Increased populations of medusae and/or ctenophores may develop wherever, or whenever, a flagellate-based food chain is favored. The effects of climate, pollution, and overfishing may, at times, act synergistically.

It is clear that several anthropogenic influences are having profound effects on our marine ecosystems. Industrial fisheries have removed, and continue to remove, vast numbers of the top-level predators of the sea; for the most part, these (teleost fish and whales) are the most recently evolved marine animals. These animals are also the most susceptible to pollution effects through bioaccumulation. By removal or debilitation of these top trophic levels, we not only provide more food to lower trophic levels, but we may also be changing the

species compositions of ecosystems. In the examples given here, medusae and/or ctenophores are becoming predominant in ecosystems formerly dominated by fish. It is well to remember, as PURCELL *et al.* (1999) have pointed out, that jellyfish may be superior competitors to fish in many respects as they feed continuously, do not satiate at natural food concentrations, usually have broad diets, often eat fish eggs and larvae, and shrink rather than die when food is limiting. Most are passive feeders that do not expend large amounts of energy in hunting and capturing food. Further, many medusae have both asexual and sexual reproduction, and all jellies have short generation times compared with fish. It is beginning to look as though the balance is being shifted from a highly evolved ecosystem in which fish or marine mammals occupy top trophic levels to an ecosystem in which environmental conditions and lessened competition favor the more ancient species like cnidarians and ctenophores.

One consequence of the establishment of the flagellate-jellyfish food chain is that the much lower energy demands of jellies compared with raptorial feeders (fish and whales), and their more rapid life cycles, can result in a rapid production of gelatinous biomass, much exceeding the total biomass of fish and whales. This is because jellies have a much lower metabolism, and consequently their total biomass can greatly exceed that of more metabolically expensive animals. It is important to remember that jellies have relatively few natural predators, and only a few species are commercially fished for human consumption. Control of jellyfish (or ctenophore) population size is primarily bottom-up control via the physical-chemical nature of the environment (temperature, salinity etc.), food availability and, for those species with a benthic stage in their life cycle, availability of suitable hard substrates. The development of huge jellyfish populations on a global scale is not a desirable result in a world where an expanding human population is demanding more and more protein from marine resources.

The hypothesis of GREVE and PARSONS that links jellyfish production to flagellate-based

food chains remains speculative, although we believe that additional evidence given in the present paper strengthens its validity. At present our knowledge of both natural and perturbed marine ecosystems remains underdeveloped to prove or disprove this hypothesis. However, certain observations and/or experiments could be undertaken to examine more closely the types of food chains discussed here. For example, it is essential that phytoplankton species composition be determined in areas undergoing anthropogenic change, as total primary productivity may not reveal differences leading to low- or high-energy food chains. Further, it is unlikely that the hypothesis holds for all species of jellies, especially not for those that are large-particle feeders and direct competitors with large raptorial fish. In this regard, it would be extremely useful to have more detailed information on diets of specific medusae and ctenophores in different types of ecosystems; such studies are presently being undertaken by Graham and Costello (in prep.). Until these types of information are available, the Greve and Parsons hypothesis remains unresolved.

Acknowledgements

We wish to thank Dr. J. E. PURCELL, Dr. W. M. GRAHAM and the anonymous reviewers for their constructive criticisms of earlier drafts of this paper.

References

- ARAI, N. M. (2001) : Pelagic coelenterates and eutrophication : a review. *Hydrobiologia*, **451**, 69–87.
- AVIAN, M. and L. R. SANDRIN (1988) : Fishery and swarmings of *Pelagia noctiluca* in the central and northern Adriatic Sea : Middle term analysis. *Rapports et Process-verbaux des Reunions. Commission internationale pour L'Exploration scientifique de la Mer Mediterranea*, **31**, 230–231.
- AZAM, F., T. FENCHEL, J.G. FIELD, J.S. GRAY, L. A. MEYER-REIL and L. A. THINGSTAD. (1983) : The ecological role of water column-microbes in the sea. *Mar. Ecol. Prog. Ser.*, **10**, 257–263.
- BRODEUR, R. D., C. E. MILLS, J.E. OVERLAND, G. E. WALTERS and J.D. SCHUMACHER (1999) : Evidence for a substantial increase in gelatinous zooplankton in the Bering Sea, with possible links to climate change. *Fish.Oceanogr.*, **8**, 296–306.
- DASKALOV, G. M. (2002) : Overfishing drives a trophic cascade in the Black Sea. *Mar. Ecol. Prog. Ser.*, **225**, 53–63.
- FENCHEL, T. (1974) : Intrinsic rate of natural increase: the relationship with body size. *Oecologia*, **14**, 317–326.
- FENCHEL, T. (1982) : Ecology of heterotrophic microflagellates. II. Bioenergetics and growth. *Mar. Ecol. Prog. Ser.*, **9**, 35–42.
- FRASER, J. H. (1969) : Experimental feeding of some medusae and Chaetognatha. *J. Fish. Res. Bd Canada*, **26**, 1743–1762.
- GOY, J., P. MORAND and M. ETIENNE (1989) : Long-term fluctuations of *Pelagia noctiluca* (Cnidaria, Scyphomedusa) in the western Mediterranean Sea. Prediction by climatic variables. *Deep-Sea Res.*, **36**, 269–279.
- GRAHAM, W. M. (2001) : Numerical increases and distributional shifts of *Chrysaora quinquecirrha* (Desor) and *Aurelia aurita* (Linne) (Cnidaria : Scyphozoa) in the northern Gulf of Mexico. *Hydrobiologia*, **451**, 97–111.
- GRAHAM, W. M. and J. H. COSTELLO (In prep.) : A biogeographic synthesis of prey capture strategies among rhizostome and semeanostome scyphomedusae.
- GRAHAM, W. M., F. PAGÈS and W. M. HAMNER (2001) : A physical context for gelatinous zooplankton aggregations : a review. *Hydrobiologia*, **451**, 199–212.
- GREVE, W. (1970) : Cultivation experiments on North Sea ctenophores. *Helg. wiss. Meeresunter.*, **20**, 304–317.
- GREVE, W. and T.R. PARSONS (1977) : Photosynthesis and fish production : hypothetical effects of climatic change and pollution. *Helg. wiss. Meeresunter.*, **30**, 666–672.
- HARBISON, G.R., L.P. MADIN and N.R. SWANBERG (1978) : On the natural history and distribution of oceanic ctenophores. *Deep-Sea Res.*, **25**, 233–256.
- HASTINGS, A. and T. POWELL (1991) : Chaos in a three-species food chain. *Ecology*, **2**, 896–903.
- HEINBOKEL, J.F. and J.R. BEERS (1979) : Studies on the functional role of tintinnids in the Southern California Bight. III. Grazing impact on natural assemblages. *Mar. Biol.*, **52**, 23–32.
- HEMPEL, G. (1978) : North Sea fisheries and fish

- stocks—a review of recent changes. *Rapports et Process-verbaux des Reunions. Conseil international pour l'Exploration de la Mer*, **173**, 145–167.
- HOBSON, L.A. and M.R. McQUOID (2001) : Pelagic diatom assemblages are good indicators of mixed water intrusions into Saanich Inlet, a stratified fjord in Vancouver Island. *Mar. Geol.*, **174**, 125–138.
- ISHII, H. and F. TANAKA (2001) : Food and feeding of *Aurelia aurita* in Tokyo Bay with an analysis of stomach contents and a measurement of digestion times. *Hydrobiologia*, **451**, 311–320.
- KOVALEV, A.V. and S.A. PIONTKOVSKI (1998) : Interannual changes in the biomass of Black Sea gelatinous zooplankton. *J. Plankton Res.*, **20**, 1377–1385.
- LONGHURST, A.R. (1985) : The structure and evolution of plankton communities. *Prog.Oceanogr.*, **15**, 1–35.
- MCQUEEN, J.D., M.R.S. JOHANNES, J.R. POST, T.J. STEWARD and D.R.S. LEAN (1989) : Bottom-up and top-down impacts of freshwater pelagic community structure. *Ecol. Monogr.*, **59**, 289–309.
- MILLS, C.E. (1995) : Medusae, siphonophores, and ctenophores as planktivorous predators in changing global ecosystems. *ICES J. Mar. Sci.*, **52**, 575–581.
- MILLS, C.E. (2001) : Jellyfish blooms : Are populations increasing globally in response to changing ocean conditions? *Hydrobiologia*, **451**, 55–68.
- NOMURA, H. and M. MURANO (1992) : Seasonal variation of meso- and macroplankton in Tokyo Bay, central Japan. *La mer*, **30**, 49–56.
- PAGÈS, F. and J.M. GILI (1991) : Effects of large-scale advective processes on gelatinous zooplankton populations in the northern Benguela ecosystem. *Mar. Ecol. Prog. Ser.*, **75**, 205–215.
- PARSONS, T.R. (1979) : Some ecological, experimental and evolutionary aspects of the upwelling ecosystem. *South African J. Sci.*, **75**, 536–540.
- PARSONS, T.R. (1992) : The removal of marine predators by fisheries and the impact on trophic structure. *Mar. Poll. Bull.*, **26**, 51–53.
- PARSONS, T.R. (1996) : The impact of industrial fisheries on the trophic structure of marine ecosystems. *In Food Webs – Integration of Patterns and Dynamics*, Polis, G.A. and K.O. Winemiller (eds.), Chapman Hall, N.Y., pp. 352–357.
- PARSONS, T.R., L.J. ALBRIGHT, F.WHITNEY, P.J. LeB WILLIAMS and C.S. WANG (1981) : The effect of glucose on the productivity of seawater : An experimental approach using controlled aquatic ecosystems. *Mar. Environ. Res.*, **4**, 229–242.
- PARSONS, T.R. and C.M. LALLI (1988) : Comparative oceanic ecology of the plankton communities of the subarctic Atlantic and Pacific Oceans. *Oceanogr. Mar. Biol. Annu. Rev.*, **26**, 317–359.
- PARSONS, T.R., R.J. LeBRASSEUR and W.E. BARRACLOUGH (1970) : Levels of production in the pelagic environment of the Strait of Georgia, British Columbia : A review. *J. Fish. Res. Bd Canada*, **27**, 1251–1264.
- PARSONS T.R., R.I. PERRY, E.D. NUTBROWN, W. HSIEH and C.M. LALLI (1983) : Frontal zone analysis at the mouth of Saanich Inlet, British Columbia, Canada. *Mar. Biol.*, **73**, 1–5.
- PARSONS, T.R. and M. TAKAHASHI (1973) : Environmental control of phytoplankton cell size. *Limnol.Oceanogr.*, **18**, 511–515.
- PURCELL, J.E. (1991) : A review of cnidarians and ctenophores feeding on competitors in the plankton. *Hydrobiologia*, **216/217**, 335–341.
- PURCELL, J.E. and M.N. ARAI (2001) : Interactions of pelagic cnidarians and ctenophores with fish : a review. *Hydrobiologia* **451**, 27–44.
- PURCELL, J.E., W.M. GRAHAM and H.J. Dumont (eds.) (2001a) : Jellyfish Blooms : Ecological and Societal Importance. Reprinted from *Hydrobiologia*, **451** : 333 pp. Dordrecht : Kluwer Academic Publ.
- PURCELL, J.E., A. MALEJ and A. BENOVIĆ (1999) : Potential links of jellyfish to eutrophication and fisheries. *Coastal Estuar. Stud.*, **55**, 241–263.
- PURCELL, J.E., T.A. SHIGANOVA, M.B. DECKER and E.D. HOUDE (2001b) : The ctenophore *Mnemiopsis* in native and exotic habitats : U.S. estuaries versus the Black Sea basin. *Hydrobiologia*, **451**, 145–176.
- PURCELL, J.E. and M.V. STURDEVANT (2001) : Prey selection and dietary overlap among zooplanktivorous jellyfish and juvenile fishes in Prince William Sound, Alaska. *Mar. Ecol. Prog. Ser.*, **210**, 67–83.
- RYTHER, J.H. (1969) : Photosynthesis and fish production in the sea. The production of organic matter and its conversion to higher forms of life vary throughout the world oceans. *Science*, **166**, 72–76.
- SHELDON, R.W., W.H. SUTCLIFFE and M.A. PARANJAPÉ (1977) : Structure of pelagic food chains and relationship between plankton and fish production. *Fish. Res. Bd. Canada*, **4**, 2344–2353.

- SHERMAN, K., C. JONES, L. SULLIVAN, W. SMITH, P. BERRIEN and L. EJSYMONT (1981) : Congruent shifts in sand eel abundance in western and eastern North Atlantic ecosystems. *Nature*, **291**, 486-489.
- SHIGANOVA, T.A. (1998) : Invasion of the Black Sea by the ctenophore *Mnemiopsis leidyi* and recent changes in pelagic community structure. *Fish. Oceanogr.*, **7**, 305-310.
- SHIGANOVA, T.A., Y.V. BULGAKOVA, S.P. VOLOVIK, Z.A. MIRZOYAN and S.I. DUDKIN (2001) : The new invader *Beroe ovata* Mayer 1912 and its effect on the ecosystem in the northeastern Black Sea. *Hydrobiologia*, **451**, 187-197.
- SPRINGER, A.M. (1992) : A review : Walleye pollock in the North Pacific - how much difference do they really make? *Fish. Oceanogr.*, **1**, 80-96.
- STOCKWELL, D.A., T.E. WHITLEGE, S.I. ZEEMAN, K.O. COYLE, J.M. NAPP, R.D. BRODEUR, A.I. PINCHUK and G.L. HUNT, Jr. (2001) : Anomalous conditions in the south - eastern Bering Sea, nutrients, phytoplankton and zooplankton. *Fish. Oceanogr.*, **10**, 99-116.
- STOECKER, D.K., P.G. VERITY, A.E. MICHAELS and L.H. DAVIS (1987) : Feeding by larval and post-larval ctenophores on microzooplankton. *J. Plank. Res.*, **9**, 667-683.
- THOMAS, W.H. and D.L.R. SEIBERT (1977) : Effects of copper on the dominance and the diversity of algae : Controlled ecosystem pollution experiment. *Bull. Mar. Sci.*, **27**, 23-33.
- UYE, S.-I. (1994) : Replacement of large copepods by small ones with eutrophication of embayments : cause and consequence. *Hydrobiologia*, **292/293**, 513-519.
- VINOGRADOV, M.E., E.A. SHUSHKINA and S.V. VOSTOKOV (2001) : Gelatinous macroplankton (jellyfish *Aurelia aurita*, ctenophores *Mnemiopsis leidyi* and *Beroe ovata*) in the Black Sea ecosystem. (Important aspects for the Caspian Sea modern ecology). 1st International Meeting of the Caspian Environment Programme. Baku, Azerbaijan, 24-26 April 2001. 5 pp.
- ZAITZEV, Yu. P. (1992) : Recent changes in the trophic structure of the Black Sea. *Fish. Oceanogr.*, **1**, 180-189.

Received July 25, 2002
Accepted August 29, 2002

Seasonal variations of sea level along the Japanese coast

Nyoman M.N. NATIH,* Masaji MATSUYAMA,* Yujiro KITADE* and Jiro YOSHIDA*

Abstract : Seasonal variation of sea level was investigated at 68 tidal stations along the Japanese coast by using monthly mean data from 1981 to 1990. The main results mostly agree with TSUMURA's results (1963) by the data from 1951 to 1960, but the details are partly different from his results. The high sea level in winter is found along the Hokkaido coast in the Okhotsk Sea, and even along the southeastern coast of Hokkaido. This high sea level is considered to be closely related to the strength of East Sakhalin Current in this season. The gentle sea level rise occurs from Mera to Uragami along the southeastern coast of Honshu from June to July, i.e., in warming season. The sea level change along Suruga Bay coast mostly agrees with the vertical mean temperature from the sea surface to 200m depth in the center of bay. The vertical mean temperature is not so increased by the surface-temperature rise because of seasonal thermocline ascent in warming season. The seasonal thermocline ascent has been frequently found off the southeast of Honshu from Boso to Kii Peninsulas, and is explained as coastal upwelling induced by the prevailing northward wind in summer. The coastal upwelling is suggested to induce such a unique variation as the gentle sea level rise and secondary minimum of the water temperature. The gentle sea level rise in the Seto Inland Sea and the southwestern coast of Japan also appears from April to May, but the sea level change slightly disagrees with the temperature change in the surface layer.

Key words : *coastal current, coastal upwelling, Japanese coast, sea level, seasonal thermocline, seasonal variations, secondary minimum of temperature*

1. Introduction

Sea level in subtropical region is well known to show a seasonal variation, i.e., a maximum during summer to early fall and a minimum during winter to early spring (e.g., PICKARD and EMERY, 1990). The sea level variations are closely connected to water temperature variations in surface and subsurface layers. But, some observations indicated the unique seasonal variations of sea level. The sea level at the Oregon coast and dynamic height off Oregon are minimum in summer in relation to the coastal upwelling induced by the southward wind (e.g., GILL, 1982). This result is in direct opposition to the usual seasonal variation seen in the subtropical region. Along the Japanese coast, the extraordinary seasonal variations are found in sea level records. The sea level along the Hokkaido coast in the Okhotsk Sea show

the peculiar seasonal variations which have two peaks in summer and early winter (TSUMURA, 1963, KONISHI *et al.*, 1987, MATSUYAMA *et al.*, 1999). Such variant phenomena are possible to be found in the seasonal variation of sea level along the Japanese coast.

TSUMURA (1963) analyzed the sea level data at about 58 tidal stations along the Japanese coast during 10 years and investigated the characteristics of annual and interannual variations of the sea level. He showed the seasonal variation of sea level along the Japanese coast and derived the interesting features, but he didn't explain the relations between the sea level variation and oceanographic phenomena. We are very interested in a relation between the seasonal variation and the oceanographic phenomena. Then we grasp the seasonal variations of sea level along the Japanese coast using the monthly mean data during the period from 1981 to 1990. The aim of this paper is to investigate the characteristics of seasonal

*Department of Ocean Sciences, Tokyo University of Fisheries

Minato-ku, Konan 4-5-7, Tokyo, 108-8477, Japan

variations of sea level in more detail, and to clarify the relation between the sea level variation and oceanic phenomena, i.e., current and temperature variations, and coastal upwelling.

2. Data and analysis

The monthly mean sea level data registered by the Coastal Movement Data Center (CMDC), Geographical Survey Institute, were used at 68 tidal stations in this study (Table 1). The same data set was already applied to investigate the inter-annual and decadal variations along the Japanese coast (SENJYU *et al.*, 1999). The tidal stations are selected around all over the Japanese coast as shown in Fig.1. Under the inverse barometric assumption with a factor of -1.0 cm/hPa, the original sea level data were corrected by using the atmospheric pressure obtained at a meteorological station near each tidal station. Monthly mean atmospheric pressure was also registered at CMDC.

3. Seasonal variations of sea level along the Japanese coast

Fig. 2 shows typical sea level variations at 9 stations along the Japanese coast for 10 years. These stations are selected as a typical station in each area. The seasonal variations are remarkable at all stations, but the amplitudes are different from each other. The amplitudes are large in the southern region (Kochi (Stn.37 shown in Fig.1), Matsuyama (Stn.48) and Kagoshima (Stn.51)) of Japan and the Japan Sea (Maizuru (Stn.62)), and small along the Hokkaido coast (Abashiri (Stn.3) and Kushiro (Stn.4)). The maximum and minimum of these variations appear mostly in early autumn and late winter, respectively. But the maximum is found at December at Abashiri (Stn.3) and Kushiro (Stn.4), as described by the previous papers (TSUMURA, 1963, KONISHI *et al.*, 1987, MATSUYAMA *et al.*, 1999, ITOH, 2000). The sea level variations are not so decent sinusoidal curve except at Kamaishi (Stn.13) and Maizuru (Stn.62), but are frequently disturbed by a few month period fluctuations. These short period fluctuations are especially remarkable between Mera (Stn.19) to Kagoshima (Stn.51), i.e. in the coast of facing to the Kuroshio. NOMITSU and OKAMOTO (1927)

Table 1. Location of the sea level stations

No.	Location	No.	Location
1	Wakkanai	36	Muroto
2	Mombetsu	37	Kochi
3	Abashiri	38	Tosashimizu
4	Kushiro	39	Hosojima
5	Tokachi	40	Oita
6	Urakawa	41	Shirahama
7	Muroran	42	Wakayama
8	Hakodate	43	Kobe
9	Matsumae	44	Uno
10	Oshoro	45	Hiroshima
11	Hachinohe	46	Tokuyama
12	Miyako	47	Uwajima
13	Kamaishi	48	Matsuyama
14	Ofunato	49	Takamatsu
15	Ayukawa	50	Komatsujima
16	Soma	51	Kagoshima
17	Onahama	52	Makurazaki
18	Katsuura	53	Kune
19	Mera	54	Misumi
20	Chiba	55	Nagasaki
21	Tokyo	56	Sasebo
22	Yokotsuka	57	Izuhara
23	Aburatsubo	58	Shimon oseeki
24	Ito	59	Hagi
25	Minami Izu	60	Hamada
26	Uchiura	61	Sakai
27	Shimizu	62	Maizuru
28	Yaizu	63	Mikuni
29	Omaezaki	64	Wajima
30	Maisaka	65	Toyama
31	Nagoya	66	Kashiwazaki
32	Toba	67	Oga
33	Owase	68	Fukaura
34	Uragami		
35	Kushimoto		

described the variations of monthly sea level along the Japanese coast to be due to both the variations of density distribution from the sea surface to 200 m depth and of atmospheric pressure. Fig. 2 supports mainly their description, but we are interested in more detailed characteristics and distortion from the sinusoidal curve of seasonal variation.

TSUMURA (1963) analyzed the sea level data at 58 stations along the Japanese coast during the period from 1951 to 1960 and summarized the mean seasonal variations of sea level without correction of atmospheric pressure as

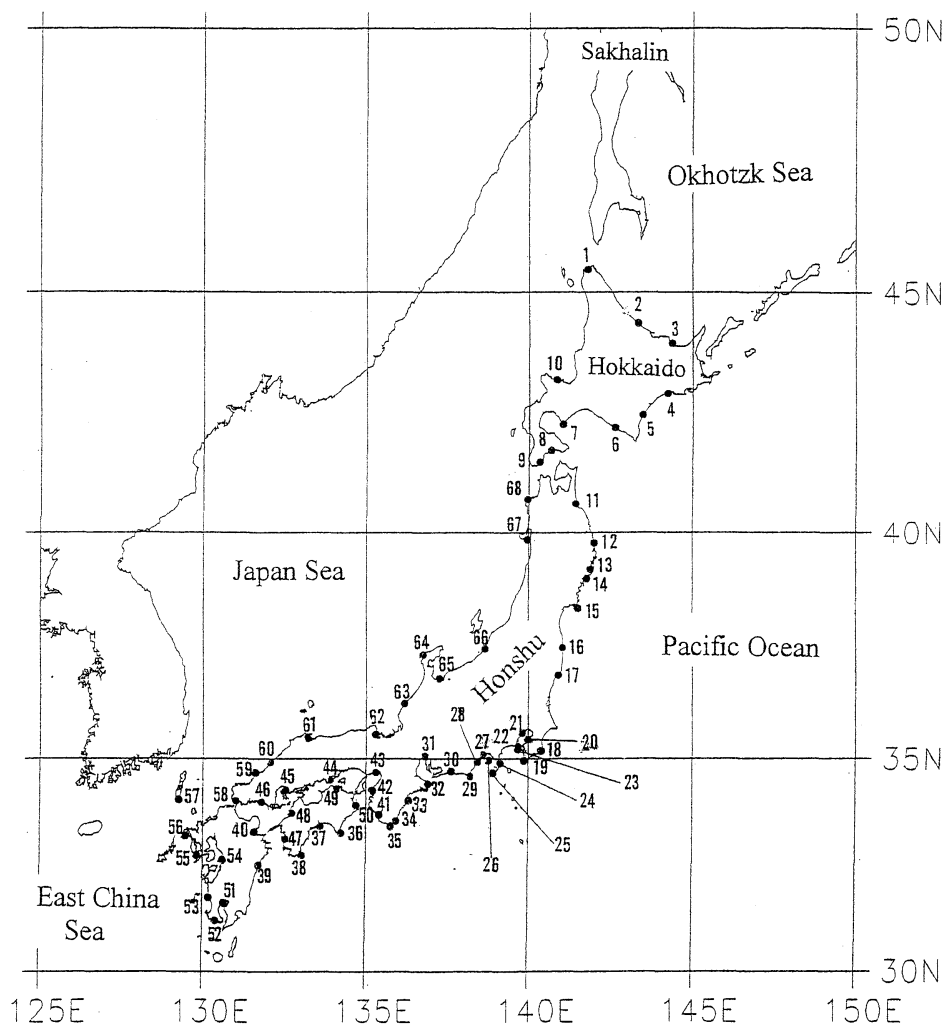


Fig. 1. Location of tide stations used in this study.

follows. (1) The maximum and minimum appear on September to October and March to May, respectively, in most stations. (2) The amplitude is the largest in the western part of the Japanese coast and the smallest in the northern part. (3) The two maximum appear along the eastern coast of Hokkaido. (4) The sea level gently rises along the southern coast of Japan from Mera (Stn. 19) to Megami (near Stn. 55) during the period from July to August. (5) In the northern part of the Japan Sea coast, north of Wajima (Stn. 64), the steep and gentle descents are seen from October to November, and from November to December, respectively.

These results are interesting features in relation to the coastal phenomena, that is, heating and cooling, wind effect and ocean currents. Fig. 3 shows the seasonal variations at all stations using the sea level data at 68 tidal stations from 1981 to 1990. These showed the similar characteristics of the seasonal variations indicated by TSUMURA (1963). Then we will try to verify the above five points by the recent tidal records, and we investigate the features of the seasonal variations in more detail.

The maximum is seen on September and October except the east coast of Hokkaido and Hamada (Stn. 60) and Sakai (Stn. 61) along the

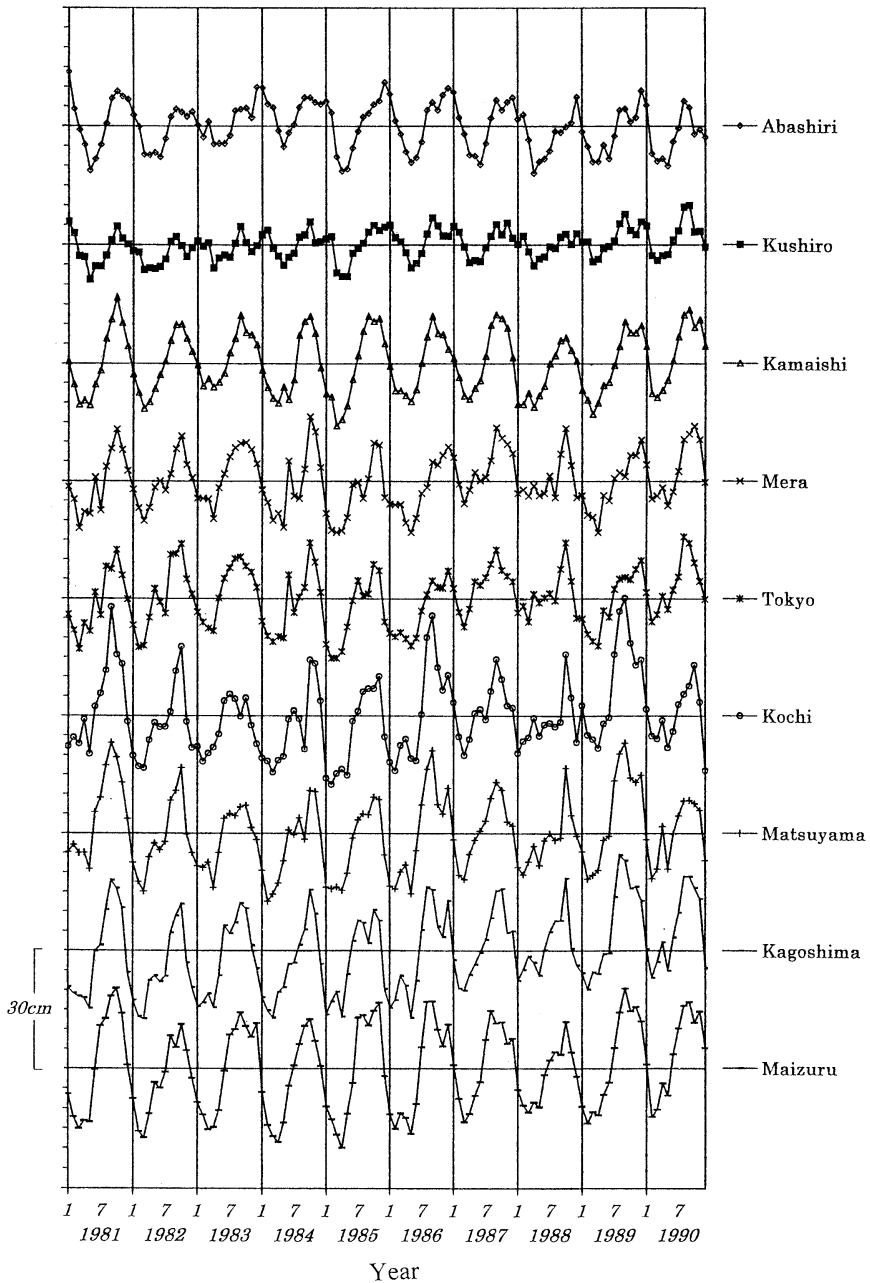


Fig. 2. Sea level variations corrected for the atmospheric pressure at nine tidal stations.

western coast in the Japan Sea. In the Japan Sea coast from Izuhara (Stn.57) to Wakkanai (Stn.1), the high sea level continues from August to October. The variations from Akune (Stn.53) to Sasebo (Stn.56) of the East China Sea coast resemble to these of the Japan Sea

coast region. Along the Pacific coast, the maximum is seen on September from Hachinohe (Stn.11) to Onahama (Stn.17), i.e., northern part of Honshu, while it is on October from Katsuura (Stn.18) to Makurazaki (Stn.52), i.e., southern part of Japan. The maximum in the

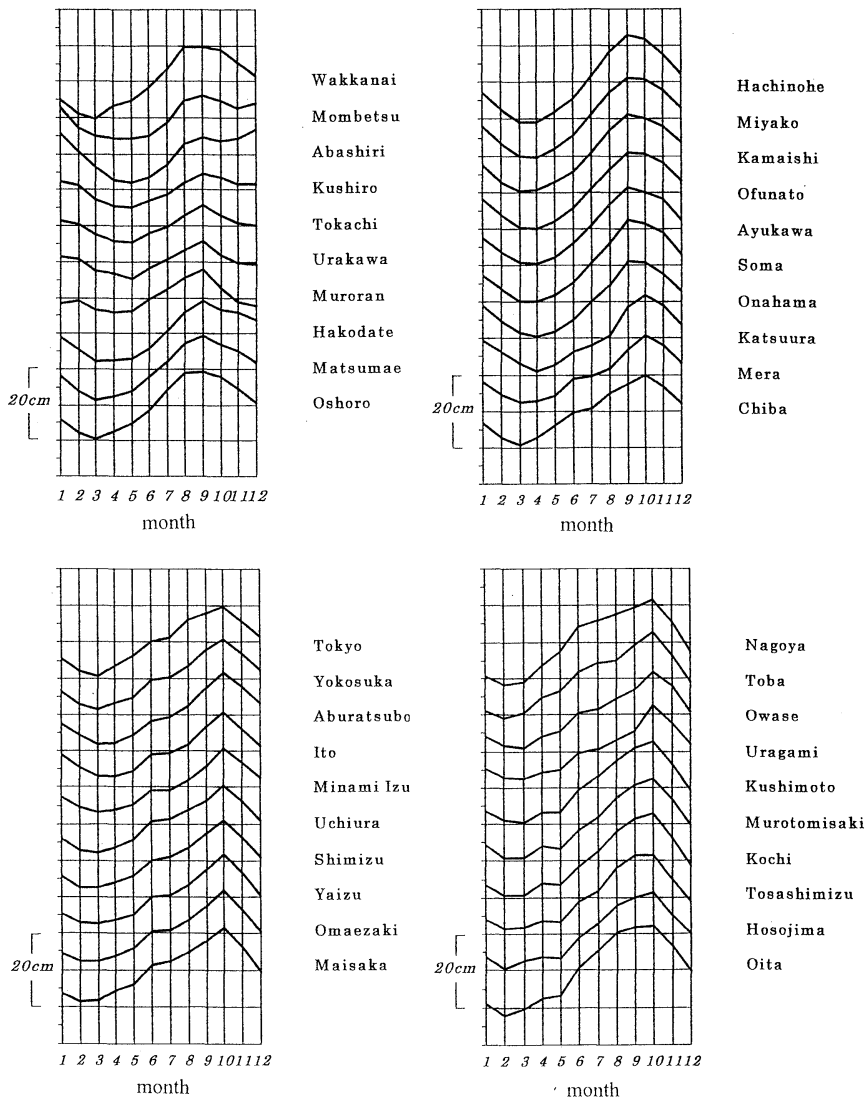


Fig. 3. Annual sea level variations at 68 tidal stations averaged from 1981 to 1990.

region from Katsuura (Stn. 18) to Makurazaki (Stn. 52) has a sharp peak, while it is a flat shape from Shirahama (Stn. 41) to Oita (Stn. 40) along the coast of the Seto Inland Sea. The minimum of the seasonal variation mostly appears between February and April, and the southern part leads the northern and eastern part by one or two month. The time difference between maximum and minimum of the seasonal variations displays the gentle ascent and steep descent along the Pacific coast.

The seasonal variations along the eastern

and southern coast of Hokkaido, i.e., Mombetsu (Stn. 2) to Muroran (Stn. 7), as shown in Fig. 1, are significantly different from the other stations in the Japanese coast, as indicated by TSUMURA (1963). Fig. 3 shows the variations of the Hokkaido coast and interesting feature with two maximum along the eastern coast from Mombetsu (Stn. 2) to Muroran (Stn. 7). The two peaks appear on September and December or January at Abashiri (Stn. 3) and Mombetsu (Stn. 2), and the peak in winter is higher than in early autumn at Abashiri (Stn.

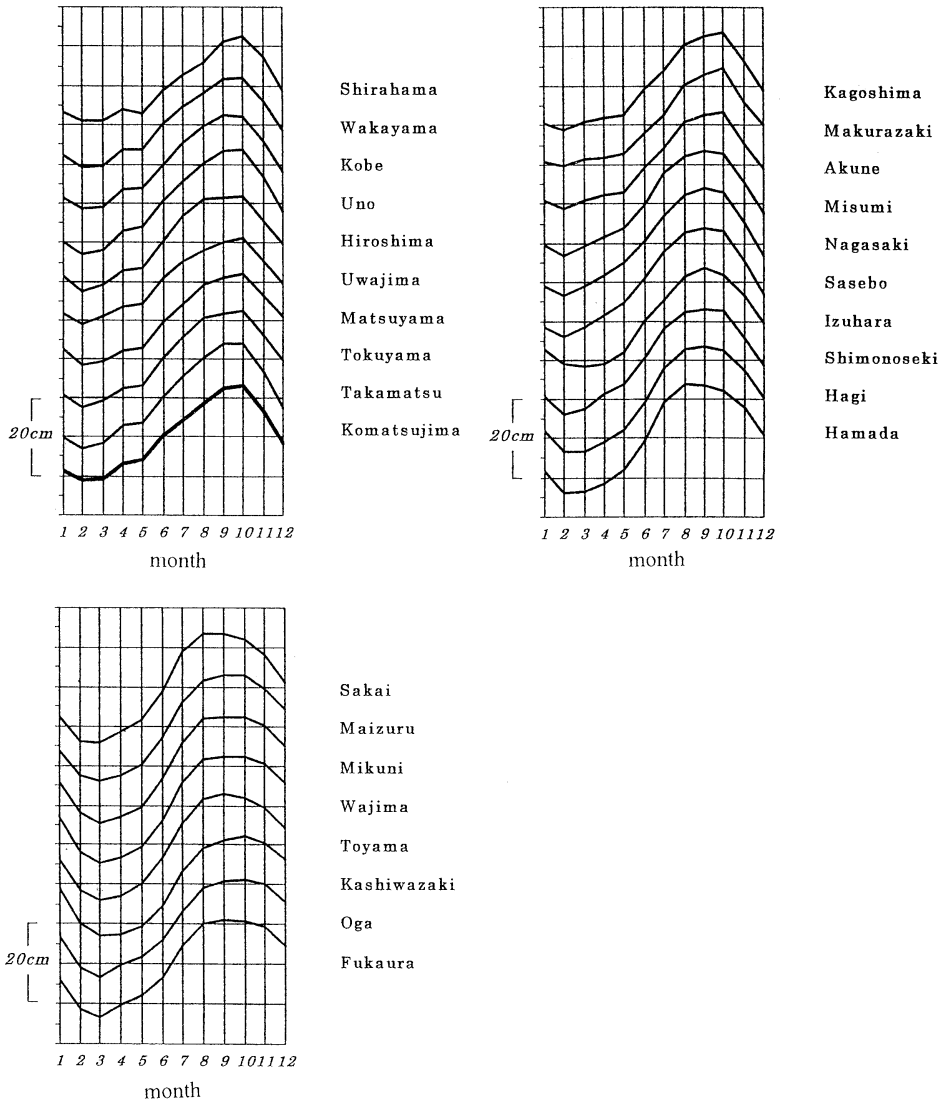


Fig. 3. (Continued)

3).

TSUMURA (1963) indicated that the sea level gently rises along the coast from Mera (Stn. 19) to Megami (Stn.55) during June to July. We can clearly find this phenomenon along the coast from Mera (Stn. 19) to Uragami (Stn. 34) during this period. In the southwestern coast from Kushimoto (Stn.35) to Hosojima (Stn. 39), including the Seto Inland Sea coast, the gentle rise of sea level appears during April to May instead of June-July. The significant difference of two-month lag is found between

Uragami (Stn.34) and Kushimoto (Stn. 35), which is a distance of 16km only. The sea level difference between both stations is very important to detect whether Kuroshio path is meandering or not along the southern coast of Japan as well (e.g., KAWABE, 1985). The westward propagation of several-day period fluctuations of sea level is also interrupted and is discontinued between both stations (NARUMI, 2002).

The other phenomenon indicated by TSUMURA (1963), which the steep descent from September to October and gentle descents from

October to December was seen in the northern part of the Japan Sea coast, couldn't be clearly found in this analysis.

4. Discussion

TSUMURA (1963) showed the seasonal variation of sea level along the Japanese coast and derived some interesting features. But, he didn't explain the relations between such the sea level variation as the above results and oceanographic phenomena. We will examine to explain these relations.

4-1 Two maximum along the eastern and southern coast of Hokkaido

The high sea level in winter is found along the coast from Mombetsu (Stn.2) to Muroran (Stn.7), and it is especially significant at Abashiri (Stn.3) and Mombetsu (Stn.2) along the Hokkaido coast in the Okhotsk Sea. The high sea level in winter in this region is related to the strength of East Sakhalin Current (WATANABE, 1963, OHSHIMA *et al.*, 2002). The southward current along the East Sakhalin coast turns eastward after arriving near the Hokkaido coast (Fig.4), so the sea level rise occur at this region by piling up of the low temperature and low salinity water (ITOH 2000). The sea level difference between Wakkanai

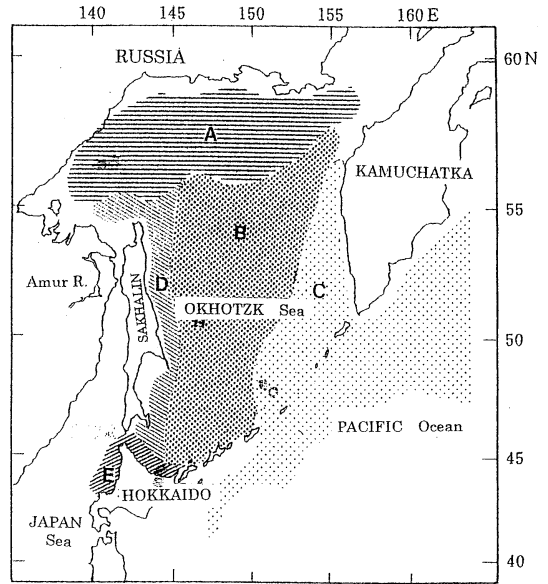


Fig. 4. Distribution of typical water mass and current in Okhotsk Sea. D is the East Sakhalin Current and E the Soya Warm Current. (After AOTA, 1987)

(Stn. 1) and Abashiri (Stn. 3) induces the Soya Warm Current (AOTA, 1975, MATSUYAMA *et al.*, 1999), so that the remarkable difference of seasonal variations between both stations directly

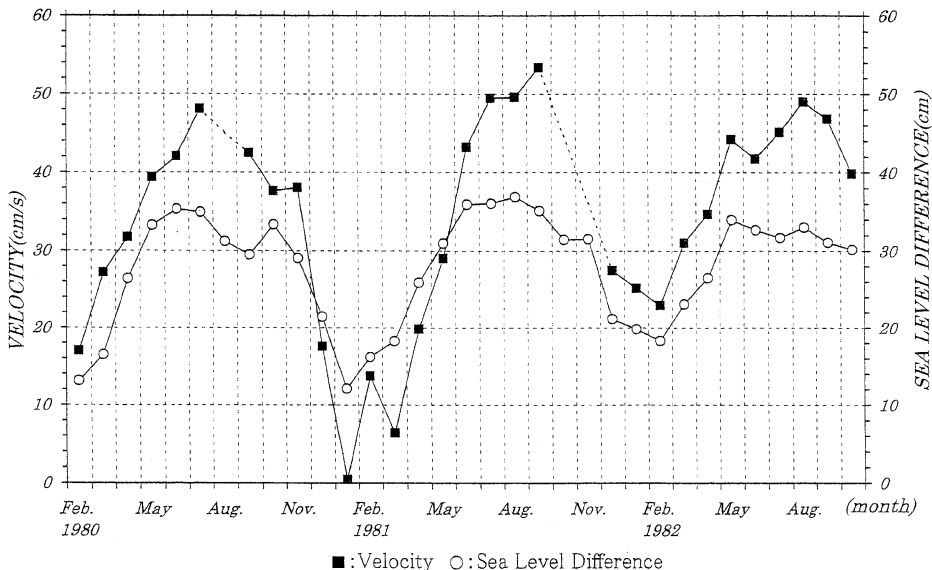


Fig. 5. Time variations of monthly-mean alongshore current 5 miles off Sarufutsu in Hokkaido and of adjusted sea level difference between Wakkanai and Abashiri (after MATSUYAMA *et al.*, 1999).

reflects the variations of the Soya Warm Current, that is, the small difference in winter indicates the weakness of the current (Fig. 5). The minimum of the sea level difference along the Hokkaido coast in the Okhotsk Sea appears on March at Wakkanai (Stn. 1) and on May at Abashiri (Stn. 3), so the Soya Warm Current indicates to be intensified from April.

The maximum of sea level in winter is also found from Kushiro to Muroran along the southeastern coast facing to the Pacific Ocean (Fig. 3). These are seen to be related to the sea level rise along the Okhotsk Sea coast from December to January. But we do not have much data to describe the relation between both phenomena in the Okhotsk Sea and the Pacific Ocean. We will investigate these phenomena in both seas, including the seasonal variation of the Oyashio.

4-2 Gentle rise of sea level along the southeastern coast of Honshu from June to July

The sea level rise is gently sloping from June to July from Mera (Stn. 19) to Uragami (Stn. 34) as seen in Fig. 3. In general, the sea level shows a sinusoidal curve as seasonal variation, and connects closely with the sea surface and subsurface temperature. Then, the small rising of sea level during June-July along the southern coast of Honshu from Boso Peninsula to Kii Peninsula is expected to connect to the low temperature in the surface and subsurface layers, as described by NOMITSU and OKAMOTO (1927).

NAKAMURA (1977) showed the seasonal variations of the temperature and salinity from the sea surface to 200m depth in and around Suruga Bay. Fig. 6 shows observation stations and the temperature distribution from the sea surface to 200 m depth at Stn. A estimated by the observational data from 1964 to 1974. From May to August, the isotherms descend near the sea surface, but they ascend in the subsurface layer. NAKAMURA (1977) called the temperature descending in the subsurface layer in this period a secondary minimum of water temperature. He presented the secondary minimum of the temperature together with the salinity maximum. T-S relation suggested the phenomena to be related to the upwelling. The

secondary minimum of the water temperature in the subsurface layer was found at the Boso coast, Sagami Bay and eastern side of the Kii Peninsula (NAKAMURA 1977). UNOKI and UNNO (1983) analyzed the distributions of secondary minimum of the subsurface water temperature from the Boso peninsula to the Kii peninsula from 1965 to 1976, and found the following three cases of appearance of the water, (1) almost the whole area, (2) limited within a partial region and (3) scarcely and scattered distribution.

The gentle rise of sea level is possible to relate on the secondary minimum indicated by NAKAMURA (1977) and UNOKI and UNNO (1983). Then we compare the sea level at Suruga Bay coast with the temperature at Stn. A in Suruga Bay and at Stn. B located at out of the bay from 1964 to 1974. Fig. 7 shows the time series of the temperature distributions at Stns. A and B shown by NAKAMURA (1977). Both stations were selected as the typical stations for the inner and outer bay, respectively. The arrows indicate the secondary minimum of the temperature in the subsurface layer, i.e., ascending of the seasonal thermocline in both stations. The temperature and salinity observations were made at every month by Shizuoka Prefectural Experimental Fishery Station. The arrows are mostly found at both stations in summer, especially August, so that the phenomena can be considered to usually exist in summer, i.e., the ascending of seasonal thermocline in August. On the other hand, Fig. 8 shows the monthly mean sea level at four tidal stations at the Suruga Bay coast from 1965 to 1974. The sea level variations resemble among four stations and show the complicated seasonal variation. The low sea level in August is found on 1965, 1967, 1969, 1970, 1973, and 1974. These years mostly agree with the years of secondary minimum in Fig. 6, but strict comparison is difficult for the difference of the sampling interval between the monthly mean data and one-time data in every month.

Then, we compare the long-term mean data between temperature and sea level. NOMITSU and OKAMOTO (1927) described the monthly mean sea level to be closely related to the density distribution from the sea surface to 200m

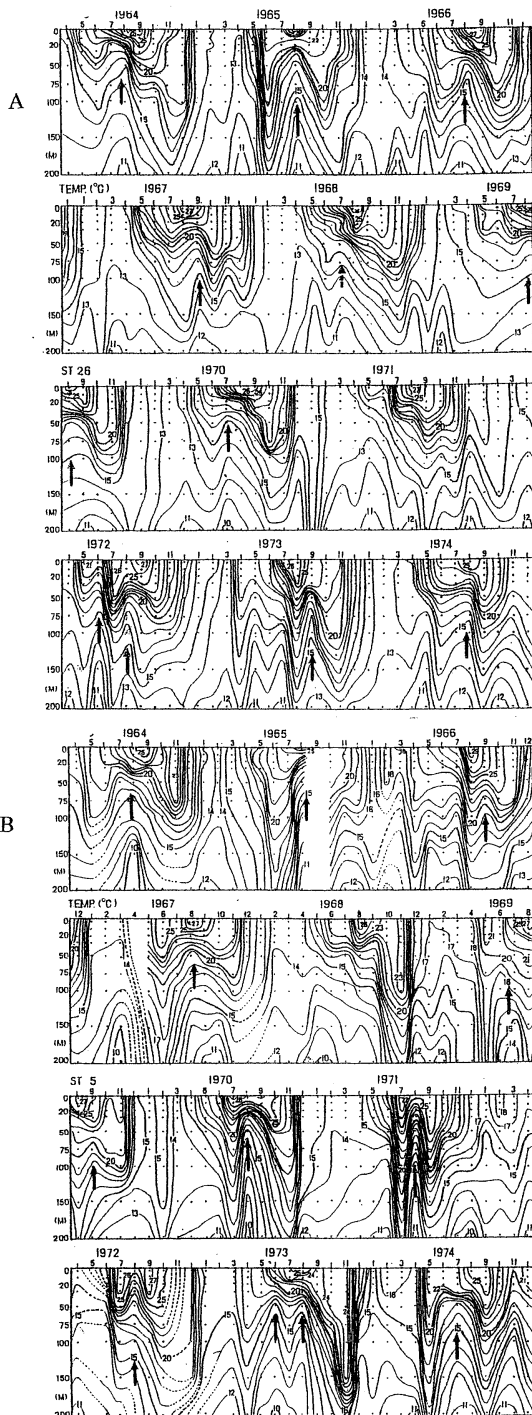


Fig. 7. Time variations of the temperature distribution at Stn. A (upper) and Stn. B (lower) from April 1964 to December 1974. Arrows show the upwelling in summer (After NAKAMURA, 1977).

days period along the southeast coast of Honshu, Japan induced by the wind. From July to August, the northward wind continues over 10 days and induces the upwelling along the Boso and Kashima coast (Fig. 10). The upwelling region propagates westward along the coast from the south of Boso Peninsula, having the characteristic of internal Kelvin waves, so that the low temperature water occupies the subsurface layer in the coastal region as such as the western coast of North America (HUYER 1977). The numerical experiments suggest the coastal upwelling due to the northward wind to be related to both gentle sloping rise of sea level at the coast and the secondary minimum of the water temperature indicated by NAKAMURA (1977).

4.3 Small sea level rise the southwestern coast of Japan in April to May

The seasonal variations of sea level also shows gentle rise in and around the Seto Inland Sea from April to May as seen in Fig. 3. Firstly the temperature variations are considered to relate to the sea level change near the coast. YANAGI (1984) investigated the seasonal variation of the temperature in this area from 1971 to 1975. He calculated the vertical mean temperature from the sea surface to bottom and for station of water depth over 50m, from the surface to 50m depth. His results show the uniform ascent of mean temperature from March to September, that is, a significant sinusoidal curve as a seasonal variation. The temperature change is different from the sea level change from April to May. As seen in Fig. 3, this anomalous seasonal change is seen at Kushimoto (Stn. 35), Murotomisaki (Stn. 36), Kochi (Stn. 37), Tosashimizu (Stn. 38) and Hosojima (Stn. 39), i.e., the southwestern coast of Japan facing to the Pacific Ocean. The reason why the gentle rise of sea level appears along the southwestern coast of Japan from April to May is not sufficiently explained in this study.

5. Summary

The seasonal change of sea level is investigated at 68 tidal stations along the Japanese coast by using the monthly mean data from

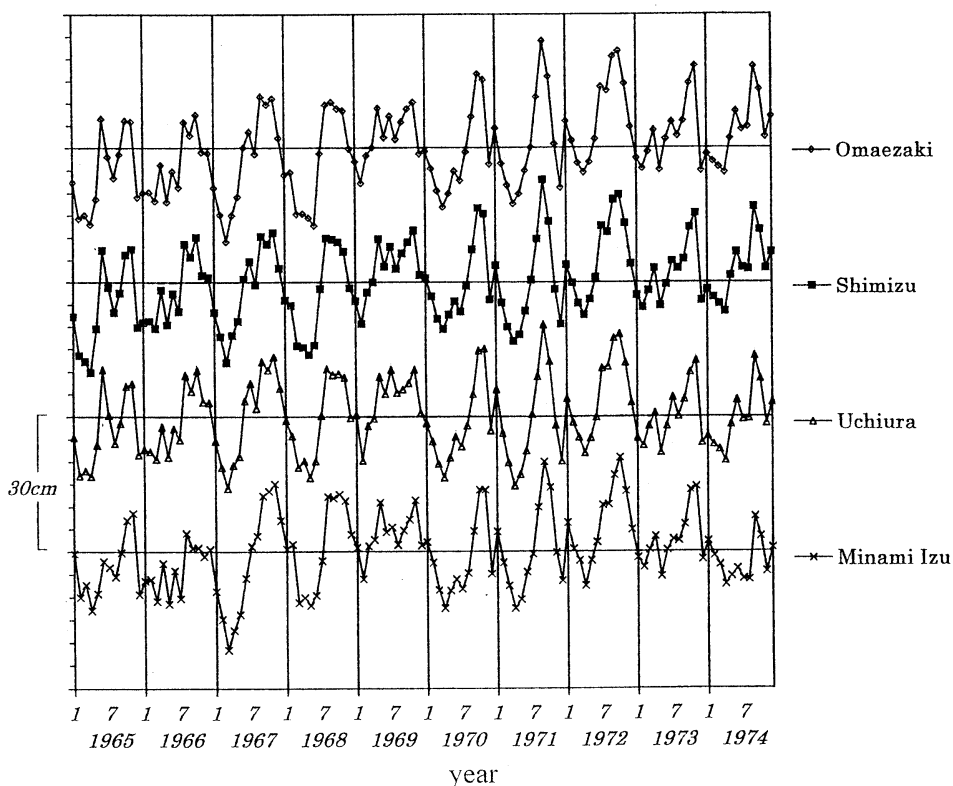


Fig. 8. Sea level Variations at Omaezaki (Stn.29), Shimizu (Stn.27), Uchiura (Stn.26) and Minami-Izu (Stn.25) from 1965 to 1974.

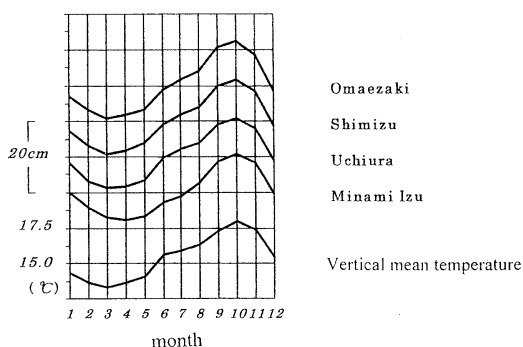


Fig. 9. Annual variations of sea level at Omaezaki, Shimizu, Uchiura and Minami-Izu, and of vertical mean temperature from the sea surface to 200m depth at Stn.26 averaged from 1964 to 1974.

change in relation to the oceanographic phenomenon such as coastal current and coastal upwelling.

The high sea level in winter is found from Mombetsu (Stn.2) to Muroran (Stn.7) along the Hokkaido Coast, and it is significant at Abashiri (Stn.3) and Mombetsu (Stn.2) along the Hokkaido coast in the Okhotsk Sea. The strength of East Sakhalin Current is considered to induce the sea level rise along the Hokkaido Coast in winter. In addition, the high sea level near Abashiri (Stn.3) in winter significantly depresses the Soya Warm Current.

The gentle sloping rise of sea level occurs from Mera (Stn.19) to Uragami (Stn.34) along the southeastern coast of Honshu from June to July. The sea level change along Suruga Bay coast agrees with the vertical mean temperature from the sea surface to 200m depth in the center of the bay. The vertical mean temperature is depressed by the seasonal thermocline

1981 to 1990. The main results mostly agree with Tsumura's results (1963) by the data during 1951 to 1960. We analyzed the seasonal change in detail and discussed the sea level

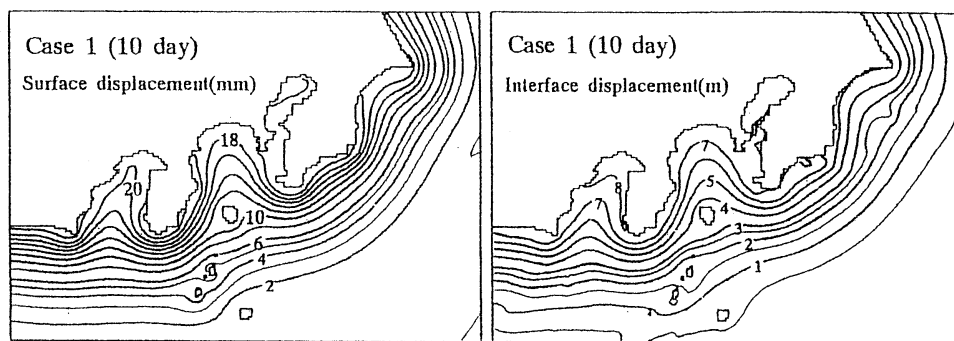


Fig. 10. Amplitude distribution of the sea level (left) and interface (right) displacement after 10 days blowing of 7ms^{-1} northward wind calculated by the two layer numerical model (After KITADE and MATSUYAMA, 2000).

ascending in spite of the surface temperature rising in this period. The phenomenon of the seasonal thermocline ascending is called as "secondary minimum of water temperature" by NAKAMURA (1977) and was frequently found in the region from the Boso Peninsula to Kii Peninsula (UNOKI and UNNO, 1983). The coastal upwelling by the northward wind in summer is suggested to induce both the gentle sea level rise and secondary minimum of the water temperature along the southeastern coast of Honshu, Japan.

The gentle sea level rise in the Seto Inland Sea and the southwestern coast of Japan also appears from April to May, but the sea level change slightly disagrees with the temperature change in the surface layer.

Acknowledgement

The authors acknowledge with many thanks to Dr. R. MURAKAMI, Geographical Survey Institute, for his contribution of the sea level data and atmospheric data, and Ms S. MATSUYAMA for her help in calculations and drawing figures. We also thank the anonymous reviewer for his valuable comments.

References

- AOTA, M. (1975) : Studies on the Soya Warm Current. *Teion Kagaku*, **33**, 151–172. (in Japanese).
- AOTA, M. (1987) : Sea of Okhotsk, *In Encyclopedia of Oceanography*. 44–46. Edited by K.Wadachi, Tokyodo-Syuppan Inc. (in Japanese).
- GILL, A.E. (1982) : *Atmosphere–Ocean Dynamics*. Academic Press Inc., Orlando, 662pp.
- HUYER, A. (1977) : Seasonal variation in temperature, salinity and density over the continental shelf off Oregon. *Limnol. Oceanogr.*, **22**, 442–453.
- IMAWAKI S. H. UCHIDA, H. ICHIKAWA, M. FUKASAWA, S. UMATANI and ASUKA Group (1997) : Time series of the Kuroshio transport derived field observations and altimetry data. *Int.WOCE Newsletter*, **25**, 15–18.
- ITOH, M. (2000) : Formation and Distribution of Okhotsk Sea Intermediate Water. Doctoral Dissertation, Hokkaido University. 62pp.
- KAWABE, M. (1985) : Sea level variations at the Izu Islands and typical stable paths of the Kuroshio. *J. Oceanogr. Soc. Japan*, **41**, 307–326.
- KISHI M.J. (1976) : Upwelling along the east coast of Izu Peninsula (1). *Umi to Sora*, **51**, 105–113.
- KISHI M.J. (1977) : Upwelling along the east coast of Izu Peninsula (2). *Umi to Sora*, **52**, 59–66.
- KITADE Y. and M. MATSUYAMA (2000) : Coastal trapped waves with several-day period caused by wind along the southeast Coast of Honshu, Japan. *J. Oceanogr.* **56**, 727–744.
- KONISHI T., E. KAMIHIRA, and T. SEGAWA (1987) : Characteristics of tide along the Japanese coast. *Marine Sciences Monthly*, **193**, 437–441. (in Japanese).
- MATSUYAMA M., M. AOTA, I. OGASAWARA and S. MATSUYAMA (1999) : Seasonal variation of Soya Warm Current. *Umi no Kenkyu*, **8**, 333–338. (in Japanese with English abstract).
- NAKAMURA Y. (1977) : The fluctuations of the oceanographic conditions in Suruga Bay and the adjacent waters. *Bull. Japan, Soc. Fish. Oceanogr.*, **30**, 8–38.
- NARUMI Y. (2002) : Several-day period fluctuations along the southern coast of Japan. Master Thesis,

- Tokyo University of Fisheries. 38pp. (in Japanese).
- NOMITSU T. and M. OKAMOTO (1927) : The causes of the annual variation of the mean sea level along the Japanese coast. *Memoirs Coll. Sci., Kyoto Imp. Univ. Ser.A*, **10**, 125-161.
- OHSHIMA K.I., M. WAKATSUCHI, Y. FUKAMACHI and G. MIZUTA (2002) : Near-surface circulation and tidal currents of Okhotsk Sea observed with the satellite-tracked drifters (submitted to *J. Geophys. Res.*).
- PICKARD G. L. and W. J. EMERY (1990) : *Descriptive Physical Oceanography*. (5th ed.). Pergamon Press, 320pp.
- SENJYU, T., M. MATSUYAMA and N. MATSUBARA (1999): Interannual and decadal sea-level variations along the Japanese coast. *J. Oceanogr.* **55**, 619-633.
- TSUMURA, K. (1963) : Investigation of the mean sea level and its variation along the coast of Japan (Part 1) regional distribution of sea level variation. *J. Geod. Soc. Japan*, **9**, 49-90. (in Japanese with English abstract).
- UNOKI S. and Y. UNNO (1983) : On the fall of water temperature in warm seasons appearing in the coastal sea of Tokai and Kanto districts, the southeast of Japan. *Bull. Japanese Soc. Fish. Oceanogr.*, **44**, 17-28. (in Japanese with English abstract).
- WATANABE, K. (1963) : On the reinforcement of the East Sakhalin Current preceding to the sea ice season off the coast of Hokkaido. *Oceanogr. Mag.*, **14**, 117-130.
- YANAGI, T. (1984) : Seasonal variations of water temperature in the Seto Inland Sea. *J. Oceanogr. Soc. Japan*, **40**, 445-450.

Received July 12, 2002

Accepted September 10, 2002

Tide, Tidal Current and Sediment Transport in Manila Bay

Wataru FUJIE*, Tetsuo YANAGI** and Fernando P. SIRINGAN***

Abstract: Tide, tidal current and residual flow in Manila Bay are calculated using two-dimensional and three-dimensional numerical models and the mean bottom stress vector is estimated. Mean bottom stress vector expresses the direction of sediment transport. Calculations of the sediment transport direction off Pampanga and along the shoreline of Cavite are in good agreement with the observations by SIRINGAN and RINGOR (1998). The sediment transport in the whole region of Manila Bay can be estimated from the result of model calculation. The bottom sediment does not flow from Manila Bay but is transported into the bay through the bay mouth.

Key words: *Sediment transport, Mean bottom stress, POM, Manila Bay*

1. Introduction

Manila Bay is located along the southern coast of Luzon Island (Fig. 1). There are many industrial factories along its coast. These factories use water of Manila Bay as cooling water or waste disposal system. Manila Bay supplies fish for the people. Recently, water quality in Manila Bay has been deteriorated by drainage from the factories that are distributed along the coast (KATO, 1999). The substance from the land is conveyed through a river and accumulates in the bay. It is important to investigate how suspended substances are transported in the bay. On the basis of the analysis of surface sediment, SIRINGAN and RINGOR (1998) showed that the transport direction of surface sediment is southward off Pampanga and northeastward off Cavite.

In this study, we calculate tidal current and residual flow using numerical model in order to examine the relationship between the current field and the surface sediment transport in Manila Bay. Tide and tide-induced residual cur-

rent are calculated using a horizontal 2-dimensional barotropic model. The wind-driven current and the density-driven current are calculated using the Princeton Ocean Model (POM). The mean bottom stress vector is estimated using calculated current field and the result is compared with the observed one.

2. Numerical model

Tide and tidal current

Tidal amplitude spectrum in Manila harbor shows that both K_1 and O_1 constituents have the amplitude of about 30 cm and M_2 and S_2 constituents have 19cm and 6 cm, respectively (Admiralty Tide Tables, 2001). Since the length of Manila Bay is about 18 km, mouth correction coefficient is 1.2 and the mean depth is about 20 m, the co-oscillation period of the bay is about 6.1 hours (UNOKI, 1993). This value is close to M_4 tidal period and M_4 constituent cannot be ignored in Manila Bay although its amplitude 3 is not known.

Along the open boundary, the sea surface elevation is prescribed by linear interpolation using harmonic constants of M_2 , S_2 , K_1 and O_1 constituents at Mariveles and Puerto Azul. The M_4 constituent is generated by the non-linear effect of M_2 tide.

The governing equations are expressed by

*Department of Earth System Science and Technology, Kyushu University, Kasuga 816-0814, Japan

**Research Institute for Applied Mechanics, Kyushu University, Kasuga 816-0814, Japan

***University of the Philippines, Diliman, Quezon City 1101, the Philippine

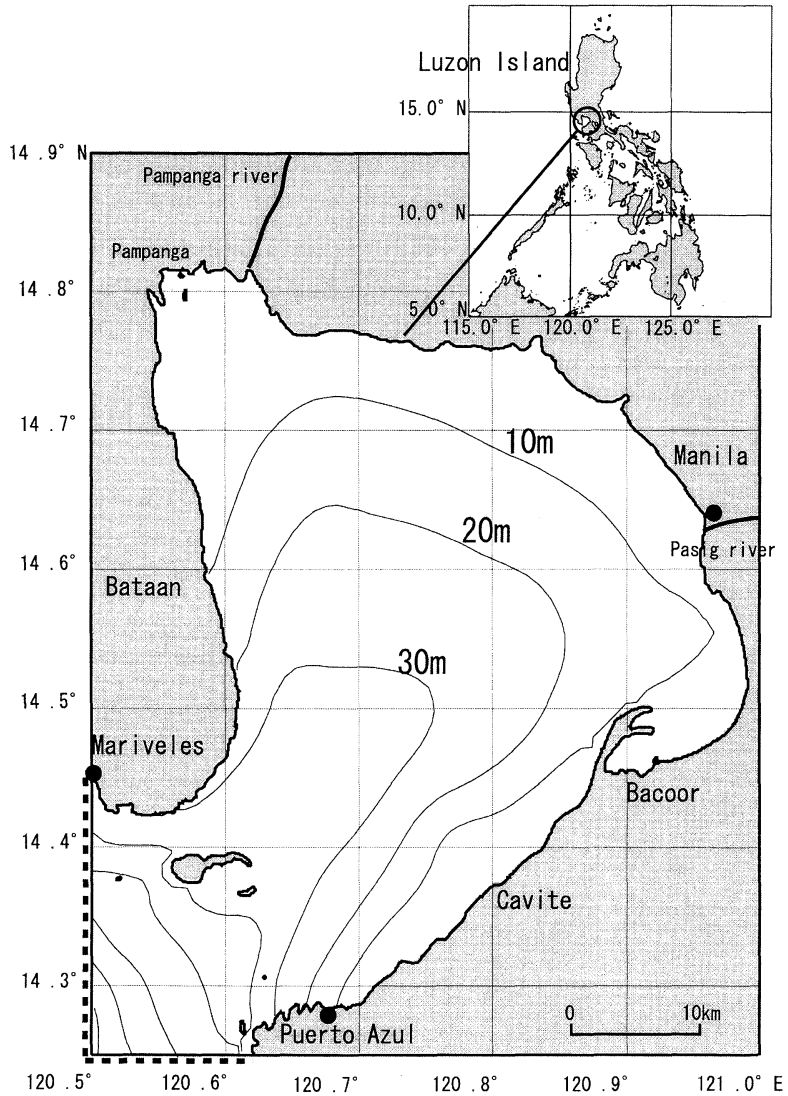


Fig. 1. Model area with bathymetry. Closed circles show the tide gauge stations. Broken line shows the open boundary of the numerical model, and thick lines show rivers flowing into Manila Bay.

$$\begin{aligned} \frac{\partial \mathbf{u}}{\partial t} + (\mathbf{u} \cdot \nabla) \mathbf{u} + f \mathbf{k} \times \mathbf{u} \\ = -g \nabla \zeta - \frac{\gamma_b^2 \mathbf{u} |\mathbf{u}|}{H + \zeta} + \nu \Delta \mathbf{u}, \end{aligned} \quad (1)$$

$$\frac{\partial \zeta}{\partial t} + \nabla \cdot \{(H + \zeta) \mathbf{u}\} = 0, \quad (2)$$

here, \mathbf{u} is the depth averaged horizontal velocity vector, ∇ the horizontal differential operator, f the Coriolis parameter ($= 3.651 \times 10^{-5} \text{ s}^{-1}$), \mathbf{k} the locally vertical unit vector, g the gravitational acceleration ($= 9.8 \text{ m sec}^{-2}$), ζ

the sea surface elevation above the mean sea level, γ_b^2 the bottom frictional coefficient ($= 2.6 \times 10^{-3}$), H the local depth, and ν the horizontal eddy viscosity ($= 10 \text{ m}^2 \text{ sec}^{-1}$). The horizontal grid size is 1000 m. Maximum depth is 81.5 m. Time step for the calculation is 2.0 sec. The integration was carried out for 510 hours (21.3 days) in all. Harmonic analysis is carried out using calculated results for last 15 days.

Calculated co-range and co-tidal charts of M_2 , S_2 , K_1 , O_1 and M_4 are shown in Fig. 2. M_2

tidal amplitude is 15.0 cm at the mouth of Manila Bay and about 20 cm in Pampanga. M_2 tidal wave travels counterclockwise from the mouth of Manila Bay to Pampanga. S_2 tidal amplitude is 4.6 cm at the mouth of Manila Bay. It becomes 6.4 cm in Pampanga. K_1 tidal amplitude is 27.5 cm at the mouth of Manila Bay and 29.0 cm in Pampanga. O_1 tidal amplitude is 25.0 cm at the mouth of the bay and 27.0 cm in Pampanga. M_4 tidal amplitude is 1.5 cm at the mouth of Manila Bay and becomes 6.0 cm in Pampanga.

Table 1 shows the ratio of tidal amplitude at the mouth to that at the head of the bay off Pampanga. Quarter-diurnal tidal amplification is the largest, about 400%, and diurnal tidal one is the smallest, about 110%, because the co-oscillation period of Manila Bay is 6.1 hours.

Figure 3 shows the comparison of observed and calculated results of M_2 , S_2 , K_1 and O_1 tides at Manila harbor. The root mean squared error is 1.1 cm for tidal amplitude and 2.9° for tidal phase. This calculation of tides well reproduces the observed result in Manila Bay.

Calculated tidal currents are shown in Fig. 4. M_2 tidal current amplitude is about 15 cm/s at the mouth of Manila Bay. It flows crossing the mouth of the bay. Off Pampanga, it becomes about 10 cm/s. S_2 tidal current amplitude is about 5 cm/s at the mouth of the bay and 5 cm/s off Pampanga. M_4 tidal current amplitude is about 5 cm/s at the mouth of the bay and becomes 5 cm/s off Pampanga. K_1 tidal current is about 12.0 cm/s at the mouth of the bay and 8.0 cm/s off Pampanga. O_1 tidal current amplitude is about 10.0 cm/s at the mouth and 9.0 cm/s off Pampanga. M_2 tidal current is most dominant in Manila Bay although K_1 and O_1 tidal amplitudes are larger than M_2 . The reason is due to the shorter period of M_2 constituent than K_1 and O_1 .

Residual flow

According to phase differences between tidal constituents, phases of M_2 , S_2 , K_1 and O_1 tides will be in agreement every 30 days. Therefore, we have to carry out 30 days calculation in order to estimate the tide-induced residual current by M_2 , S_2 , K_1 , O_1 and M_4 constituents, which is shown in Fig. 5. The speed of tide-

induced residual current is less than 1 cm/s, with the exception of 5 cm/s at the mouth of the bay. A clockwise circulation is generated at the mouth of the bay.

We calculate the wind-driven and density-driven currents using Princeton Ocean Model (BLUMBERG and MELLOR, 1987). Please refer to POM users guide (MELLOR, 1996) about the details of the governing equations. The horizontal grid size is the same as that 5 used for tide and tidal current. The vertical division is 14.

We applied a radiation condition along the open boundary as follows:

$$\frac{\partial \bar{U}}{\partial t} \pm C_e \frac{\partial \bar{U}}{\partial x} = 0, \quad (3)$$

$$C_e = \sqrt{gH} \quad (4)$$

Here, \bar{U} is a vertically integrated residual flow velocity, C_e the phase velocity of long wave and H the water depth. Calculation is carried out for 40 days. The time step is 2 seconds for the external mode. As for the internal mode, it is 120 seconds that is 60 times the external mode.

There are 2 major rivers flowing into Manila Bay, Pampanga River in Pampanga and Pasig River in Manila city (Fig. 1). We ignore many small rivers around Pampanga because of their small discharges (Siringan and Ringor, 1998). Average sea surface heat flux in 1993 and 1994 are estimated from ECMWF (European Centre for Medium-Range Weather Forecast).

Figure 6 (a) shows the average wind direction and speed from 1961 to 1995 at Manila. From February to May, wind direction is from southeast. From June to September, wind direction is from southwest. From November to January, wind direction is from northeast. We calculate three types of wind-driven currents, for southeast, southwest and northeast winds. They correspond to April, September and November. Therefore, sea surface heat flux (Fig. 6b) and river discharge (Fig. 6c) in April, September and November are considered as boundary conditions of the model calculation.

Calculated wind-driven and density-driven currents in April, September and November are shown in Fig. 7, respectively. Large variability is seen in the wind-driven and density-driven currents field. Although wind-driven

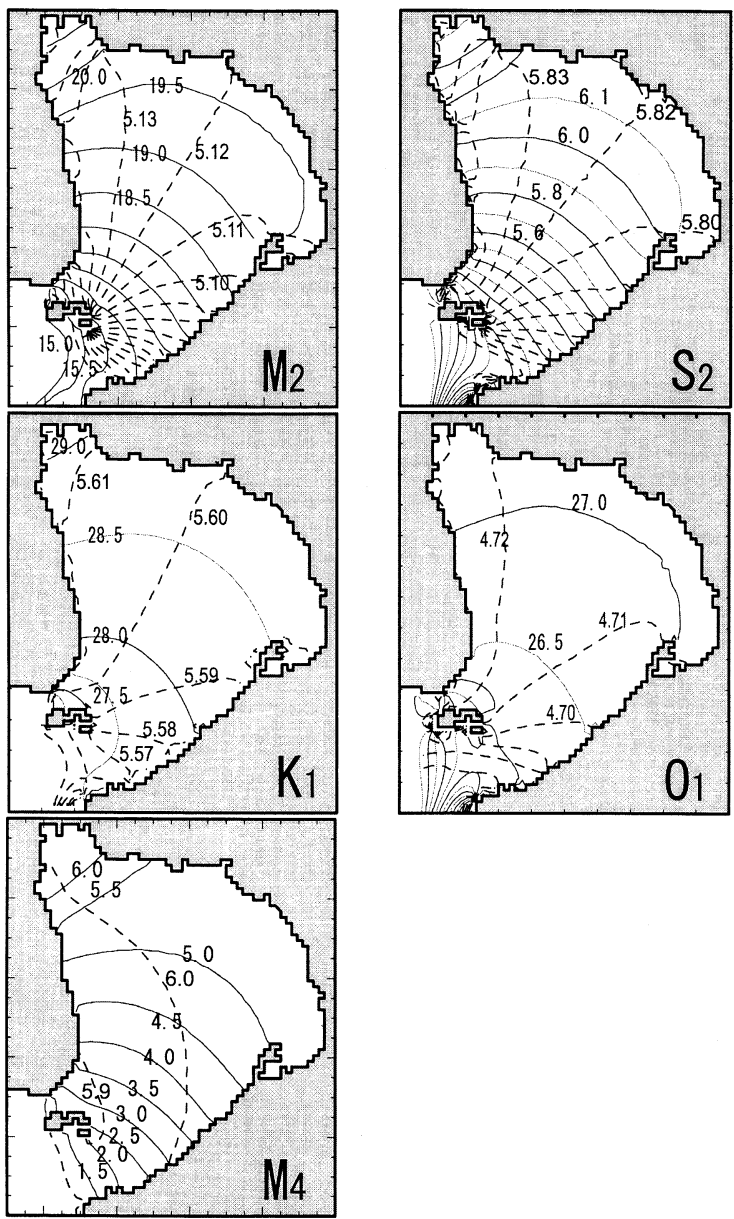


Fig. 2. Calculated co-range (thin line, unit in cm) and co-tidal (dashed line, unit in radian)charts of M_2 , S_2 , K_1 , O_1 and M_4 constituents.

Table 1 Tidal amplification ratio of each constituent from the mouth to the bay head in Manila Bay.

Constituent	M_2	S_2	K_1	O_1	M_4
Amplification ratio(%)	130	133	107	110	400

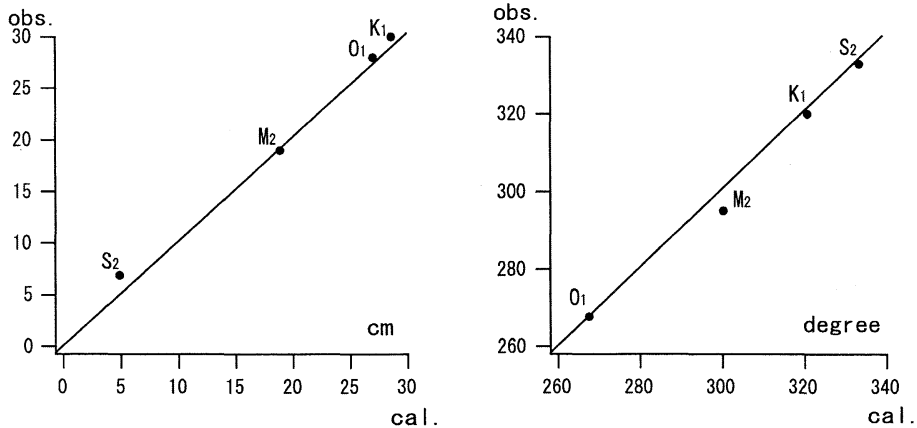


Fig. 3. Comparison of observed and calculated results of tidal amplitude and phase at Manila harbor.

current predominates in the surface layer, its influence is small in the bottom layer. Wind-driven and density-driven currents speed is about 5 cm/s above the bottom. Near the head of the bay, they flow along the wind direction. In the place where depth is large, the compensated flow is dominant.

Sediment transport

The mean bottom stress vector is calculated using obtained results of M_2 , S_2 , K_1 , O_1 and M_4 tidal currents, tide-induced residual current, wind-driven and density-driven currents. The mean bottom stress $\bar{\tau}_B$ is calculated by the following equation (Yanagi and Fuji-ie, 2001).

$$\bar{\tau}_B = \rho_w C_D \frac{1}{T} \int_0^T u \sqrt{u^2} dt, \quad (5)$$

$$u = u_{M_2} + u_{S_2} + u_{K_1} + u_{O_1} + u_{M_4} + u_T + u_r, \quad (6)$$

where $\rho_w (=1.022 \text{ kg/m}^3)$ denotes the water density, $C_D (=0.0024)$ the bottom drag coefficient, $T (=30 \text{ days})$ the averaging period, each of $u_{M_2} + u_{S_2} + u_{K_1} + u_{O_1}$ and u_{M_4} is tidal current velocity vector, u_T is tide-induced residual current, and u_r is velocity vector of residual flow whose components are density-driven and wind-driven currents. Here over bar means the average in 30 days.

Horizontal distributions of calculated mean bottom stress vector in April, September and November are shown in Fig. 8. Mean bottom stress toward northeast is common at the mouth of the bay in April, September and November. The sediment transport direction is

toward west along the shoreline at the north-eastern head of the bay in April and November. Off Cavite, although the transport direction in September is toward northeast, it is toward southwest in November. In April, it is toward southeast. Such variation is due to the seasonal variation of wind-driven current.

Figure 9 (a) shows averaged sediment transport vector in April, September and November and Fig. 9 (b) the sediment transport path estimated by the field observation of Siringan and Ringor (1998). From the calculation off Pampanga, the sediment transport is toward southeast. Off Bataan, the sediment transport is toward north. Off Cavite, the sediment transport is toward northeast (Fig. 9a). These calculation results agree with the observation results by SIRINGAN and RINGOR (1998). From the calculation result, there is a convergence of sediment transport in the center of Manila Bay and sediment transport is into the bay at the mouth of the bay.

3. Conclusion

The average sediment transport direction in Manila Bay is calculated by averaging the mean bottom stress vector in April, September and November. The results are in agreement with the results of field observation by SIRINGAN and RINGOR (1998). Therefore, the result of this study can explain the sediment transport in a long time scale.

The seasonal variation in the direction of

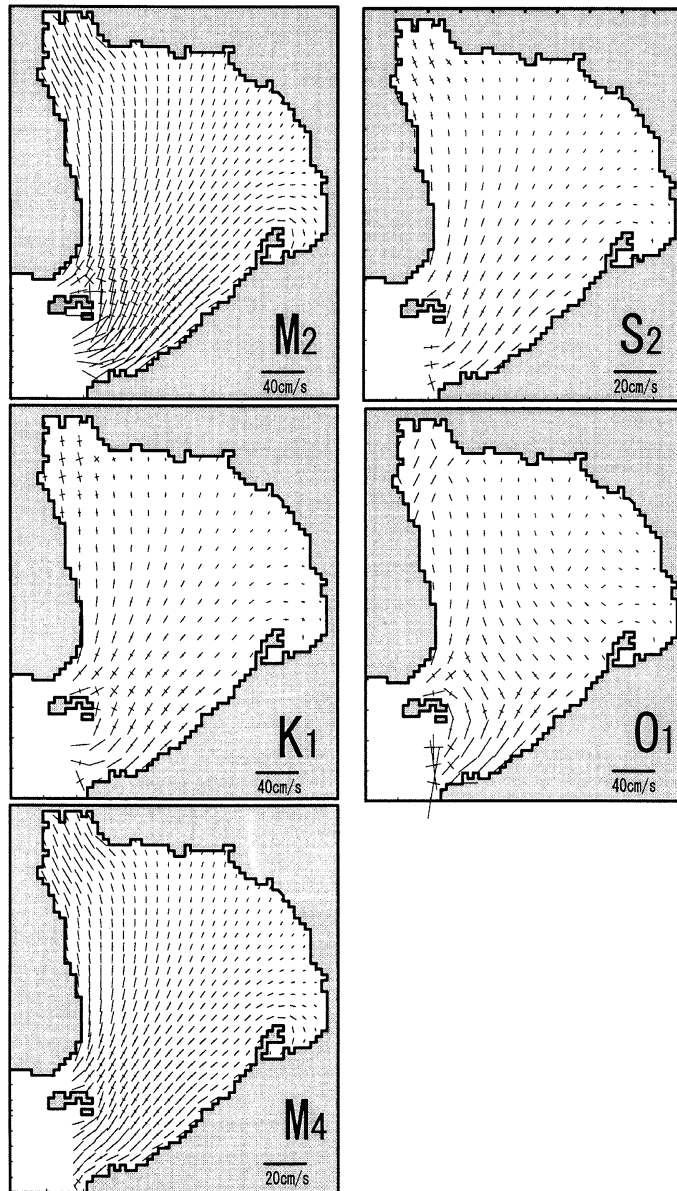


Fig. 4. Calculated long and short axes of M_2 , S_2 , K_1 , O_1 and M_4 tidal current ellipses.

sediment transport in Manila Bay, mainly seen at the shallow area, depends on the variability of wind-driven and density-driven currents.

It is very interesting that transport vector is directed into the bay at the mouth of Manila Bay. This result suggests that bottom sediments are always transported from the bay mouth into the bay and sediments do not flow from Manila Bay. Therefore, the prevention of

contamination from the land is very important in Manila Bay in order to preserve the sediment environment there.

Next, we will calculate the transport direction of various substances such as suspended matter.

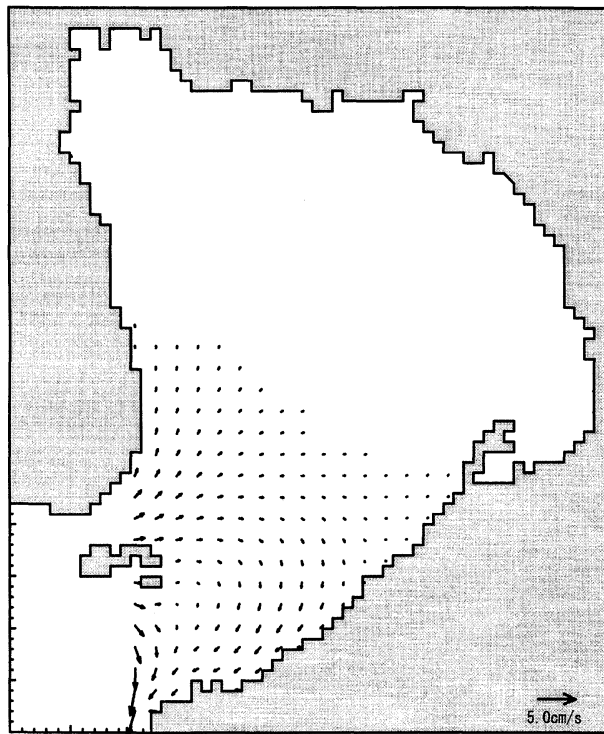


Fig. 5. Calculated tide-induced residual current by M_2 , S_2 , K_1 , O_1 and M_4 constituents. Only the flow velocities larger than 0.5cm/s are shown.

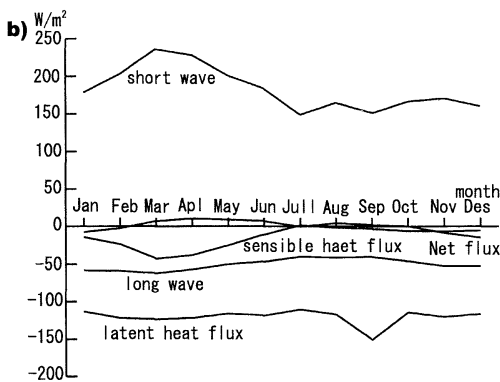
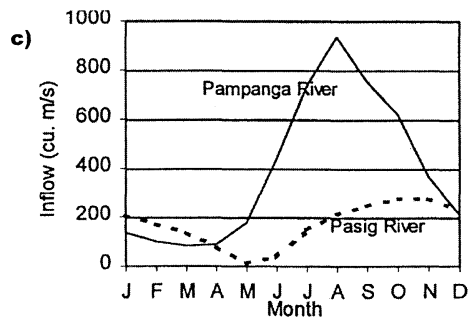
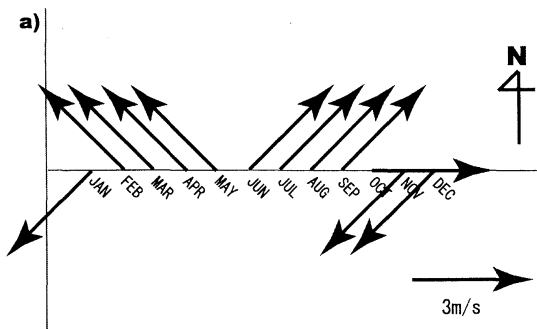


Fig. 6. Wind speed and direction at Manila. (average in 1961–1995, Philippine Atmospheric, Geophysical and Astronomical Services Administration) (a). Heat flux in Manila Bay (average over 1993–1994, ECMWF). Positive value represents downward heat flux(b). River discharge from Pampanga and Pasig rivers(SIRINGAN and RINGOR, 1998)(c).

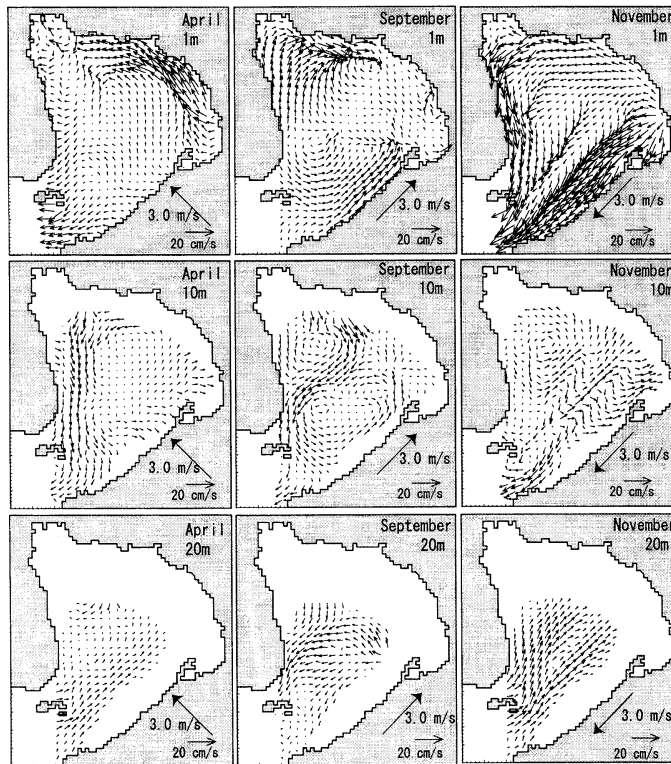


Fig. 7. Wind-driven and density-driven currents calculated for April, September and November.

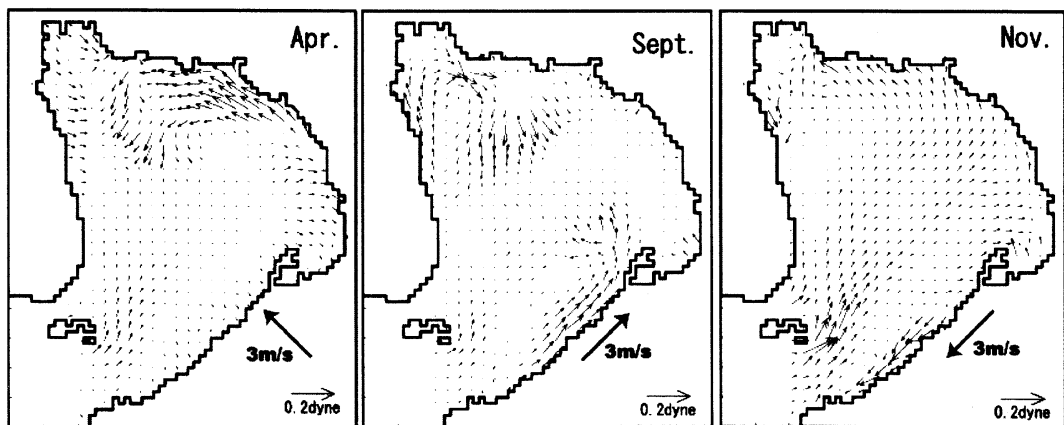


Fig. 8. Horizontal distribution of mean bottom stress vector during 30 days in Manila Bay in April, September and November.

References

ADMIRALTY Tide TABLES (2001) : Indian Ocean and South China Sea (Including tidal stream tables): The hydrographer of the Navy; 3, 416p.
 BLUMBERG, A. F. and G. L. MELLOR (1987) : A description of a three dimensional coastal ocean

circulation model. Three-Dimensional Coastal Ocean Models, Coastal and Estuarine Sciences, Vol. 4, N. Heaps, ed., Amer. Geophys. Union, 1-16.
 KATO, S. (1999) : Current Status of Water Quality in Philippines: Public Health and Environment Research Division, Mie Pref. Science & Technology

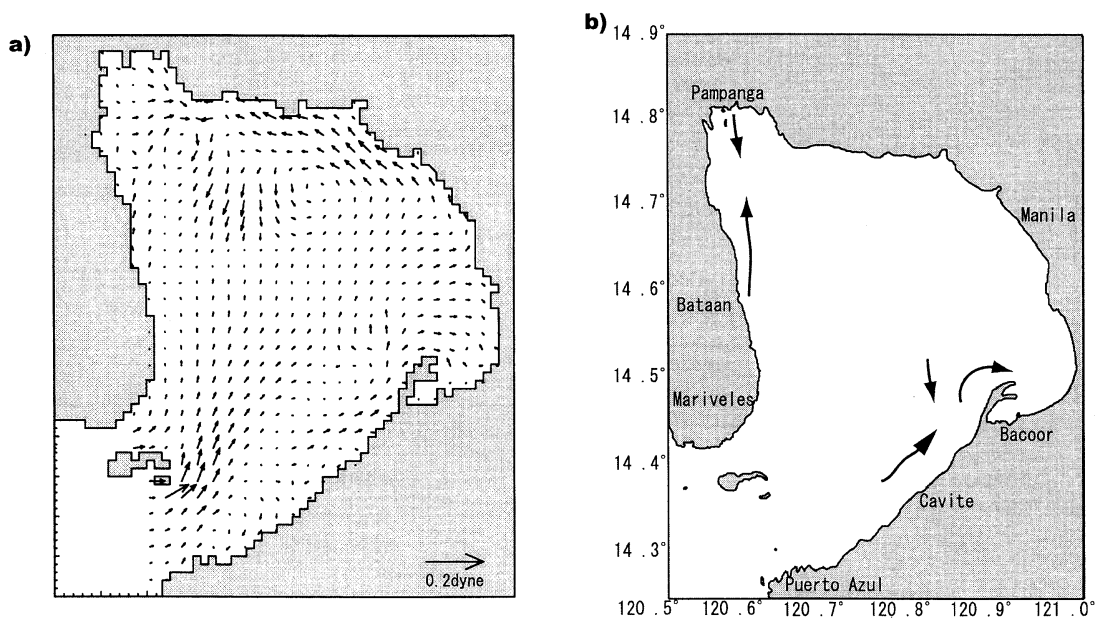


Fig. 9. (a) Calculated horizontal distribution of average mean bottom stress vector throughout the year. (b) Observed pattern of sediment transport path by Siringan and Ringor (1998).

Promotion Center Report, 19, 23–33.

UNOKI, S. (1993) : Coastal physical oceanography, Tokai Univ. Press. 674pp. (in Japanese).

MELLOR, G. L. (1996) : Users guide for a three-dimensional, primitive equation, numerical model. Princeton University, 38pp.

SIRINGAN, F. P. and L. RINGOR (1998) : Changes in bathymetry and their implications to sediment

dispersal and rates of sedimentation in Manila Bay. Science Diliman, 2, 12–26.

YANAGI, T. and W. FUJI-IE (2001) : Transport of bottom sediment in the coastal sea of Okinawa, Umi-no-kenkyu, 10 (6), 485–494 (in Japanese).

Received June 6, 2002

Accepted September 30, 2002

Seasonal Variations in Circulation and Salinity Distributions in the Upper Gulf of Thailand: Modeling Approach

Anukul BURANAPRATHEPRAT^{*1}, Tetsuo YANAGI^{*2} and Pichan SAWANGWONG^{*1}

Abstract : Seasonal variations in circulation and salinity distributions in the upper Gulf of Thailand are investigated by using a 2-D hydrodynamic model. The computed results of circulation are used as inputs in a simple model to calculate salinity distribution to verify the computed results with those of the observation from a previous study. The model succeeds to reproduce salinity distribution that confirms the reliability of computed circulation. During the southwest monsoon, a clockwise gyre is generated near the head of the Gulf with northward inflow and southward outflow in the southwest and the southeast of the upper Gulf, respectively. However, there is no complete gyre during the northeast monsoon, just flow along the coast from the east to the west, and then flow out of the Gulf at the southwest, consecutively. The results roughly inform the oceanographic condition regarding the occurrence of strong eutrophication in the eastern part of the upper Gulf during the southwest monsoon. More realistic 3-D hydrodynamic model and ecological model will be used to investigate the mechanism of this phenomenon in the future.

Key words : *Gulf of Thailand, wind-driven current, seasonal variation, salinity distribution*

1. Introduction

The upper Gulf of Thailand (Fig.1) is located in the tropical region at 13°N and 100°E. It is surrounded by land in the eastern, northern and western sides, and is open to the lower Gulf of Thailand via the southern border. It has an approximate area of 10⁴ km² with the maximum depth of 40 m at the southeastern area. The area is under the two-monsoon wind system, the dry northeast (November to January) and the wet southwest monsoon (May to August). The northeast wind during the northeast monsoon brings cool and dry air from Siberia, while the west to southwest winds bring moist air from the Indian Ocean into the region (SOJISUPORN, 1994).

The upper Gulf is one of the significant economic areas for the Thai nation. Large-scale farming of the green mussel is largely confined

to coastal areas in the upper region of the Gulf of Thailand, and the major mussel-producing provinces are all close to Bangkok where major markets are located (CHALERMWAT and LUTZ, 1989). Fisheries are also important in such a shallow area. Although overfishing has almost wiped out the high-priced fish species, the income from local fishery is still a major one. Furthermore, maritime activities are rapidly stimulated in present time because of industrial development. Therefore, many commercial ports are developed and located around the upper Gulf. However, tourism and recreation activity are also important for the nation income and cannot be overlooked.

Rapid country development and population growth have resulted in pollution problem and deterioration of the Gulf condition. Anyway, the most conspicuous and widespread pollution impact on the marine environment of the Gulf is perhaps eutrophication (CHONGPRASITH and SRINETH, 1998). And consequently, massive blooms of phytoplankton frequently occurred in the area, especially in the eastern side of the upper Gulf of Thailand (SOJISUPORN, 1994;

^{*1}Department of Aquatic Science, Faculty of Science, Burapha University

T. Saensuk, A. Muang, Chonburi 20131 Thailand

^{*2}Research Institute for Applied Mechanics, Kyushu University

Kasuga, Fukuoka, 816-8580 Japan

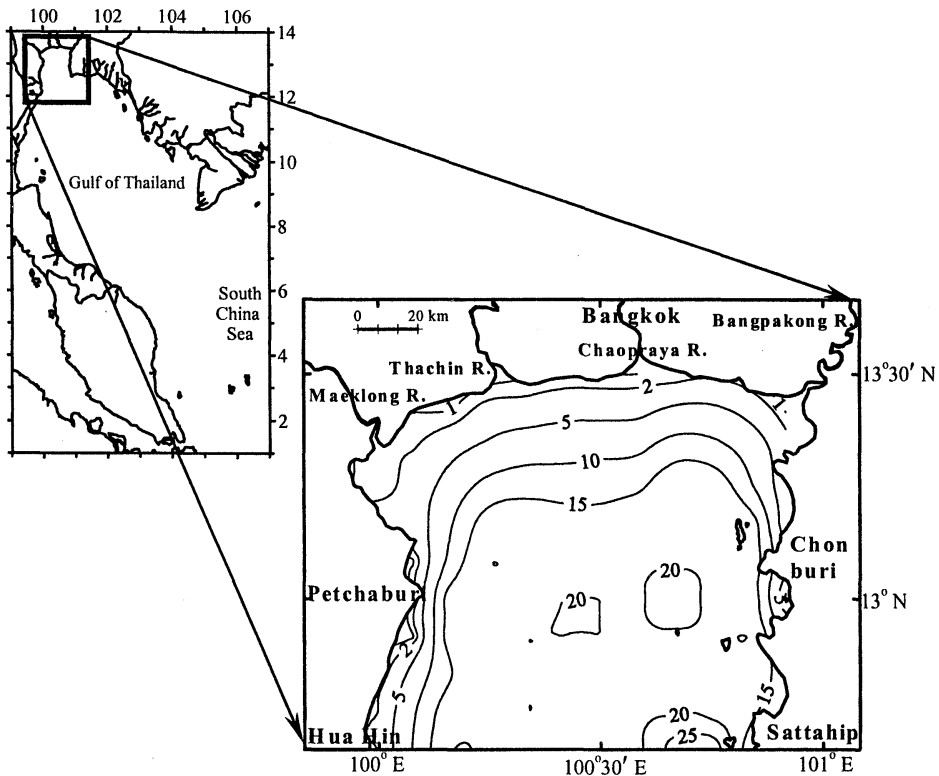


Fig. 1. The upper Gulf of Thailand. Contours show the depth in meters.

CHONGPRASITH and SRINETH, 1998). One of the major causes of phytoplankton bloom is from excessive nutrients and organic pollutants carried down by major rivers in the head of the upper Gulf, namely the MaeKlong, the Thachin, the Chaopraya and the Bangpakong, located from the west to the east, respectively. However, the reason why blooming frequently appeared in the eastern part of the upper Gulf is still not understood well.

According to the importance and problems of the upper Gulf of Thailand, understanding in oceanographic condition becomes the vital key to access the ways to use it sustainably. Many studies have been done (e.g. NEDECO, 1965; NEELASRI, 1981; SOJISUPORN and PUTIKIATIKAJORN, 1998) but their results of circulation are different depending on the methods and assumptions of the authors. Therefore we cannot clarify the oceanographic view of the area and still in doubt at present time. As

for the seasonal variation of 3-D circulation in the whole area of the Gulf of Thailand, numerical experiment (YANAGI and TAKAO, 1998) is already conducted. However the information on the upper Gulf is limited because their mesh size is too large as 10 km.

Although direct measurement is the best way to get the oceanographic information, it consumes very much time and budget. With the hope to get the general information of seasonal variation of the circulation in this area, this is a try to investigate the circulation in the upper Gulf by using a 2-D hydrodynamic model. And, the results of circulation will be applied as inputs to calculate the seasonal salinity distributions, which will be compared with those of the observation from a previous study.

2. Numerical experiment

In order to find out the horizontal circulation

of the upper Gulf of Thailand, a prognostic numerical model developed by BUNPAPONG *et al.* (1985), and BURANAPRATHEPRAT and BUNPAPONG (1998) is adopted. This model uses ADI (Alternating Direction Implicit) technique to solve the governing momentum and continuity equations shown as follows:

$$\frac{\partial u}{\partial t} - 2\Omega \sin \phi \cdot v + gD \frac{\partial \eta}{\partial x} = T_{sx} - T_{bx}, \quad (1)$$

$$\frac{\partial v}{\partial t} - 2\Omega \sin \phi \cdot u + gD \frac{\partial \eta}{\partial y} = T_{sy} - T_{by}, \quad (2)$$

and

$$\frac{\partial u}{\partial x} + \frac{\partial v}{\partial y} + \frac{\partial \eta}{\partial t} = 0, \quad (3)$$

where x and y are distance in east - west and north - south directions (m), respectively, u and v are transports per unit width (m^2/s) in x and y directions, respectively, η is water elevation (m), g is gravitational acceleration (9.8 m/s^2), D is averaged depth (m), t is time (s), Ω is angular velocity of the Earth rotation ($7.29 \times 10^{-5} \text{ rad/s}$), ϕ is latitude (radian), T_{sx} and T_{sy} are wind stress terms in x and y directions, respectively, and T_{bx} and T_{by} are bottom stress terms in x and y directions, respectively. The general forms of surface and bottom stress terms are presented in equations (4) and (5).

$$T_s = k_s |W| W, \quad (4)$$

$$T_b = k_b |V| V, \quad (5)$$

where k_s is wind stress coefficient (1.1×10^{-6}), and k_b is bottom stress coefficient (2.5×10^{-6}) (BUNPAPONG *et al.* 1985), W is wind velocity at 10 m above sea level (m/s), and V is water current vector (m/s). In the momentum equations (equations (1) and (2)), we neglect the terms of horizontal viscosity because they are considered to be very small in order of magnitude when comparing with other terms. The spherical coordinate is used with grid spacing 1×1 minute in latitude and longitude (about 1.7 km), respectively. Thus, the spatial derivative terms in equation (1) to (3) will be transform according to equation (6) and (7).

$$\frac{\partial}{\partial x} = \frac{1}{a \cos \phi} \frac{\partial}{\partial \lambda} \quad (6)$$

and

$$\frac{\partial}{\partial y} = \frac{1}{a} \frac{\partial}{\partial \phi}, \quad (7)$$

where a is average radius of the Earth ($6.37 \times 10^6 \text{ m}$), ϕ and λ are latitude and longitude (radians), respectively.

The mean depth from the navigation chart, and the 8-year (1990–1998) averaged wind field from ECMWF (European Center of Medium Range Weather Forecast) (Fig. 2) are employed as inputs in computation. The model is taken initially at rest or no-motion condition. Normal component of volume transport is specified as zero along the solid coastal boundary. At the sea boundary, water elevation at the east (Sattahip) and the west (Hua Hin) end points (Fig.1), calculated by using the harmonic analysis technique, are linearly interpolated to fill in all grids along the open boundary between them. The predominant tidal constituent from SOJISUPORN and PUTIKIATIKAJORN (1998) are used for the harmonic calculation of tidal elevation, whose values are shown in Table 1. The monthly mean river discharges from the Hydrographic Department, and BOONPHAKDEE *et al.* (1999) are conditions at the river boundary. The model is operated with time step of 1800s, and running time for 30 days.

3. Seasonal circulation

The results of seasonal circulation due to the monsoon winds plus the tide-induced residual current are presented in Fig.3. Currents have averaged magnitude of 0.44, 0.40, 0.70, and 0.36 cm/s in the northeast, the transition from the northeast to the southwest (NE-SW), the southwest, and the transition from the southwest to the northeast monsoon (SW-NE), respectively. During the northeast monsoon, circulation has trend to flow in counter-clockwise direction along the coastline from the east to the head of the Gulf, and then flows to the west, respectively. This current continues flowing southward along the west coast, and finally runs out of the Gulf in the southwestern part. The counter-clockwise flow presented in the northeast monsoon becomes weaker in the NE-SW transition period. A clockwise gyre appears at the northwestern

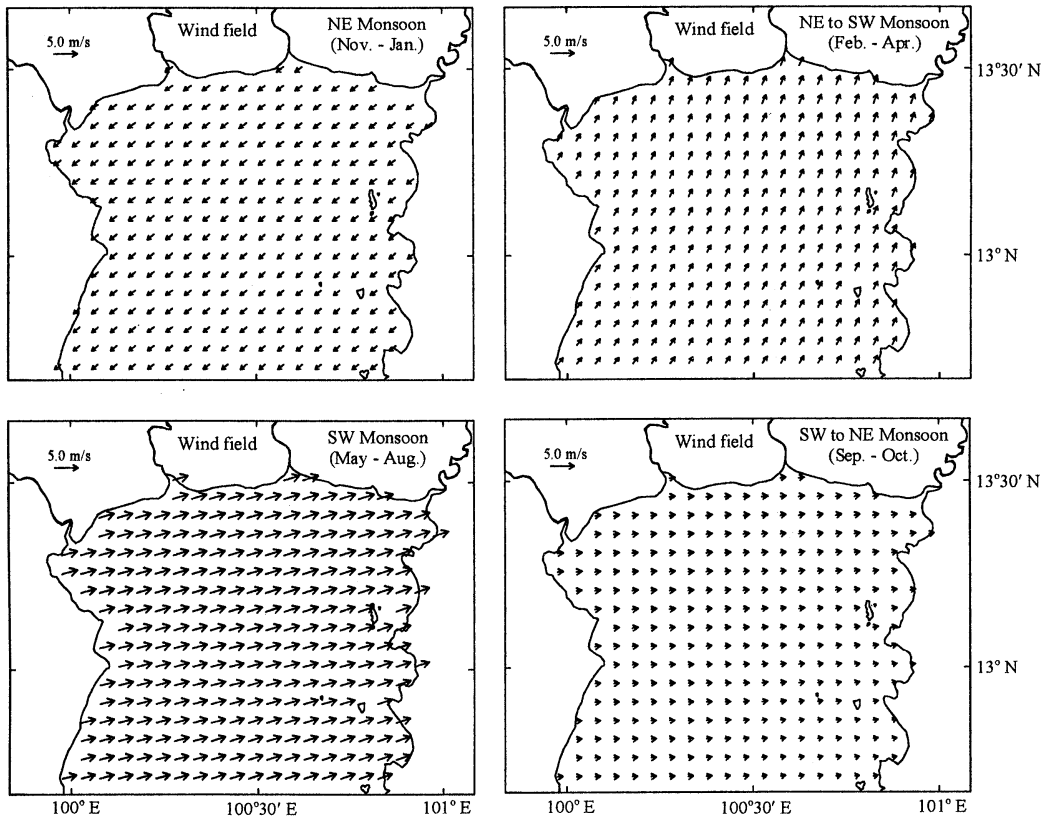


Fig. 2. Seasonal wind fields over the upper Gulf of Thailand

Table 1 Major harmonic constituents used to calculate the tidal elevation at the sea boundary.

Tidal Constituent	Hua Hin		Sattahip	
	Amplitude(m)	Phase(degree)	Amplitude(m)	Phase(degree)
K ₁	0.609	167	0.587	162
O ₁	0.396	117	0.393	112
M ₂	0.327	140	0.261	121
S ₂	0.158	213	0.123	192

part of the Gulf. Strong northward currents can be observed along the eastern coast in this season, which are the same as those in the previous season.

Circulation during the southwest monsoon dramatically changes from that during the northeast monsoon. The counter-clockwise flow vanishes in this season, but a big strong clockwise gyre appears near the head of the Gulf. The current flowing into the Gulf in the southwestern part separates into two directions, the northward along the west coast, and

the northeastward to the central of the lower half of the Gulf. The northward flow along the chain of eastern islands is still observed but the magnitude is weaker than those in the two previous seasons. Strongest currents from main rivers are perceived during the SW-NE transition period because of high river discharge in this period. However, over all current in the Gulf is weaker and more complicate than other time. The clockwise gyre disappears and retreats as a weak clockwise flow along the coast in the northwestern area.

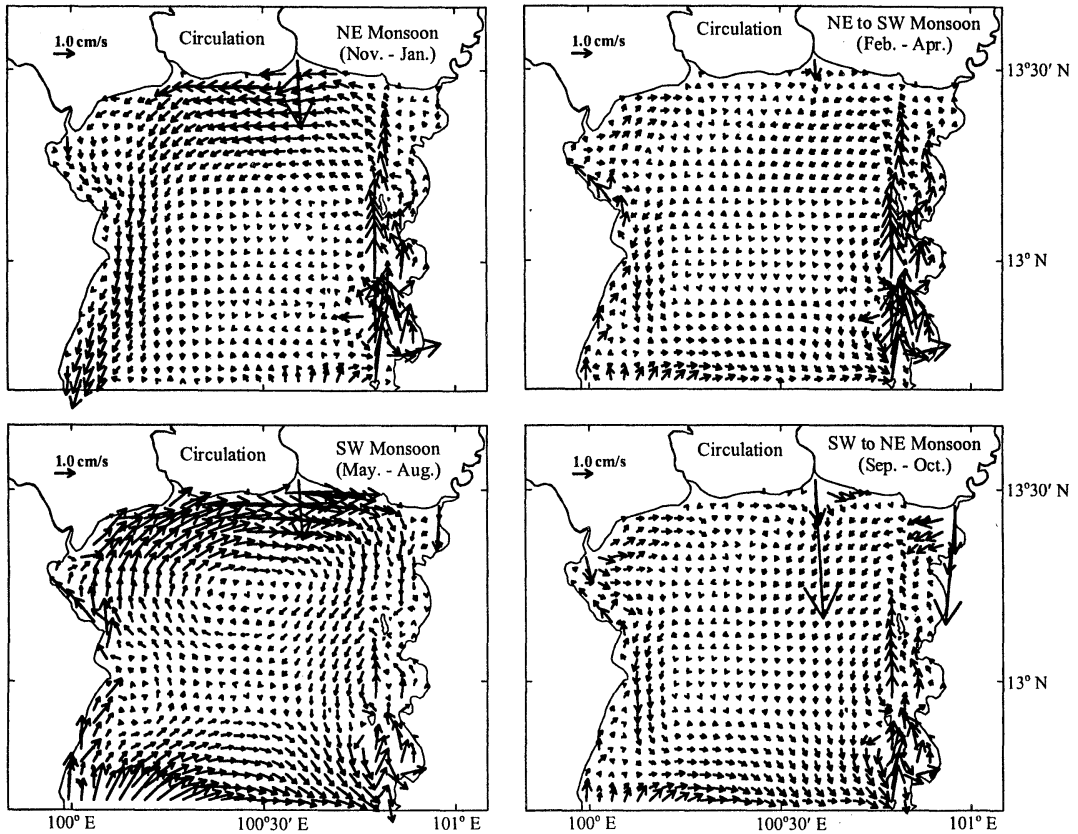


Fig. 3. Calculated seasonal circulation in the upper Gulf of Thailand.

3. Salinity distribution experiment

In this study, because of the lack of measured current data to be verified with the computed results, we have to try to simulate the seasonal salinity distribution in the upper Gulf of Thailand by using computed circulation as input. And the results will be compared with the picture of the seasonal distribution of sea surface salinity in the same area (Fig. 4), which was intensively measured and presented by NEDECO (1965). The objective of the study is to examine if the computed results of seasonal circulation can reproduce the salinity distribution in the same way as those from the measurement. Vertical stratification is developed only in the central and southern parts of the Gulf of Thailand throughout the year and the water column is vertically mixed near the head of the Gulf because $\log_{10}(H/U^3)$ is smaller than 2.5 (H ; water depth in meters, U ; tidal current

amplitude in m/sec) there (YANAGI *et al.*, 2001).

The governing equation to calculate salinity distribution is shown below:

$$\frac{\partial s}{\partial t} + u \frac{\partial s}{\partial x} + v \frac{\partial s}{\partial y} = K_h \left(\frac{\partial^2 s}{\partial x^2} + \frac{\partial^2 s}{\partial y^2} \right), \quad (8)$$

where s is salinity (psu), and K_h is the horizontal diffusivity (m^2/s). The detail how to consider the value of K_h will be described later.

We use the spatial coordinate in the same way as that in the circulation model, with the central scheme of the finite difference technique. Time step is 3600s with running time of 1,200 days because the solutions become stable at the day of 1,100. Salinity at the river boundaries are fixed and set as zero, while those at the sea boundary are assumed to depend on the observed results in Fig.4. Values of K_h are adjusted seasonally depending on the computed results of salinity. If the K_h is too small, some errors will be generated in the results. Thus, we

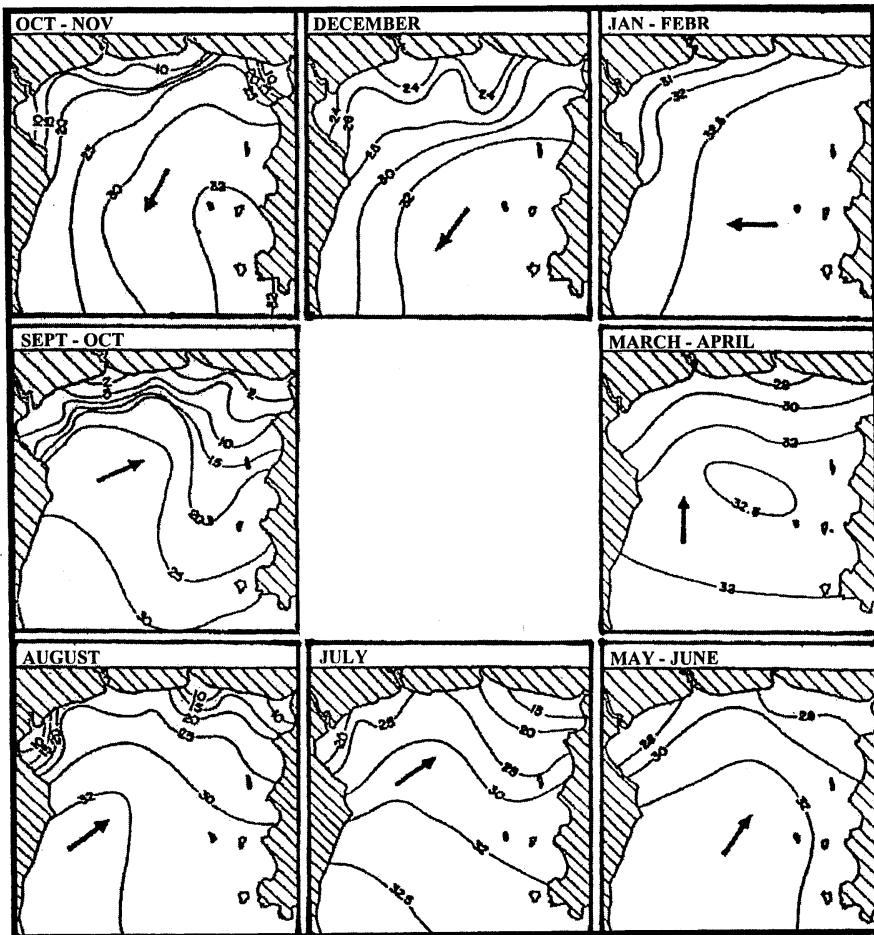


Fig. 4. Seasonal variations in salinity distribution in the upper Gulf of Thailand. Arrows show the wind direction (NEDECO, 1965).

Table 2 The list of some parameters used as inputs in computation of salinity distribution

Seasons	Initial sal.(psu.)	Boundary sal.(psu.)	K_h (m ² /s)
Northeast	31.0	33.0	1.5
Northeast to Southwest	29.0	32.0	1.5
Southwest	25.0	32.5	30.0
Southwest to Northeast	20.0	30.0	15.0

choose the minimum K_h value in each operation that can maintain the reliable outputs. The values of salinity for initial and boundary conditions, and K_h are summarized and presented in Table 2.

The computed results of seasonal distribution of salinity in the upper Gulf of Thailand are shown in Fig.5. Salinity is quite high

during the northeast monsoon with tendency of low salinity in the west coast. Anyway, low salinity also appears in the east coast just near the Bangpakong river mouth. In the NE-SW period, a plume of low salinity water occurs in the northwestern area, while higher salinity arises as the background in the entire area. A meander of low salinity appears from the mid-west

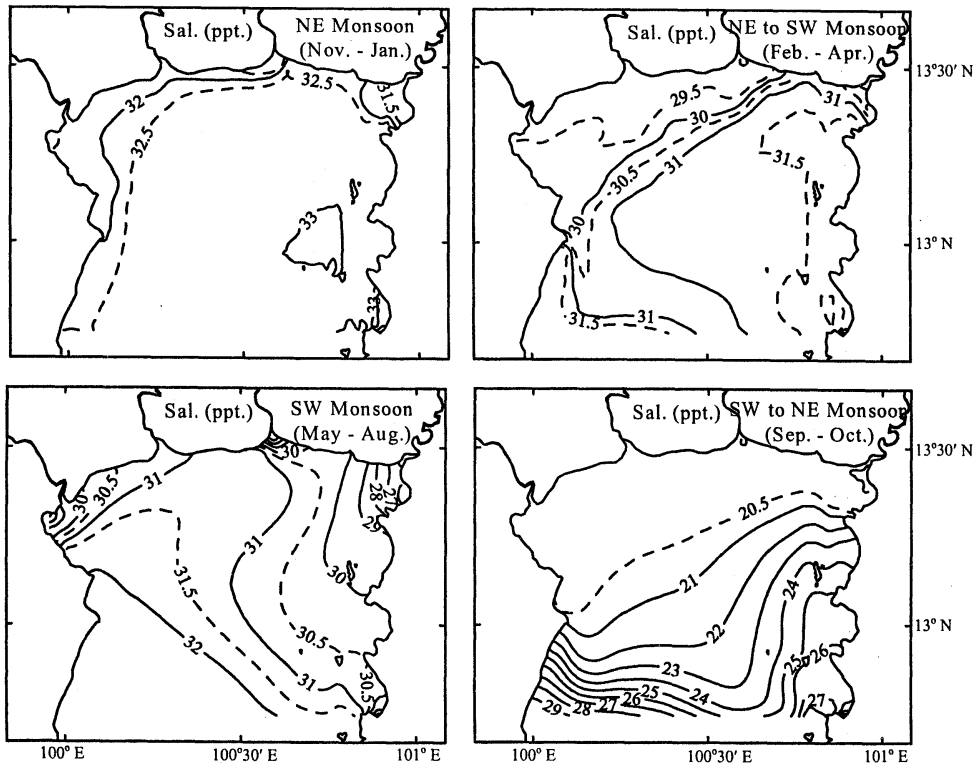


Fig. 5. Computed salinity distribution in the upper Gulf of Thailand.

coast to the central of the southern end. However, the salinity distribution is dramatically shifted from those in the two previous seasons during the southwest monsoon. Relatively high and low salinity presents in the west and the east coasts, respectively. Lowest salinity can be observed near the Bangpakong river mouth, and the values are gradually high along the east coast from this area to the sea boundary. The contours illustrate that high salinity from the west coast penetrates to the east near the mid-north coast, while low salinity percolates from the east to the west in the mid-Gulf. During the SW-NE transition period, except the sea boundary region, salinity is quite low in the remaining area. High salinity water from the south advances into the Gulf along the east coast, while it retreats because of the low salinity water mass in the southwestern site. As a result, salinity in the upper half of the Gulf is lower in the west than that in the east.

4. Discussions

Unfortunately, we have no raw numerical data from the previous studies to be correlated mathematically with the computed results of salinity distribution. Therefore, we can just compare the figures of the measured from a previous study with those of the computed by this study. However, it is quite clear that the computed results of salinity distribution (Fig. 5) coincide with those of the measured (Fig. 4), although the former represents the depth-averaged salinity while the latter are the values at the sea surface. Good comparisons are observed during the mid-northeast and the mid-southwest monsoons. Because the patterns of wind field at these times are quite stable, which can generate the unique and stable patterns of circulation and salinity distributions. On the contrary, it is quite hard to reproduce the observed patterns during the monsoon transition because of the year-to-year variation in the time of monsoon change.

From the success to reproduce the salinity

distributions, we can refer them back to the patterns of circulation. The figures of salinity distribution (Fig. 5) and seasonal circulation (Fig. 3) illustrate the closed gyre occurring only in the southwest monsoon. While in the northeast monsoon, the closed gyre cannot be generated. It may be from the interaction between wind direction and coastal morphology. The main balance in the momentum equations of (1) and (2) is between the surface and bottom stresses because the horizontal scale of the upper Gulf (about 100 km) is much smaller than the Rossby's deformation length λ of 370 km ($\lambda = (gH)^{1/2}/f$; $g=9.8 \text{ m/s}^2$, $H=15\text{m}$ and $f=3.3 \times 10^{-5} \text{ rad/s}$). Strong west and southwest wind during the southwest monsoon will push water in the shallow region along the north coast to move strong and fast to the east. And when the current batters the east coast, it will reflect back to the west along the central line separating the northern and the southern Gulf due to the horizontal geometry, generating a closed clockwise circulation. However, during the northeast monsoon, strong northeast wind just induced water movement consecutively along the coast from the north to the west, and then flows out of the Gulf at the southwestern boundary. This counter-clockwise flow is compensated by the northward inflow of seawater along the east coast. Therefore, the closed gyre cannot occur, just flows along the coast from east to north, to west, and then flows out at the southwest, respectively.

The frequent occurrence of phytoplankton bloom in the northeastern Gulf should be discussed here as well. This phenomenon can be mentioned to the eutrophic condition from high nutrient accumulation in the area. The study of NRCT-JSPS (1998) pointed out the significant source of nutrient from the Bangpakong River. Anyway, the results of circulation and salinity distribution suggest the oceanographic condition promoting the condition other than loading from the Bangpakong River. It is obvious that nutrient loads from four main rivers in the upper Gulf (Fig. 1) are very high depending on large freshwater discharge in wet season, which is the time of the southwest monsoon. The west and southwest wind prevailing over the upper Gulf (> 6

months per year: ECMWF data) will generate the clockwise gyre near the head of the Gulf (Fig. 3), which let discharges from the river mouths flow from the west to the east along the north coast. As we can see in the salinity distribution during the southwest monsoon (Fig. 5) that indicates the influence of discharge from the Chaopraya river over the area near the Bangpakong river mouth and the eastern coast of the Gulf. Not only freshwater but also contaminants such as nutrients are also driven to the east. Therefore, this terminal area will suffer from the nutrient transport and then the eutrophic condition is promoted for long period of the year.

However, the above reason for the eutrophic condition is just a possible assumption according to the results from this study. We will have to investigate the details of mechanism by using 3-D hydrodynamic model and ecosystem model in the near future. The 3-D model can let us know more realistic oceanographic condition because it include effects not only from wind, tide, and river discharge but also from horizontal density difference (density driven current), and sea surface height. And, we will use the ecosystem model, which considers the biological factors to investigate the mechanism of the phenomenon.

5. Conclusions

The seasonal variations in circulation and salinity distributions in the upper Gulf of Thailand are investigated by using a 2-D hydrodynamic model. Comparable results of salinity distributions from the computation and those from the observation confirm the reliability of computed circulation. During the southwest monsoon, a clockwise gyre is generated near the head of the Gulf with northward inflow and southward outflow in the southwest and the southeast of the upper Gulf, respectively. However, there is no closed gyre during the northeast monsoon, just flows along the coast from east to west, and then flows out of the Gulf at the southwest, consecutively.

Acknowledgements

The authors would like to thank Dr.KASHANE Chalermwat from Burapha Uuniversity for his

kind support and suggestions, and the Department of Aquatic Science, Faculty of Science for facilitation.

References

- BOONPHAKDEE, T., P. SAWANGWONG and T. FUJIWARA (1999) : Freshwater discharge of Bangpankong River flowing into the inner Gulf of Thailand. *La mer*, **37**, 103–110.
- BUNPAPONG, M., R.O. REID and E. WHITAKER (1985) : An investigation of hurricane-induced forerunner surge in the Gulf of Mexico. Research Conducted Through Texas A & M Research Foundation Project 4667. Texas A&M University, 201 pp.
- BURANAPRATHEPRAT, A. and M. BUNPAPONG (1998) : A two dimensional hydrodynamic model for the Gulf of Thailand. Proceedings of The IOC/WESTPAC Fourth International Scientific Symposium, 469–478.
- CHALERMWAT, K. and R.A. LUTZ (1989) : Farming the green mussel in Thailand. *World Aquaculture*, **20**, 41–46.
- CHONGPRASITH, P. and V. SRINETH (1998) : Marine water quality and pollution of the Gulf of Thailand. *In* SEAPOL Integrated Studies of the Gulf of Thailand, Vol.1, ed. By D.M. Johnston, Southeast Asian Programme in Ocean Law, Policy and Management.
- NEDECO (1965) : A study on the siltation of the Bangkok Port Channel. The Hage, Holland.
- NEELASRI, K. (1981) : Analysis of the observed current during the inter-monsoon period. *In* the 2nd Seminar on Water Quality and Living Resources in Thai Water, 57–63.
- NRCT-JSPS (1998) : An integrated study on physical, chemical and biological characteristics of the Bangpakong Estuary. Final Report Cooperative Research NRCT-JSPS, the National Research Council of Thailand (NRCT) and the Japan Society for the Promotion of Science (JSPS), 127 pp.
- SOJISUPORN, P. (1994) : Density-driven and wind-driven current in the upper Gulf of Thailand. Proceedings IOC-WESTPAC 3rd International Scientific Symposium, 374–385.
- SOJISUPORN, P. and P. PUTIKATIKAJORN (1998) : Eddy circulation in the upper Gulf of Thailand from 2-D tidal model. Proceedings of The IOC/WESTPAC Fourth International Scientific Symposium, 515–522.
- YANAGI, T. and T. TAKAO (1998) : Seasonal variation of three-dimensional circulations in the Gulf of Thailand. *La mer*, **36**, 43–55.
- YANAGI, T., S.I. SACHOEMAR, T. TAKAO and S. FUJIWARA (2001) : Seasonal variation of stratification in the Gulf of Thailand. *J. Oceanogr.*, **57**, 461–470.

Received July 9, 2002

Accepted October 1, 2002

資料

第40巻第3号掲載欧文論文要旨

T.R. パーソンズ・C.M. ラリ : クラゲ個体群の爆発的増大 : 原因であり得る事象に関する一仮説の再検討

クラゲ(刺胞動物および/または有櫛動物)の大規模なブルームの生産を、海洋におけるナノ植物プランクトンの生産を基礎とする特定の食物連鎖と関連づける一つの仮説が多角的に論じられる。この型の低エネルギーの食物連鎖が高エネルギーの食物連鎖(珪藻が基礎となり、大型の肉食者、魚類、鯨類を支えるもの)といかに対照的であるかということを示す証拠が、化石の記録および現代の海洋から提示される。最近の人為活動が海洋に与えている影響(汚染や乱獲を含む)が、提唱された仮説との関連で議論される。また、クラゲの大量発生をもたらす自然事象も検討される。

Nyoman M. N. Natih*・松山優治*・北出裕二郎*・吉田次郎* : 日本沿岸の潮位の季節変動

日本周辺の68潮位観測点で1981年から1990年に得られた記録を解析し、潮位の季節変動を調べ、海洋現象との関係について議論した。1951年から1960年の同様の記録を解析した津村(1963)と非常によく似た結果が得られたが、一部異なる点も見つけられた。北海道のオホーツク海岸から南東海岸で冬季に潮位が高くなるが、東サハリン海流が強化されるためであると考えられる。房総半島の布良から紀伊半島の浦神まで6月から7月に潮位上昇が緩やかになり、海面から200mまでの平均水温の季節変化と非常によく対応していた。この海域では夏季の表層下に水温第二極小と呼ばれる季節温度躍層の上昇が見られ、このため昇温期であるにもかかわらず、200m深までの平均水温の上昇は緩やかで、潮位も上昇しないことがわかった。この時期の季節温度躍層の上昇は、連吹する南からの風により起こされた湧昇が南岸を伝播するためと推測された。4月から5月に本州の南西岸から瀬戸内海で水位上昇が緩やかになるが、理由は明らかではない。(*東京水産大学海洋環境学科 〒108-8477 東京都港区港南4-5-7)

藤家 亘*・柳 哲雄**・フェルナンド・シリガン*** : マニラ湾における堆積物輸送経路

マニラ湾における4月、9月、11月の平均的な流動場を数値モデルで計算し、その結果を用いて平均海底面応力ベクトルを計算した。平均海底面応力ベクトルは堆積物の輸送方向を表す。Pampanga沖とCaviteの海岸線において計算から得られた堆積物の輸送方向はSiringan and Ringor (1998)による観測結果とよく合っていた。マニラ湾全域の堆積物の輸送方向を計算結果から考察した。その結果マニラ湾全体において、堆積物は流出せず、湾外の堆積物が湾口部をとおって流入していることが明らかとなった。

(*九州大学総合理工学府大気海洋環境システム学専攻 〒816-8580 福岡県春日市春日公園6丁目1番地, **九州大学応用力学研究所 〒816-8580 福岡県春日市春日公園6丁目1番地, ***University of the Philippines, Diliman, Quezon City 1101, the Philippine)

アヌクル・ブラナプラスブラット*・柳 哲雄**・ピチャン・サワンゴング* : タイランド湾奥の循環流と塩分分布に季節変動 : モデル計算

タイランド湾奥の循環流と塩分分布の季節変動を水平2次元数値モデルを用いて研究した。計算した循環流を用いて塩分分布を計算し、それを観測結果と比較することで、計算結果を検証した。南西モンスーン時にタイランド湾奥には時計回りの閉じた循環流が形成される。しかし、北東モンスーン時には反時計回り不完全な循環流しか形成されない。このような循環流の季節変動は湾奥東部のバンパコン河口域で南西モンスーン時にのみ富栄養化が進むという観測事実とよく対応している。

(*Department of Aquatic Science, Burapha University, T. Saensuk, A. Muang, Chonburi 20131, Thailand, **九州大学応用力学研究所, 〒816-8580 春日市春日公園6-1)

学 会 記 事

1. 2002年5月28日(火)東京水産大学海洋環境棟会議室において幹事会が開かれた。

43回総会議案を検討した。その後、評議員会が開かれた。

2. 2002年6月1日(土)日仏会館会議室において、平成14年度学術研究発表会が開かれた。発表題目と発表者は次の通り。

午前(10:00~12:00)

1. 発電所冷却水による閉鎖性内湾の流動・水質環境改善の可能性について……………○高野泰隆(榎水科コン)・柴崎道廣(助海生研)・和田 明(日大・生産工)
2. 太平洋域におけるCO₂海洋隔離技術の検証……………○長谷川一幸(日大・生産工)
3. ALACEフロートを用いた日本海中・深層の流速・水温の観測……………○柳本大吾・平 啓介(東京大)
4. 台風通過に伴い発生する相模湾の急潮の予報モデル……………○井桁庸介・北出裕二郎・松山優治(東水大)
5. 本州南岸の潮位変動特性……………○鳴海吉洋・根本雅生・長島秀樹(東水大)
6. 半日周期内部潮汐の地形による散乱……………○川村有二・北出裕二郎・松山優治(東水大)

午後(13:40~14:40)

7. ノリ育苗期における網の色彩と発芽体の数・サイズおよび付着量との関連……………○森永 勤・稲田真理・荒川久幸(東水大)・小林千果夫・坂田能光(助千葉県水振公)
 8. 褐藻類アラメ遊走子および配偶体の生残へ及ぼす海中懸濁粒子と堆積粒子の影響……………○荒川久幸・森永 勤(東水大)
 9. イセエビの脱皮と摂餌活動……………○小池 隆・山崎博貴(三重大・生資)
3. 2002年6月1日(土)日仏会館会議室において、第43回(平成14年度)総会が開かれた。議事の概要は次の通り。

1) 平成13年度事業報告

(a) 庶務

会員移動状況

	平成13年 4月	入会	退会	逝去	資格変更	平成14年 3月
名誉会員	2	-	-	-	-	2
正会員	274	9	8	5	-	270
学生会員	3	2	-	-	-	5
賛助会員	13	-	2	-	-	11

(b) 活動状況

- 評議員会 1回(H13/5/14)
 幹事会 5回(H13/5/14, 7/23, 9/12, 11/19, H14/3/30)
 総会 1回(H13/5/27 日仏会館於)
 学術研究発表会 1回(H13/5/27 日仏会館於)
 学会誌発行 38巻4号-39巻4号
 学会賞授与 寺崎誠会員(東京大学 H13/5/27)

(c) 編集

- 39(2), 39(3), 39(4), 40(1)
 (1) 第39巻第1号(2001)から表紙のデザインを変更
 (2) 2002年度(第40巻第2号)より編集委員会を交代、次期編集委員長:吉田次郎氏(東京水産大)

2) 平成13年度収支決算および監査報告

収入の部

費目	金額
前年度繰越金	175,159
正会員会費	1,081,500
学生会員会費	12,000
賛助会員会費	150,000
学会誌売上金	318,353
広告料	50,000
別刷り印刷費	1,233,985
著者負担印刷費	540,000
雑収入	41,394
寄付金収入	130,000
合計	3,732,391

支出の部

費目	金額
学会誌印刷費	2,550,000
送料・通信費	227,338
事務費	683,612
交通費	22,470
会議費	21,527
学会賞経費	73,165
雑費	59,400
次年度繰越金	94,879
合計	3,732,391

3) 平成14年度事業計画(案) 審議 40(3)

下記原案通り承認された。
 評議員, 総会, 学術研究発表会および幹事会, 学会誌の刊行
 平成14年度学会賞授与および平成15年度受賞候補者の推薦
 その他

4) 平成14年度予算(案) 審議

原案通り承認された。

収入の部

費目	金額
前年度繰越金	94,879
正会員会費	1,620,000
学生会員会費	20,000
賛助会員会費	110,000
学会誌売上金	300,000
広告料	60,000
別刷り印刷費	300,000
著者負担印刷費	300,000
雑収入	50,120
寄付金収入	1
合計	2,855,000

支出の部

費目	金額
学会誌印刷費	1,800,000
送料・通信費	205,000
事務費	700,000
交通費	24,000
会議費	23,000
学会賞経費	75,000
雑費	25,000
予備費	3,000
合計	2,855,000

5) その他

引き続き平啓介会員への学会賞授与と受賞記念講演が行われた。また終了後アトレ恵比寿「桃花宮」で懇親会が開かれ盛会裡に終了した。

4. 新入会員(正会員・学生会員)

氏名	所属・住所	紹介者
柳本大吾	東京大学海洋研究所 〒164-8639 中野区南台1-15-1	平 啓介
成田美穂	東京水産大学海洋環境学科 環境システム学講座 〒108-8477 港区港南4-5-7	森永 勤
岡本 研	東京大学大学院農学生命学 研究科生圏システム学専攻科 〒113-8657 文京区弥生1-1-1	石丸 隆
堀本奈穂	東京水産大学海洋環境学科 生物環境化学講座 〒108-8477 港区港南4-5-7	山口征矢
乙部弘隆	東京大学海洋研究所 大槌臨海研究センター 28-1102 岩手県上閉伊郡大槌町 赤浜2-106-1	長島秀樹

5. 所属・住所等変更

川名吉一郎 〒737-0197 広島県呉市広末広2-2-2
 独立行政法人産業技術総合研究所中国センター
 金成誠一 〒350-0067 埼玉県川越市三光町38-1
 アクティ川越3-401
 塩本明弘 〒236-8648 横浜市金沢区福浦2-12-4
 独立行政法人水産総合研究センター中央水産研
 究所海洋生産部物質環境研究室
 真鍋武彦 兵庫県立農林水産技術センター(名称変
 更)
 平 啓介 〒102-8471 東京都千代田区1-6
 日本学術振興会
 中川平介 広島大学大学院生物圏科学研究科
 水産増殖学研究室

6. 退会

大橋善八 岩淵義郎 岡市友利 稲葉榮生 大沼治夫
 上原研吾

7. 受贈図書

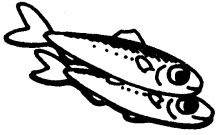
しおさい 18
 NTT R&D 51 (6・7・8・9)
 水産工学研究所技報 24
 広島日仏協会報 156

Bulletin of the National Science Museum 28 (1・2)
NII News (国立情報学研究所ニュース) 10・11
高知大学海洋生物教育研究センター研究報告 21
RESTEC 49
農業工学研究ニュース 21
農場工学研究所研究成果情報 13
養殖研ニュース 49

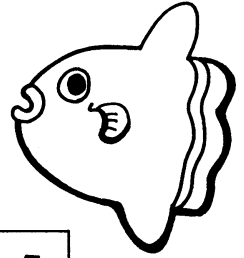
Journal of the Korean Society of Oceanography 37
(1・2)
海洋水産研究 22 (3・4) 23 (1・2)
海洋与湖沼 32 (3・4・5・6) 33 (1・2・3・4)
青島海洋大学学报 30 (3・4) 31 (1・2)
Ocean and Polar Research 24 (1・2)

賛 助 会 員

アレック電子株式会社	神戸市西区井吹台東町7-2-3
株式会社 イーエムエス	神戸市中央区多聞通3-2-9
有限会社 英和出版印刷	文京区千駄木4-20-6
株式会社 内田老鶴圃 内田 悟	文京区大塚3-34-3
財団法人 海洋生物環境研究所	千代田区内神田1-18-12 北原ビル
株式会社 川合海苔店	大田区大森本町2-31-8
ケー・エンジニアリング株式会社	台東区浅草橋5-14-10
国土環境株式会社	世田谷区玉川3-14-5
三洋測器株式会社	渋谷区恵比須南1-2-8
株式会社 高岡屋	台東区上野6-7-22
テラ株式会社	世田谷区代田3-41-8 代田ウエスト5F
日本海洋株式会社	北区栄町9-2
株式会社 三菱総合研究所 (社会システム部)	千代田区大手町2-3-6
渡邊機開工業株式会社	愛知県渥美郡田原町神戸大坪230



海洋生物資源を大切に利用する企業でありたい
 ——青魚(イワシ・サバ・サンマ)から宝を深し出す——



母なる海・海には愛を!

La mer la mère, l'amour pour la mer!



SHIDA

信田缶詰株式会社

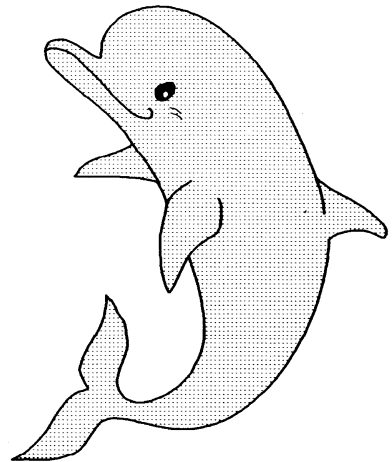
〒288 千葉県銚子市三軒町2-1 TEL 0479(22)7555 FAX 0479(22)3538

●製造品・水産缶詰・各種レトルトパウチ・ビン詰・抽出スープ・他

街をきれいにしてイルカ?

事業内容

- 産業廃棄物、一般廃棄物の収集運搬処理
- 各種槽、道路、側溝の清掃
- 上下水道、排水処理施設運転管理
- 下水道管内TVカメラ調査
- 総合ビル管理
- その他上記に付随する一切の業務



 **株式会社 春海丸工営**

本社 〒312 茨城県ひたちなか市長砂872-4 ☎029-285-0786 FAX285-7519
 銚子支社 〒288 千葉県銚子市長塚町6-4490-1 ☎0479-22-4733 FAX22-4746
 水戸支社 〒310 茨城県水戸市中央 2-2-6 ☎029-226-9639 FAX226-9855

Chelsea Instruments

(Chelsea社は、曳航式CTD計の専門メーカーです。)

Aquashuttle/Aquapack

曳航器・アクアシャトル

最適航速 8-20ノット

アーマードケーブルでリアルタイム測定可

CTD ロガー・アクアパック

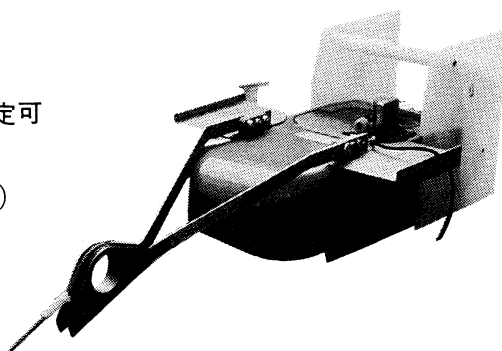
電導度 1~55 mS/cm (0.01 mS/cm)

温度 -2~32 °C (0.005 °C)

深度 0~200 m

蛍光光度 0.01 μg ~ 100 μg/l

メモリー 50,000 データ (標準)



CI

CHELSEA
INSTRUMENTS
LIMITED



**Biospherical
Instruments
Inc.**

日本総代理店

ケー・エンジニアリング株式会社

〒111 東京都台東区浅草橋5-14-10

TEL 03-5820-8170

FAX 03-5820-8172

日仏海洋学会入会申込書

(正会員・学生会員)

	年度より入会	年	月	日	申込
氏名					
ローマ字		年	月	日	生
住所 〒					
勤務先 機関名					
電話					
自宅住所 〒					
電話					
紹介会員氏名					
送付金額		円	送金方法		
会誌の送り先 (希望する方に○をつける)			勤務先 自宅		

(以下は学会事務局用)

受付	名簿	会費	あて名	学会
	原簿	原簿	カード	記事

入会申込書送付先：〒150-0013 東京都渋谷区恵比寿 3-9-25

(財) 日仏会館内

日 仏 海 洋 学 会

郵便振替番号：00150-7-96503

日仏海洋学会編集委員会 (2002-2003年度)

委員長: 吉田次郎

委員: 落合正宏, 田中祐志, 長島秀樹, 前田 勝, 門谷 茂, 柳 哲雄, 渡邊精一

海外委員: H. J. CECCALDI (フランス), E. D. GOLDBERG (アメリカ), T. R. PARSONS (カナダ)

幹事: 田中祐志, 北出裕二郎

日仏海洋学会役員・評議員 (2002-2003年度)

顧問: ユベール・ブロシェ ジャック・ロベール アレクシス・ドランドール ミシェル・ルサージュ
ロベール・ゲルムール ジャック・マゴー レオン・ヴァンデルメルシュ オーギュスタン・ベルク
ユベール・セカルディ オリビア・アンサール ピエール・カブラン

名誉会長: ビエール・スイリ

会長: 須藤英雄

副会長: 山口征矢 今脇資郎

幹事: (庶務) 前田 勝 森永 勤

(会計) 小池 隆 山崎秀勝

(編集) 田中祐志 北出裕二郎

(研究) 有元貴文 長島秀樹

(渉外) 石丸 隆 小池康之

監事: 岸野元彰 村野正昭

編集委員長: 吉田次郎

評議員:	青木三郎	有元貴文	有賀祐勝	今脇資郎	石丸 隆	磯田 豊	岩田静夫
	岡市友利	奥田邦明	梶浦欣二郎	鎌谷明善	岸野元彰	黒田一紀	小池勲夫
	小池 隆	小池康之	齊藤誠一	佐伯和昭	佐藤博雄	須藤英雄	関 文威
	関根義彦	千手智晴	平 啓介	高橋正征	高野健三	隆島史夫	田中祐志
	谷口 旭	寺崎 誠	鳥羽良明	中田英昭	中田喜三郎	長島秀樹	永田 豊
	平野敏行	福田雅明	前田明夫	前田昌調	前田 勝	松生 治	松山優治
	村野正昭	森永 勤	門谷 茂	八木宏樹	山口征矢	柳 哲雄	山崎秀勝
	吉田次郎	渡邊精一	和田 明				(52名会長推薦評議員含む)

2002年8月25日印刷
2002年8月30日発行

う み

第40巻
第3号

定価 ¥ 1,600

編集者 吉 田 次 郎

発行所 日 仏 海 洋 学 会

財団法人 日仏会館内

東京都渋谷区恵比寿3-9-25

郵便番号: 150-0013

電話: 03 (5421) 7 6 4 1

振替番号: 00150-7-96503

印刷者 佐 藤 一 二

印刷所 (有)英和出版印刷社

東京都文京区千駄木4-20-6

郵便番号: 113-0022

電話: 03 (5685) 0 6 2 1

う み

第40巻 第3号

Notes originales

Carbon Dioxide and Air-Sea CO ₂ Flux in Coral ReefHiroyuki FUJIMURA, Tamotsu OOMORI, Yukio KITADA and Tsukasa MAEHIRA	99
Jellyfish Population Explosions: Revisiting a Hypothesis of Possible CausesT. R. PARSONS and C. M. LALLI	111
Seasonal variations of sea level along the Japanese coastNyoman M. N. NATH, Masaji MATSUYAMA, Yujiro KITADE and Jiro YOSHIDA	123
Tide, Tidal Current and Sediment Transport in Manila BayWataru FUJIE, Tetsuo YANAGI and Fernando P. SIRINGAN	137
Seasonal Variations in Circulation and Salinity Distributions in the Upper Gulf of Thailand: Modeling ApproachAnukul BURANAPRATHEPRAT, Tetsuo YANAGI and Pichan SAWANGWONG	147
Faits divers	157
Procès-verbaux	158

原 著

サンゴ礁海域における二酸化炭素分圧と大気-海洋間のCO ₂ フラックス藤村弘行, 大森 保, 北田幸男, 真栄平司	99
クラゲ個体群の爆発的増大: 原因であり得る事象に関する一仮説の再検討T. R. パーソンズ, C. M. ラリ	111
日本沿岸の潮位の季節変動.....Nyoman M. N. NATH, 松山優治, 北出裕二郎, 吉田次郎	123
マニラ湾における堆積物輸送経路.....藤家 巨, 柳 哲雄, フェルナンド・シリガン	137
タイランド湾奥の循環流と塩分分布に季節変動: モデル計算アヌクル・ブラナプラサプラット, 柳 哲雄, ピチャン・サワンゴング	147
資 料	
第40巻第3号掲載欧文論文の和文要旨	157
学会記事	158

2002年8月

日 仏 海 洋 学 会